Report of Investigation 2021-4

SEDIMENTOLOGY AND RESERVOIR QUALITY OF THE NANUSHUK FORMATION (ALBIAN-CENOMANIAN) IN CORES FROM THE NATIONAL PETROLEUM RESERVE–ALASKA AND ADJOINING STATE LANDS TO THE SOUTH

David L. LePain and Kenneth P. Helmold, editors

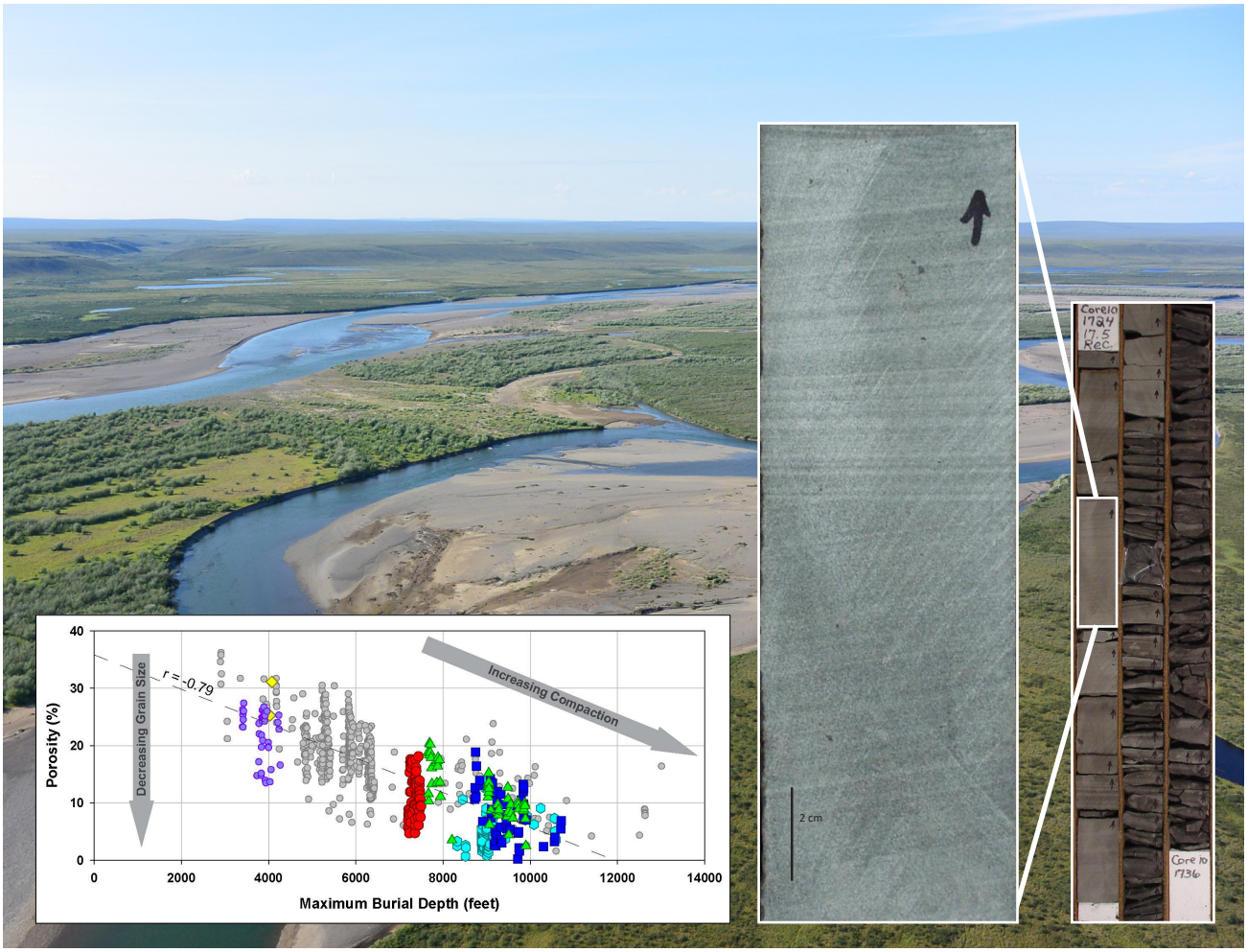

Published by
STATE OF ALASKA
DEPARTMENT OF NATURAL RESOURCES
DIVISION OF GEOLOGICAL & GEOPHYSICAL SURVEYS
2021

SEDIMENTOLOGY AND RESERVOIR QUALITY OF THE NANUSHUK FORMATION (ALBIAN-CENOMANIAN) IN CORES FROM THE NATIONAL PETROLEUM RESERVE–ALASKA AND ADJOINING STATE LANDS TO THE SOUTH

David L. LePain and Kenneth P. Helmold, editors

Report of Investigation 2021-4

State of Alaska
Department of Natural Resources
Division of Geological & Geophysical Surveys

STATE OF ALASKA
Mike Dunleavy, Governor

DEPARTMENT OF NATURAL RESOURCES
Corri A. Feige, Commissioner

DIVISION OF GEOLOGICAL & GEOPHYSICAL SURVEYS
Steve Masterman, State Geologist and Director

Publications produced by the Division of Geological & Geophysical Surveys (DGGS) are available for free download from the DGGS website (dggs.alaska.gov). Publications on hard-copy or digital media can be examined or purchased in the Fairbanks office:

Alaska Division of Geological & Geophysical Surveys
3354 College Rd., Fairbanks, Alaska 99709-3707
Phone: (907) 451-5010 Fax (907) 451-5050
dggspubs@alaska.gov | dggs.alaska.gov

DGGS publications are also available at:
Alaska State Library,
Historical Collections & Talking Book Center
395 Whittier Street
Juneau, Alaska 99811

Alaska Resource Library and Information Services (ARLIS)
3150 C Street, Suite 100
Anchorage, Alaska 99503

Suggested citation:
LePain, D.L., and Helmold, K.P., 2021, Sedimentology and reservoir quality of the Nanushuk Formation in cores from the National Petroleum Reserve–Alaska and adjoining state lands to the south: Alaska Division of Geological & Geophysical Surveys Report of Investigation 2021-4, 78 p., 6 sheets. https://doi.org/10.14509/30726

Background photo. View toward the west of the Colville River, a few miles upstream from Umiat and south of Wolf Creek 3. **Overlying photos.** Box photo showing the lower part of core 10 from the Wolf Creek 3 well. The close-up photo to the left of the box shows hummocky or swaley cross-stratified, very fine-grained sandstone at a depth of approximately 1,725 feet. Note the wave ripple cross-lamination above the black arrow. Porosity versus maximum burial depth plot for Nanushuk sandstone in wells across the North Slope. See Chapters A and B for details.

INTRODUCTION

Several large discoveries of high API gravity oil have been announced recently in the Nanushuk Formation in the Colville delta region on Alaska's North Slope. Published estimates of recoverable resources total approximately 1.5 billion barrels of oil. Accumulations are in stratigraphic traps developed in deltaic sandstones, some associated with lowstands of relative sea level. These discoveries have reignited interest in stratigraphic traps in the Nanushuk and other Brookian formations. Underscoring the remaining potential, the U.S. Geological Survey (USGS) recently estimated a mean, undiscovered, technically recoverable volume of 8.7 billion barrels of oil in the Nanushuk and Torok Formations (Houseknecht and others, 2017).

This two-chapter volume summarizes the Alaska Department of Natural Resources' study of cores from the Nanushuk and upper Torok Formations in the Fish Creek 1, Square Lake 1, Wolf Creek 3, and Grandstand 1 test wells, drilled as part of the U.S. Navy's effort to explore for hydrocarbons in the Naval Petroleum Reserve No. 4 in the 1940s and early 1950s. The name of the reserve was subsequently changed to the National Petroleum Reserve–Alaska (NPRA) in 1976. In addition to these legacy wells, this volume includes cores from the Nanushuk Formation in the Umiat 18 well, drilled by Linc Energy in 2013. This report continues the practice started with publication of the three-volume report summarizing DNR's work on the USGS Wainwright test well 1 (Decker and LePain, 2016; Helmold, 2016; and LePain, 2016) by integrating an analysis of the stratigraphic setting, sedimentology, and sedimentary petrology of the cored succession.

Chapter A by LePain and Helmold includes detailed core descriptions and an analysis of the depositional setting and reservoir potential of Nanushuk sandstone in these wells. Core descriptions are included as six large format sheets. Chapter B by Helmold and LePain presents a detailed analysis of Nanushuk sandstone composition and reservoir quality in the studied cores. Together, these reports will advance the exploration for undiscovered resources in the Nanushuk Formation.

REFERENCES

Decker, P.L., and LePain, D.L., 2016, Subsurface relationships of Albian-Cenomanian shallow marine to nonmarine topsets of the Nanushuk Formation, northwestern NPRA, northern Alaska, *in* LePain, D.L., Stratigraphic and reservoir quality studies of continuous core from the Wainwright #1 coalbed methane test well, Wainwright, Alaska: Alaska Division of Geological & Geophysical Surveys Report of Investigation 2016-3-1, p. 1–3, 1 sheet. https://doi.org/10.14509/29655

Helmold, K.P., 2016, Sedimentary petrology and reservoir quality of Albian-Cenomanian Nanushuk Formation sandstones, USGS Wainwright #1 test well, western North Slope, Alaska, *in* LePain, D.L., Stratigraphic and reservoir quality studies of continuous core from the Wainwright #1 coalbed methane test well, Wainwright, Alaska: Alaska Division of Geological & Geophysical Surveys Report of Investigation 2016-3-3, p. 37–57. https://doi.org/10.14509/29657

Houseknecht, D.W., Lease, R.O., Schenk, C.J., Mercier, T.J., Rouse, W.A., Jarboe, P.J., Whidden, K.J., Garrity, C.P., Lewis, K.A., Heller, S.J., Craddock, W.H., Klett, T.R., Le, P.A., Smith, R.A., Tennyson, M.E., Gaswirth, S.B., Woodall, C.A., Brownfield, M.E., Leathers-Miller, H.M., and Finn, T.M., 2017, Assessment of undiscovered oil and gas resources in the Cretaceous Nanushuk and Torok Formations, Alaska North Slope, and summary of resource potential of the National Petroleum Reserve in Alaska, 2017: U.S. Geological Survey Fact Sheet 2017–3088, 4 p. https://doi.org/10.3133/fs20173088

LePain, D.L., and Decker, P.L., 2016, Lithofacies analysis of the Wainwright #1 continuous core, western Arctic Slope, Alaska: Transition from lower to upper delta plain environments in the Albian-Cenomanian Nanushuk Formation, *in* LePain, D.L., Stratigraphic and reservoir quality studies of continuous core from the Wainwright #1 coalbed methane test well, Wainwright, Alaska: Alaska Division of Geological & Geophysical Surveys Report of Investigation 2016-3-2, p. 5–35, 1 sheet. https://doi.org/10.14509/29656

Contents

Figures

Chapter A

Chapter B

Tables

Chapter A

Chapter B

Sheets

CHAPTER A: CORE DESCRIPTIONS, SEDIMENTOLOGY AND RESERVOIR POTENTIAL OF THE NANUSHUK FORMATION (ALBIAN–CENOMANIAN), EASTERN NATIONAL PETROLEUM RESERVE–ALASKA

David L. LePain[1] and Kenneth P. Helmold[2]

INTRODUCTION

This report presents core descriptions and a discussion of facies associations recognized in cores from the Nanushuk Formation in Fish Creek test well 1, Square Lake test well 1, Wolf Creek test well 3, and Umiat 18, located in the eastern part of the National Petroleum Reserve Alaska (NPRA), and Grandstand test well 1, located on state land south of Umiat (fig. 1). Cores from the Torok Formation in the Fish Creek and Grandstand test wells are also included. The four test wells were drilled as part of the U.S. Navy's extensive program to explore for oil in the NPRA from 1944 through 1953 which, at that time, was referred to as Naval Petroleum

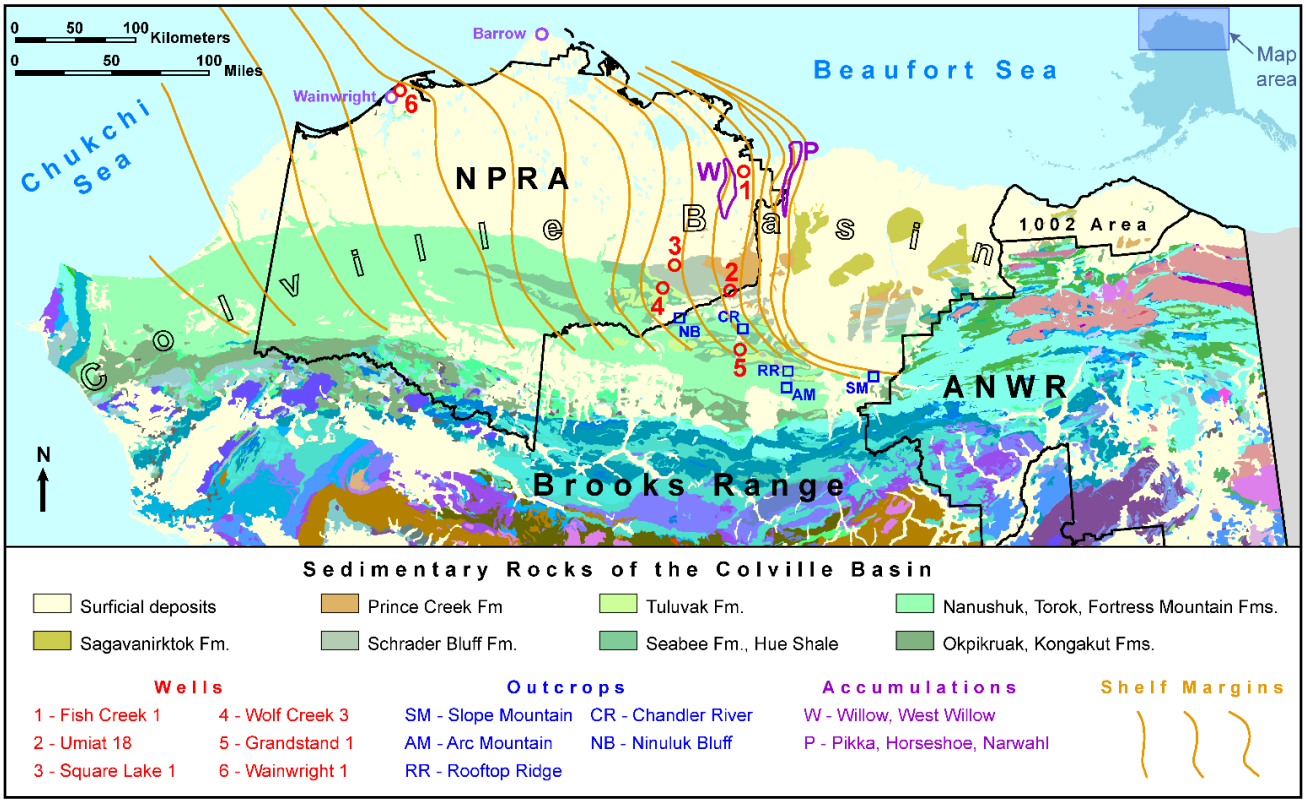

Figure 1. Simplified geologic map of northern Alaska showing the cored wells addressed in this report. Numbered dots correspond to wells: 1, Fish Creek 1; 2, Umiat 18; 3, Square Lake 1; 4, Wolf Creek 3; 5, Grandstand 1. Purple polygons show the approximate locations of Willow (W) and Pikka (P). Yellow lines show the approximate locations of Nanushuk lowstand shelf margins. Shelf margins from Houseknecht (2019). Geology from Wilson and others (2015).

[1] Alaska Division of Geological & Geophysical Surveys, 3354 College Rd., Fairbanks, Alaska 99709-3707; david.lepain@alaska.gov
[2] Alaska Division of Oil & Gas, 550 W. 7th Avenue, Suite 800, Anchorage, Alaska 99501-3560; helmold@alaskan.com

Reserve No. 4 and the exploration program as Pet 4 (Reed, 1958). The Pet 4 program included the drilling of several dozen wells and extensive geophysical and surface geological investigations (Reed, 1958). Cuttings were collected from the test wells at regular intervals and many wells were extensively cored. Lithological descriptions of cuttings and cores were carried out by U.S. Geological Survey geologists Florence Rucker Collins and Florence Robinson and published in the U.S. Geological Survey Professional Paper 305 series. Extensive investigations of the surface geology were summarized in the U.S. Geological Survey Professional Paper 303 series. Umiat 18 was drilled by Linc Energy in 2013 on the south limb of Umiat anticline, in the southeastern corner of the NPRA. Complete, detailed core descriptions accompanied by modern facies analyses are not available in the public domain for these wells. LePain and Kirkham (2001) and LePain and others (2017, 2018) presented core descriptions for selected segments of these wells and discussed implications for the depositional setting and reservoir potential of the Nanushuk in the eastern NPRA. This report presents the complete core descriptions.

The four U.S. Navy wells included in this report were drilled to test Cretaceous strata for oil and each was extensively cored (fig. 2). Fish Creek test well 1, referred to hereafter as Fish Creek 1, located approximately 1.5 miles (2.4 km) northeast of an oil seep, was spudded on May 17, 1949 in the Gubik Formation and reached total depth at 7,020 feet in the Torok Formation (Collins, 1959a; Bird, 1988). During the Pet 4 program, the Nanushuk was not recognized in the well (Collins, 1959b). Fish Creek 1 was sited near the center of a large gravity anomaly and was not drilled on a previously defined structure. The well was considered a stratigraphic test (Reed, 1958). Oil and a small volume of gas were encountered in thin sandstone and siltstone beds separated by beds of clay shale, which are now considered part of the Nanushuk Formation, and a small volume of oil was produced (Collins, 1959a). Square Lake test well 1, referred to hereafter as Square Lake 1, was spudded on January 26, 1952 in the Gubik Formation, and reached total depth at 3,987 feet in the upper Torok Formation (Collins, 1959b; Bird, 1988). Square Lake 1 was drilled to test Cretaceous rocks on an anticline defined by early reflection seismic data and resulted in discovery of a small gas field (Collins, 1959b). Wolf Creek test well 3, referred to hereafter as Wolf Creek 3, was spudded on August 20, 1952 in unconsolidated alluvium, encountered the Nanushuk Formation at a depth of 30 feet, and reached total depth at 3,760 feet in the upper Torok Formation (Collins, 1959b; Bird, 1988). Wolf Creek 3 was drilled on the crest of an anticline defined by surface mapping, with the objectives being to test for oil and gas below the depth of a gas-bearing sand encountered at 1,500 feet in the Wolf Creek 1 well and to better understand facies changes (Collins, 1959b). Minor shows of oil and a small amount of gas were encountered. Grandstand test well 1, referred to hereafter as Grandstand 1, was spudded on May 1, 1952 in unconsolidated alluvium, encountered the Nanushuk Formation at a depth of 110 feet, and reached total depth at 3,939 feet in the Torok Formation (Robinson, 1958; Bird, 1988). Grandstand 1 was drilled on the north limb of the Grandstand anticline to test for petroleum in sandstones of Early Cretaceous age (Robinson, 1958). No shows of oil or gas were encountered. All four test wells are vertical and measured depths equal true vertical depths.

Umiat 18 was spudded on March 10, 2013, in the Gubik Formation, and reached total depth at 2,600 feet measured depth in the Torok Formation (Alaska Oil and Gas Conservation Commission (AOGCC) Umiat 18 well history; fig. 2). The well was drilled on the south limb of Umiat anticline to confirm the presence of producible hydrocarbons (AOGCC Umiat 18 well history). This structure is east-southeast-trending and fault-cored (Herriott and others, 2018), and forms the trap for Umiat field (Molenaar, 1982). Oil was initially discovered at Umiat during the early years of the Pet 4 program and by the end of 1952 eleven test wells had been drilled. Umiat field is estimated to

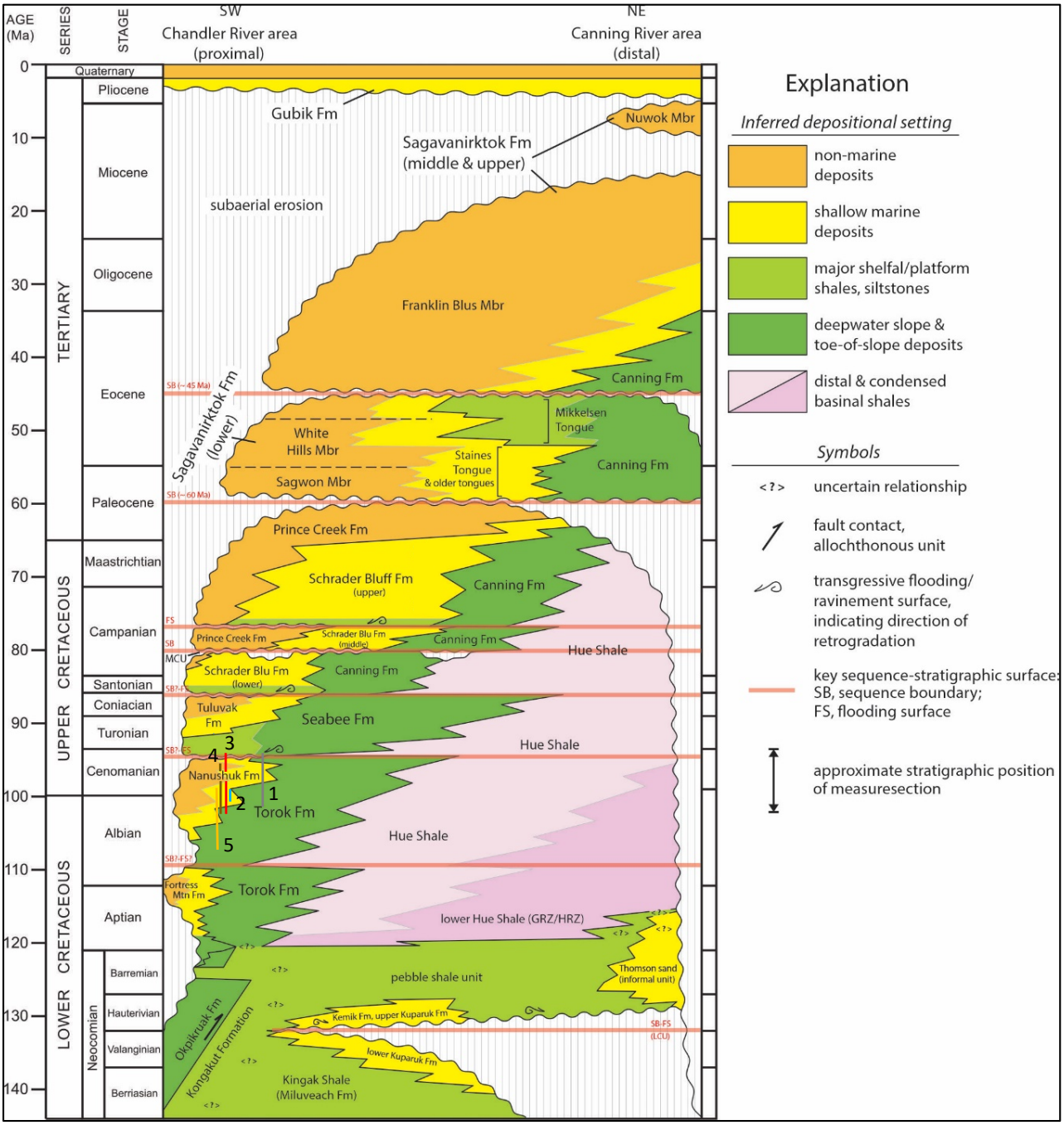

Figure 2. Generalized stratigraphy of the Brookian sequence, central North Slope, Alaska. The Kingak Shale, Kemik sandstone, and pebble shale unit comprise the Beaufortian sequence. The approximate stratigraphic positions of the cores addressed in this report are shown by the vertical lines. The gray line (1), Fish Creek 1; blue line (2), Umiat 18; red line (3), Square Lake 1; brown line (4), Wolf Creek 3; orange line (5), Grandstand 1. Modified from Decker and others (2009).

contain recoverable reserves of 70 MMBO (Molenaar, 1982). Shimer and others (2014) utilized the Umiat test wells from the Pet 4 program to investigate the sedimentology and reservoir properties of the Nanushuk Formation in this field.

GEOLOGIC SETTING

The wells addressed in this report penetrate Cretaceous strata of the Brookian sequence, including significant thicknesses of the Albian-Cenomanian Torok and Nanushuk Formations

(fig. 2). These units comprise genetically related components of a giant clinothem that fills the western two-thirds of an east-west-trending Mesozoic–Cenozoic foreland basin extending from the Alaska-Yukon border in the east to the Chukchi Sea coast in the west, and continuing offshore to the Herald arch (figs. 1 and 3; Bird and Molenaar, 1992; Houseknecht, 2019). The onshore part of the foreland basin, referred to as the Colville basin, is bounded by a subsurface rift shoulder to the north and a north-vergent fold and thrust belt comprising the Brooks Range orogen to the south (figs. 1 and 3). The basin formed in response to the orogenic load and was subsequently filled by detritus shed from it, and from more distant sources on the Chukchi platform and Chukotka (Houseknecht, 2019; Helmold and LePain, 2021, this volume).

The Nanushuk Formation is a succession of complexly intertonguing marine and nonmarine strata interpreted as marine shelf, deltaic, strandplain, fluvial, and alluvial overbank deposits (fig. 2; Ahlbrandt and others, 1979; Huffman and others, 1985, 1988; LePain and Kirkham, 2001; LePain and others, 2009; LePain and Decker, 2016; Houseknecht, 2019). Thickness estimates for the unit range from 9,020 feet in coastal exposures along the Chukchi Sea in the west (Ahlbrandt and others, 1979) to a zero edge approximately 40 mi (65 km) east of Umiat (Houseknecht, 2019; fig. 1). Large river systems flowed east, down the axis of the foreland basin, supplying an enormous volume of sediment to delta, shelf, slope, and basin settings. Transverse rivers with steeper gradients flowed northward and northeastward from the ancestral Brooks Range, supplying sediments to the same range of depositional systems as the east-flowing river systems. The influence of these river systems can be seen on seismic data sets from which a series of eastward younging lowstand shelf margins have been mapped across the onshore east-west extent of the Nanushuk depositional system (fig. 1; Houseknecht, 2019). U/Pb ages on detrital zircons provide absolute age estimates for Nanushuk lowstand shelf margins, which range in age from 115 Ma in the west to 97.9–97.8 Ma (±0.7–1.1 Ma) in the east (Lease and Houseknecht, 2017). In the eastern part of the Nanushuk's depositional extent, shelf margins are sigmoid-shaped,

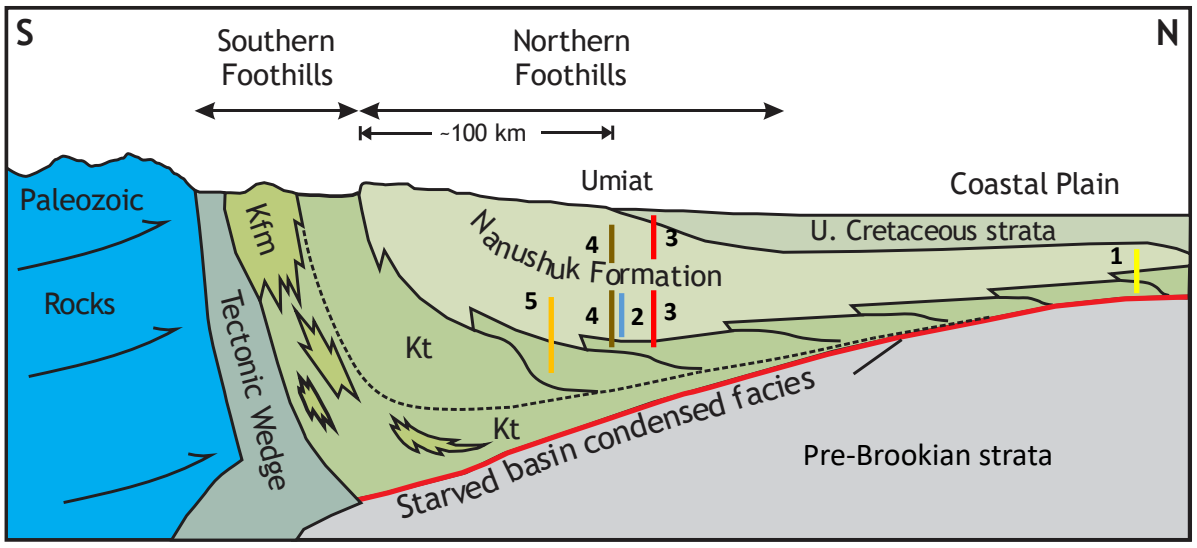

Figure 3. Generalized north-south cross-section through the Colville basin at the approximate longitude of Umiat showing the gross stratal geometries of Lower Cretaceous Brookian formations. The approximate stratigraphic positions of the cores addressed in this report are shown by the vertical lines. Kfm – Fortress Mountain Formation; Kt – Torok Formation. The yellow line (1), Fish Creek 1; blue line (2), Umiat 18; red line (3), Square Lake 1; brown line (4), Wolf Creek 3; orange line (5), Grandstand 1. Modified from Mull (1985) and Houseknecht and Schenk (2001).

trending north-south in the east-central NPRA, curving around to an east-west-trend on adjoining state lands to the south (fig. 1; Houseknecht, 2019, his fig. 5), showing the influence of east- and north-flowing river systems.

Early workers interpreted Nanushuk deltas as river-dominated (Brown and Fisher, 1969, their high-constructive delta model; Ahlbrandt and others, 1979; Huffman and others, 1985, 1988). Despite their river-dominated interpretation, Huffman and others (1985, 1988) recognized a greater wave influence on delta front facies east of the Meade arch. This change in delta style appears to correspond roughly to a pronounced change in shelf margin trajectory recognized in seismic datasets (Houseknecht, 2019). More recently, Nanushuk deltas in the eastern NPRA and in outcrop to the south and southeast have been interpreted as storm wave-influenced, consistent with earlier work (LePain and Kirkham, 2001; LePain and others, 2004; LePain and others, 2009; LePain and others, 2018). Tide-generated features have been observed locally in outcrop and in core, but the successions studied do not show a strong tidal signature overall.

A note of caution is warranted before proceeding. Coastlines that include deltaic depocenters tend to be complex. Coastal depositional systems can vary significantly along strike from deltaic headlands to broad interdistributary areas characterized by non-barred bays, barrier islands and associated back-barrier lagoons, estuaries, and strandplains, depending on the relative importance of sediment supply and river, wave, and tidal energy, which typically vary along strike in response to changes in coastal geomorphology (Boyd and others, 1992). Multiple contemporaneous deltas can vary from river-dominated to wave-dominated depending on their positions along the coastline and whether they face the open ocean or a low-energy coastal embayment, as documented for the Ferron Sandstone (Ryer and Anderson, 2004). A single delta lobe, the product of one progradational episode, can vary from strongly river-dominated to strongly wave-influenced along its progradational trajectory (Ryer and Anderson, 2004). Deltas can also display a distinct asymmetry due to oblique wave approach resulting in greater wave influence on the up-drift side and river influence on the down-drift side (Bhattacharya and Giosan, 2003). There is no reason to expect less complexity in Nanushuk coastal depositional systems.

FACIES ASSOCIATIONS IN CORE

Six facies associations are recognized in the studied cores. Most of the cores presented in this report are from the Nanushuk Formation, but a significant number of Torok cores that were cut in Fish Creek 1 and Grandstand 1 are included. Brief descriptions and interpretations of facies associations are presented here. Core descriptions are presented in sheets 1–5. Lithofacies comprising the six associations are summarized in table 1 and shown on the core descriptions but are not discussed in this report. The ichnofabric index of Droser and Bottjer (1986) is used to qualitatively characterize the degree of bioturbation in cores from Square Lake 1 and Wolf Creek 3; the bioturbation index of Taylor and Goldring (1993) is used to qualitatively characterize the degree of bioturbation in cores from Fish Creek 1 and Umiat 18; bioturbation was not characterized in cores from Grandstand 1. Specific ichnogenera identified while describing the cores are shown on the core descriptions at the depths where they were encountered. A similar suite of facies associations has been recognized in Nanushuk outcrops and in cores from Wainwright 1, and are described in detail, along with component facies, by LePain and others (2009) and LePain and Decker (2016). Photographs of core boxes from Fish Creek 1, Wolf Creek 3, Square Lake 1, and Grandstand 1 are from D'Agostino and Houseknecht (2002). Core box photographs of Umiat 18 were shot by Weatherford Laboratories for Linc Energy and are available from the Alaska Geologic Materials Center. All depths mentioned in this report and shown on sheets 1–5 are measured depths from the top

Table 1. Summary of facies recognized in core from the Nanushuk Formation, Fish Creek 1, Square Lake 1, Wolf Creek 3, Grandstand 1, and Umiat 18, eastern NPRA.

Facies		Characteristics	Trace Fossils	Bioturbation Index (BI)	Ichnofabric Index (II)	Process Interpretation
Fl	Laminated mudstone	Dark gray to brown claystone, siltstone, and mixtures of clay and silt; plane-parallel laminated, locally developed fissility; appears unbioturbated. Minor interbedded coarse siltstone and very-fine-grained sandstone. Typically in undisturbed beds, but present locally in packages with apparent dips up to 25 degrees from paleohorizontal.	No trace fossils	0	1	Suspension settling in low-energy, subaqueous settings. Fissility due to subparallel alignment of clay particles resulting from burial-related compaction. Coarser-grained siltstone and very-fine-grained sandstone interbeds record deposition from episodic unidirectional currents and, in shallow marine settings, subsequent local reworking by short-period waves. Absence of bioturbation records stressed depositional setting due either to high sediment flux, low dissolved oxygen levels in bottom waters, or a combination of both factors. Dipping strata associated with small slide blocks.
Flb	Laminated bioturbated mudstone	Similar to Fl, but with slightly to moderately disrupted laminae due to sparse to moderate bioturbation. Intermediate between Fl and Fm.	Discrete trace fossils commonly visible, including *Phycosiphon* and *Palaeophycus*	1–4	2-4	Suspension settling in low-energy, subaqueous settings. Coarser-grained siltstone and very-fine-grained sandstone interbeds record deposition from episodic unidirectional currents and subsequent local reworking by short-period waves. Oxygenated bottom waters supported a diverse burrowing infauna.
Fm	Massive mudstone	Medium gray to brown clay shale, claystone, siltstone, and mixtures of clay and silt; lacks fine-scale laminations; blocky fabric and orange-brown siderite nodules are common; mottled appearance due to bioturbation, occassional vertical traces filled with coarser sediment.	Typically no discrete traces recognizable; vertical traces locally	1–5?	2-5?	Clay shale, claystone and fine siltstone deposited from suspension in low-energy, subaqueous settings. Coarser silt deposited from density underflows. Mottled appearance suggests sediment disruption by burrowing organisms in oxygenated setting.
Fc	Coal and carbonaceous mudstone	Thin coaly stringers up to 0.2 feet thick and carbonaceous mudstones; coals commonly include high ash content.	Discrete trace fossils rare	0-1	1-2	Low-lying, minor peat accumulations and/or rafted peat mats.
Sr	Ripple cross-laminated sandstone	Light gray to beige coarse siltstone to fine-grained sandstone in beds up to a foot or more thick; locally includes muddy foreset laminae with relatively abundant plant detritus; uniform foreset dip direction; locally preserved, small, asymmetric ripple bedforms. Rhizoliths are locally preserved.	*Skolithos*; rare *Thalassinoides*?	0–3	1-3 or 4	Deposition from unidirectional currents in which equilibrium current ripple bedforms developed and migrated down-current. Where rhizoliths have been recognized, deposition occurred in shallow water or the beds were subsequently exposed.
Swr	Ripple cross-laminated sandstone	Light gray to beige coarse siltstone to very fine-grained sandstone in beds up to 1 foot thick; locally preserved wave ripple bedforms and complex, bundled sets with scalloped lower set boundaries.	*Skolithos*	0-2	1-2	Reworking of silt and sand by short-period waves in shallow, subaqueous setting.
Sx	Cross-bedded sandstone	Light gray to light brown, fine- to medium-grained sandstone with foreset laminae dipping 10–25 degrees relative to paleohorizontal; foresets appear planar and in sets from 0.3 to greater than 1 ft thick.	No trace fossils	0	1	Deposited from steady, unidirectional flows in which equilibrium dune bedforms developed; foresets record down-current migration of bedforms.

Table 1, continued. Summary of facies recognized in core from the Nanushuk Formation, Fish Creek 1, Square Lake 1, Wolf Creek 3, Grandstand 1, and Umiat 18, eastern NPRA.

Facies		Characteristics	Trace Fossils	Bioturbation Index (BI)	Ichnofabric Index (II)	Process Interpretation
Sl	Plane-parallel laminated very fine to fine-grained sandstone	Light gray to light brown, moderately to well sorted, very-fine- to fine-grained sandstone in beds from 0.01 to greater than 1 ft thick displaying plane-parallel to gently wavy lamination; parting lineation visible locally. Some alternating sandstone and organic-rich silty sandstone laminae.	*Skolithos*, locally developed escape structures	0–3	1-3 or 4	Deposited under upper flow-regime conditions, most likely from unidirectional flows. Alternating sandstone and organic-rich silty sandstone laminae record fluctuating current strength, possibly related to tides. Where associated with HCS, may record deposition from combined flows.
Sm	Massive sandstone	Light gray to light brown, very-fine- to medium-grained sandstone characterized by an apparent lack of sedimentary structures; locally includes pebbles of gray chert, siderite, and mudstone rip-ups.	Locally burrow mottled	0–4	1-4	Records high sediment supply and/or rapid deposition with no subsequent traction transport.
Shcs	Hummocky/ swaley cross-stratified sandstone	Light gray to light brown, very fine- to fine-grained sandstone characterized by low-angle laminae dips, dip direction changes over short vertical distances (from inches up to one foot), low-angle laminae truncations below flat laminae to laminae dipping at low angles in opposite direction; parting lineation prominent locally. Where tentatively identified, swaley cross-stratification is shown on the core descriptions with a symbol and in the facies column as Sscs.	*Palaeophycus*, *Skolithos*, *Schaubcylindrichnus*, fugichnia	0-1?	1-2?	Records sediment reworking and deposition from waning, oscillatory-dominant combined flows above storm wave-base in marine setting.
Scb	Convolute laminated sandstone	Light gray to light brown, very-fine- to fine-grained sandstone in beds from 0.01 to greater than 1 ft thick; bedding and internal stratification, if present, are deformed and characterized by irregular, chaotic folds and steep bed/laminae dips; beds commonly broken.	*Thalassinoides*, *Teichichnus*, and *Skolithos*	0–3?	1-3?	Soft-sediment deformation. Several possible mechanisms, but given context likely due to rapid deposition on muddy, water-rich substrates.
Sb	Burrow-mottled sandstone	Light gray to light brown, very-fine- to fine-grained sandstone in beds from 0.02 to 0.6 ft thick characterized by extensive intense bioturbation.	*Phycosiphon*, *Skolithos*, *Teichichnus*, and *Thalassinoides*; possible *Diplocraterion* and *Rosselia*	3–5	3-5	Reworking of sand beds at or very near the depositional surface by burrowing organisms in a marine or marine-influenced setting.
SFl	Heterolithic sandstone and mudstone	Light gray to light brown coarse siltstone/very-fine- to fine-grained sandstone and dark gray to dark brown mudstone; sandstone and mudstone are thinly interbedded, beds from 0.01 to 0.5 ft thick.	*Skolithos*	0–3	1-3 or 4	Deposited under fluctuating energy conditions. Coarse silt and sand transported to depositional site as bedload and mudstone as suspended load.

Bioturbation index is from Taylor and Goldring (1993); Ichnofabric index is from Droser and Bottjer (1986). When our work on these core began in 2000 we used Droser and Bottjer's scheme (Wolf Creek 3 and Square Lake 1 test wells). When the Fish Creek and Umiat 18 cores were described in 2017 and 2018, we used Taylor and Goldring's scheme as it had become more widely used by sedimentologists.

of the Kelly bushing. Available information indicates the four test wells are vertical wells; Umiat 18 is slightly deviated (at total depth the measured depth in 2,600 feet whereas the true vertical depth is 2,515.36 feet).

Facies association 1 – Slope

Description – Facies association 1 (FA1) consists mostly of massive to thinly laminated, dark brown-gray to gray clay shale, silty clay shale, and mudstone (fig. 4A). Thin laminations are locally well-developed and defined by subtle color variations (lighter brown-gray to gray laminae alternating with darker laminae). Laminae of light to medium gray siltstone and very fine-grained sandstone are locally present and typically range in thickness from less than 0.01 feet to 0.1 feet (fig. 4B); sandstone in beds up to a few feet thick are rare (sheet 1, 6003.5–6007.1 feet). Siltstone and sandstone are either massive, internally laminated, or current ripple cross-laminated, and some laminae include two or three of these structures in an organized vertical sequence representing nearly complete to partial Bouma sequences (Tabcd, Tacd, Tbcd, Tb, Tcd) (fig. 4C). Fine-scale stratigraphy is generally undisturbed, except for locally developed convolute laminae and micro-load structures on the undersides of some coarser siltstone and very fine-grained sandstone laminae (fig. 4D). Visible indications of bioturbation, including discrete trace fossils and obvious bioturbation fabrics, are absent (BI 0?). In Fish Creek 1, bedding attitudes range from flat-lying to gently dipping (up to 10 degrees; fig. 4A). Some cores in the lower part of the cored interval from Grandstand 1 include dramatic examples of FA1 in which laminae dip up to 25 degrees from paleohorizontal throughout the vertical extent of the core (figs. 4E and 25). FA1 has only been recognized in Fish Creek 1 and Grandstand 1, where it comprises most of the cores from the Torok Formation (sheets 1 and 5).

Interpretation –FA1 was deposited in a slope setting from suspended plumes of fine-grained sediment discharged from deltaic distributaries

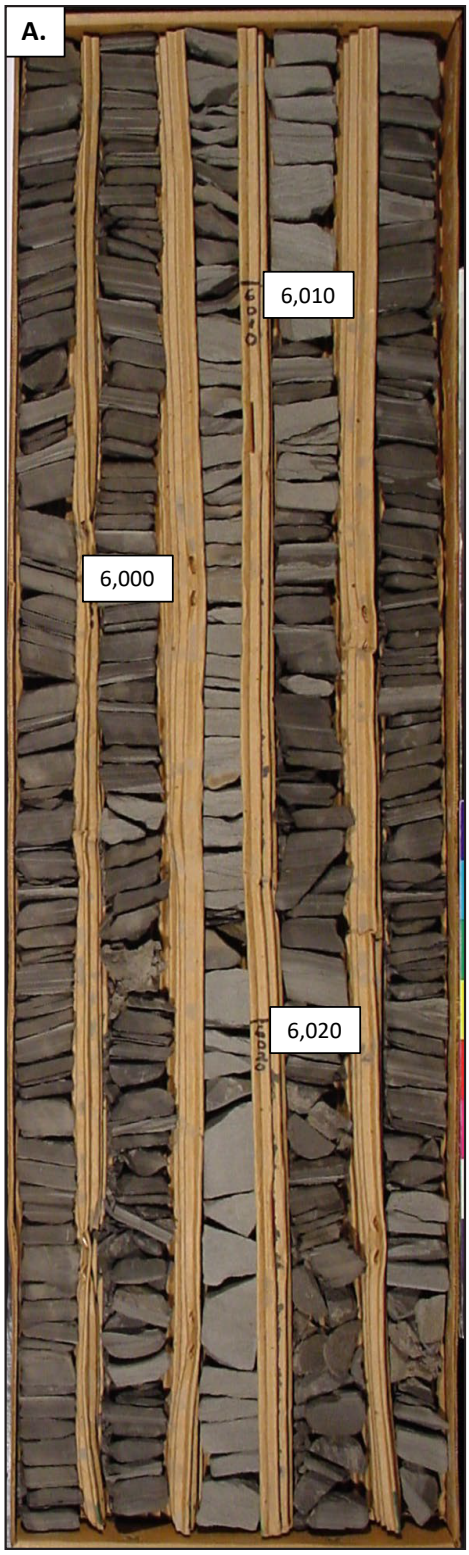

Figure 4. Photographs showing characteristics of FA1. **A.** Core box photograph showing the succession of silty clay shale, siltstone, and minor very fine-grained sandstone in the Torok between approximately 6,022–5,578 feet in Fish Creek 1. Each core row is 3.28 feet (1 meter) long. Core box photograph modified from D'Agostino and Houseknecht (2002).

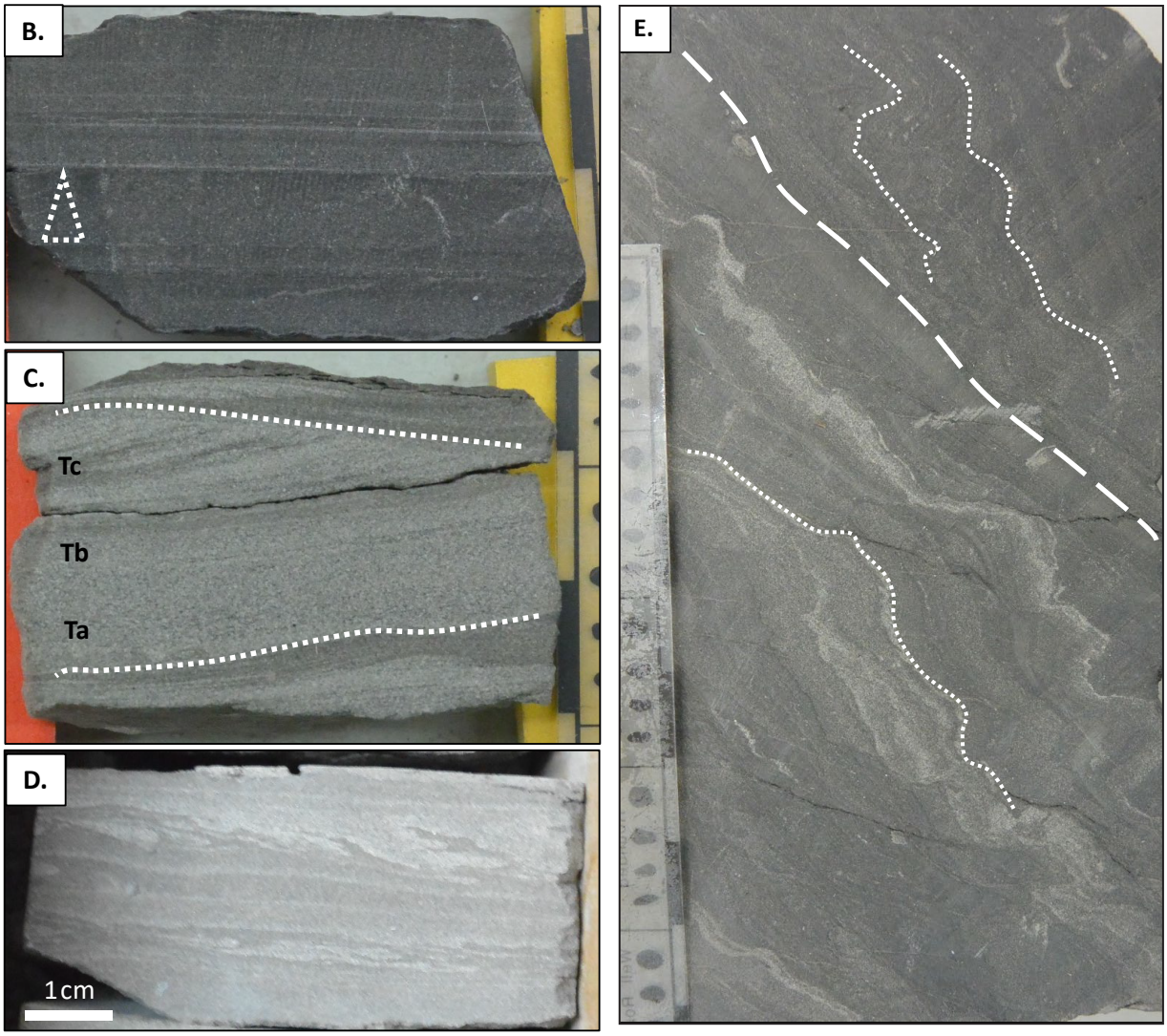

Figure 4. B. Laminae in the Torok Formation at 6,011.3 feet in Fish Creek 1. Note normal size grading in several laminae grading from fine siltstone to silty claystone. **C.** Very fine-grained sandstone with Bouma Tabc divisions at 5,582.4 feet in Fish Creek 1. **D.** Small-scale flame structures near the base of siltstone bed at 5,544.7 feet in Fish Creek 1. Horizontal white bar is 0.39 inches (1 cm) long. **E.** Dipping laminae of silty clay shale and siltstone at 3,738 feet in Grandstand 1. Dashed white line (long dashes) shows contact between two packages of strata dipping at slightly different angles (white dotted lines). Scale in all photos graduated in centimeters.

up-dip to the west and southwest (Houseknecht and Schenk, 2001). Laminated mudstones were deposited from fluid mud layers or very dilute turbidity currents. Coarser-grained laminae and beds of siltstone and sandstone with complete and partial Bouma sequences represent dilute turbidites, possibly related to the distal reaches of hyperpycnal flows (Mulder and others, 2003). Houseknecht and Schenk (2001) noted that bioturbation in slope mudstones of the Torok is rare, consistent with the absence of bioturbation fabrics in facies association 1. Packages of dipping laminae in Grandstand 1 are interpreted to be part of small slide blocks.

Facies association 2 – Distal Shelf

Description – Facies association 2 (FA2) consists of medium brown-gray to gray clay shale, silty clay shale, and mudstone. Medium to light gray to light brown siltstone and very fine-grained sandstone are common to abundant in solitary laminae (less than 0.01 feet thick) and thin beds up to approximately

0.3 feet thick (fig. 5A); siltstone and sandstone also comprise horizontally laminated successions up to 10 feet thick (sheet 1, 3,171–3,181 feet). Internally, siltstones and sandstones are massive to horizontally laminated (fig. 5B, Sheet 1, Fish Creek 1 3,378.2 feet); ripple cross-laminations are present locally, as are graded laminae. Fine-grained carbonaceous material is concentrated along the top of some siltstone and sandstone laminae, and most are slightly micaceous. The degree of bioturbation in mudstone,

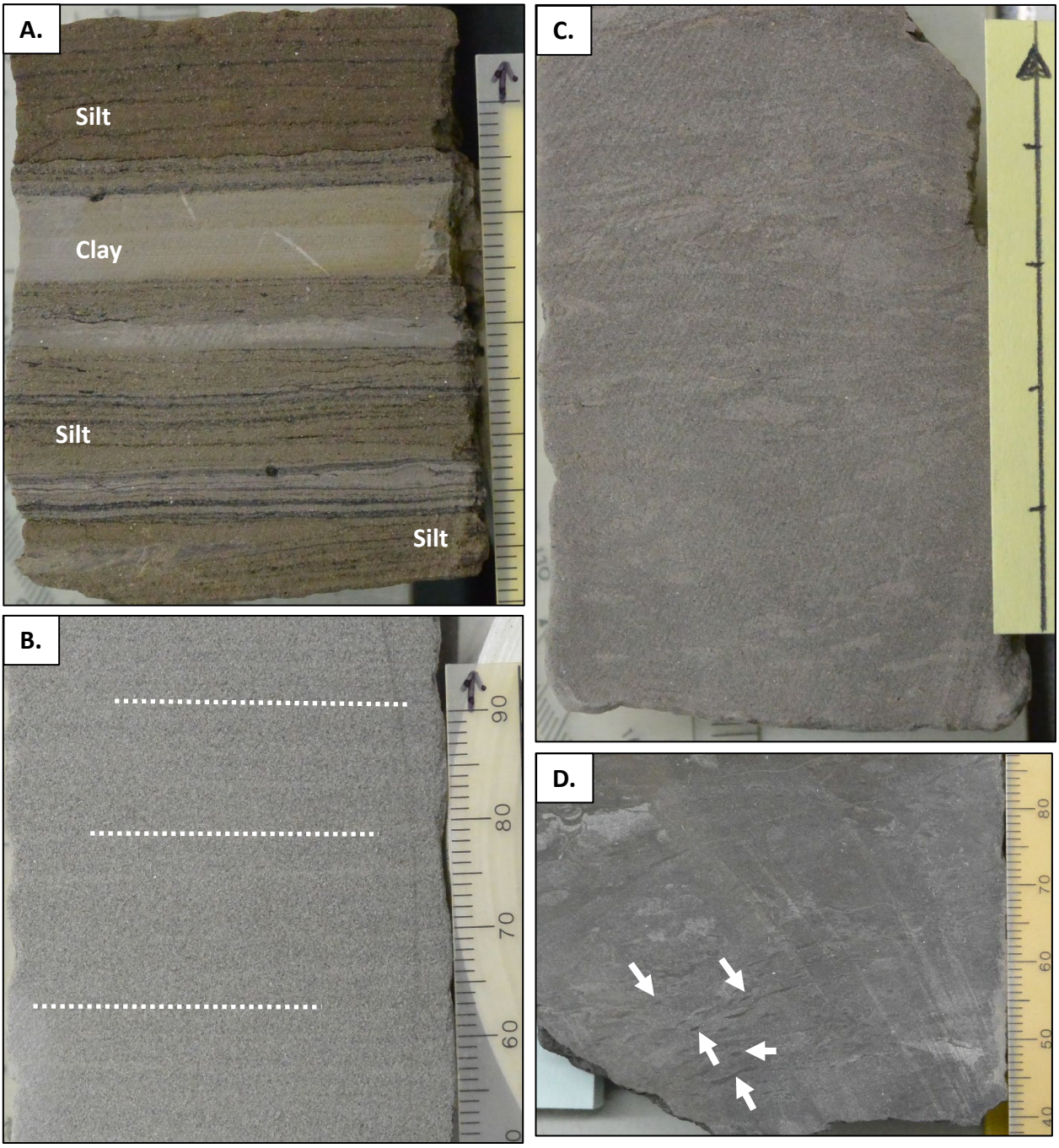

Figure 5. Photographs showing characteristics of FA2. **A.** Undisturbed siltstone and claystone laminae at 2,977 feet in Fish Creek 1. Brown color in siltstone due to residual oil. BI 0. **B.** Unbioturbated, faintly laminated siltstone at 3,384 feet in Fish Creek 1. BI 0. **C.** Bioturbated mudstone at 2,963.2 feet in Fish Creek 1. BI 3–4. Bioturbation appears to be absent, or rare, in Torok slope deposits and is common in the distal shelf facies. **D.** Burrow-mottled mudstone at 3,742 feet Wolf Creek 3. Note Phycosiphon burrows near base of core (white arrows). BI 4-5. Visible scale in all photographs in centimeters; scale in A, B, and D also graduated in millimeters.

siltstone and sandstone ranges from absent (figs. 5A–B, BI 0) to intense (figs. 5C–D, BI 4–5), but is typically absent to moderate (BI 0–3). Bioturbation appears to define a distal *Cruziana* ichnofacies. FA2 differs from FA1 by the greater number of thin siltstone and sandstone laminae and the common presence of bioturbation. FA2 comprises most of the Nanushuk cores in Fish Creek 1 (sheet 1, 3,981–2,700 feet) and is common in the deeper cores from Wolf Creek 3 (sheet 2, 3,740–3,746 feet), Square Lake 1 (sheet 3, 3,910–3,987 feet), and Grandstand 1 (sheet 5, 2,694–2,710 feet). Based on Collins' (1959b) cuttings descriptions, this association is likely common in many of the deeper uncored intervals in Wolf Creek 3, Square Lake 1, and Grandstand 1. FA2 is likely gradational above FA1, except where associated with sea level lowstands.

Interpretation – FA2 was deposited in a distal shelf setting, below storm wave base. Clay shale, silty clay shale, and mudstone were deposited from plumes of suspended sediment discharged from deltaic distributaries and from plumes of fine-grained sediment re-suspended by major storms affecting the Nanushuk shelf. Siltstone and very fine-grained sandstone were deposited from frequent dilute shelf turbidity currents (turbidites; Mulder and Alexander, 2001) and possibly hyperpycnal flows (hyperpycnites; Mulder and others, 2003; Bhattacharya and MacEachern, 2009) that reached middle to outer shelf settings. Some examples of FA2 could have been deposited in upper slope settings during sea level lowstands. We recognize that distal shelf and slope settings can include similar processes and facies, making it difficult to differentiate successions deposited in these settings without seismic data.

Facies association 3 – Offshore Transition—Prodelta

Description – Facies association 3 (FA3) consists of interbedded mudstone, siltstone, and very fine- to fine-grained sandstone commonly forming the lower part of sandier-upward successions (fig. 6A, above 3,908 feet, and fig. 6B). Silty clay shale is present locally as a minor component. Mudstone beds are dark to medium gray, range in thickness from 0.01 feet to over 1 foot, and include a variety of facies, including horizontally laminated, current and wave ripple cross-laminated, and highly bioturbated beds (table 1). Siltstone and sandstone are medium to light gray and occur as thin laminae and beds ranging in thickness from less than 0.01 foot to approximately 1.5 feet. Sandstone is moderately- to well-sorted and bounding contacts tend to be sharp and planar, or sharp with minor erosional relief. Some beds include features found in dilute turbidites (Tabc, Ta, Tab, Tbc, Tc beds; fig. 7A, stacked Ta laminae, and fig. 8A, solitary Tab bed marked by white triangle). Horizontal, plane-parallel lamination, current ripple cross-lamination (fig. 7B), wave-ripple cross-lamination (fig. 7C), and soft-sediment deformation features (fig. 7D) are common to abundant in siltstone and sandstone. In some sandstone beds, horizontal laminations grade up- and down-section over short stratigraphic distances (less than a foot) to gently dipping laminations, and lamina dip directions commonly reverse, suggesting the presence of hummocky cross-stratification (HCS; fig. 7E, Square Lake 1, approximately 3,595 feet). Bioturbation in mudstone is generally moderate to intense (BI 3–5; figs. 8A–D), and is sporadic in siltstone and sandstone, ranging from absent (fig. 7E, BI 0) to intense (BI 4–5; figs. 8C and E). Where present in the latter lithology, bioturbation is greatest in the uppermost part of beds (0.05 to 0.2 feet; fig. 8E), but can extend through the entire thickness of thinner beds (fig. 8C). Bioturbation defines a *Cruziana* ichnofacies and discrete traces are commonly recognizable, including *Planolites*, *Palaeophycus*, *Schaubcylindrichnus*, *Phycosiphon*, *Teichichnus*, and *possible Rosselia and Chondrites* (figs. 8A–E).

FA3 differs from FA2 in the greater abundance of sandstone beds, paucity of clay shales, and greater variety of sedimentary structures. FA3 is common in cores from the lower part of the Nanushuk in Wolf Creek 3, Square Lake 1, Grandstand 1 and Umiat 18 (sheets 2–5), and is also present in cores

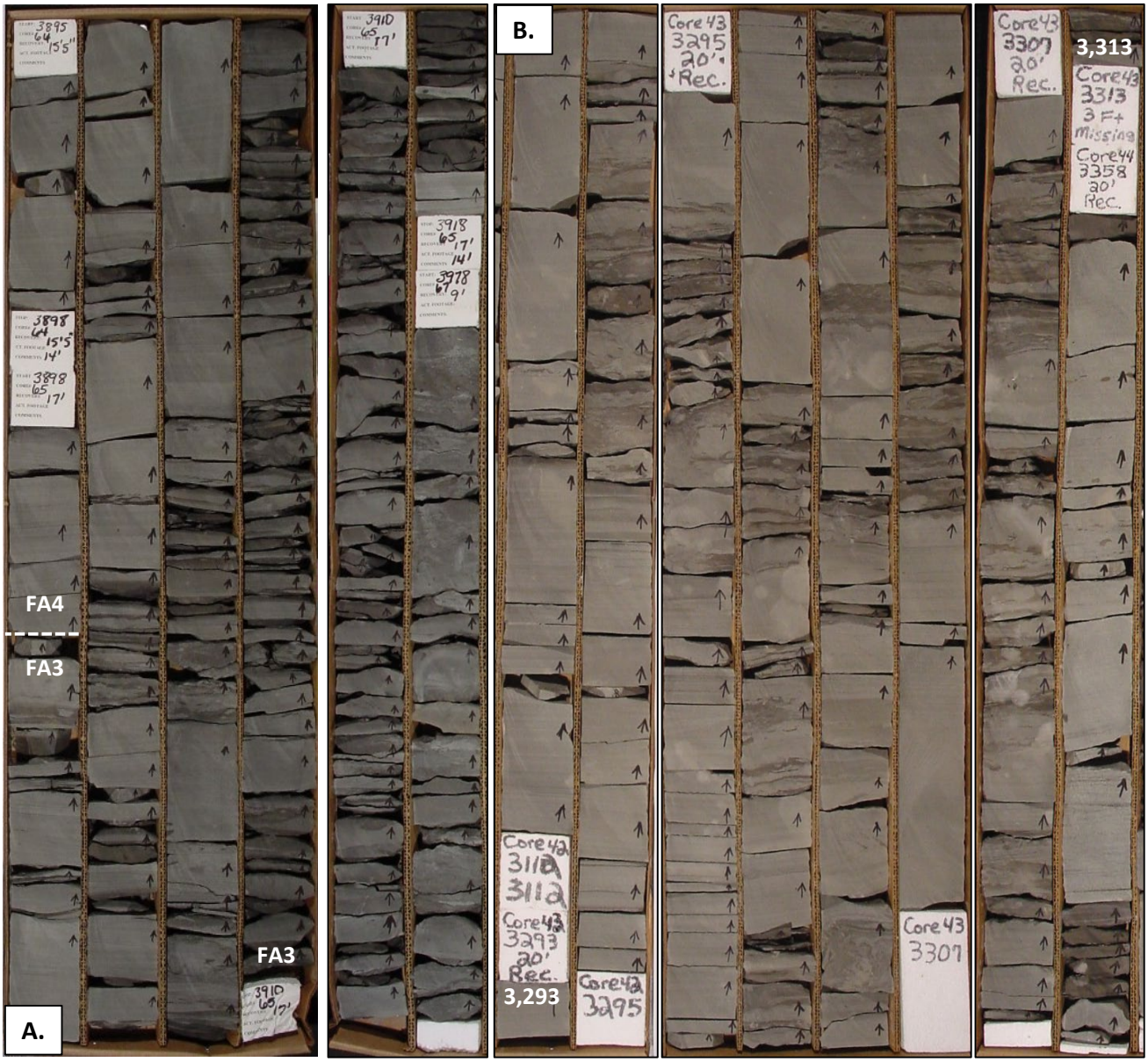

Figure 6. Core box photographs showing gross lithologies in FA3. **A.** Cored part of a coarsening-upward parasequence from 3,898.5 feet (white dashed line) to 3,910 feet (FA3 label bottom center of box) in Square Lake 1 assigned to FA3 showing lithologic characteristics. In distal settings FA2 commonly grades up-section to FA3, and the two associations differ in the greater number of sandstone interbeds in the latter. **B.** Cored part of a coarsening-upward parasequence consisting of FA3 from 3,293 feet to 3,313 feet in Wolf Creek 3. Cuttings and the SP log suggest FA3 forms part of the base of a parasequence that continues up-section to approximately 3,120 feet (Sheet 6). Each core row is 3.28 feet (1 meter) long. Core box photos modified from D'Agostino and Houseknecht (2002).

from the upper part of the formation in Square Lake 1 (sheet 3). Based on cuttings descriptions (Collins, 1959b; Robinson, 1958), this association is likely common in the intervening uncored intervals in Wolf Creek 3, Square Lake 1, and Grandstand 1. FA3 is gradational above FA2.

Interpretation – In the Wolf Creek 3 and Square Lake 1 cores, FA3 includes facies elements common to wave-influenced offshore transition settings (see Walker and Plint, 1992; Reading and Collinson, 1996), but also includes features typically found in river-dominated proximal prodelta

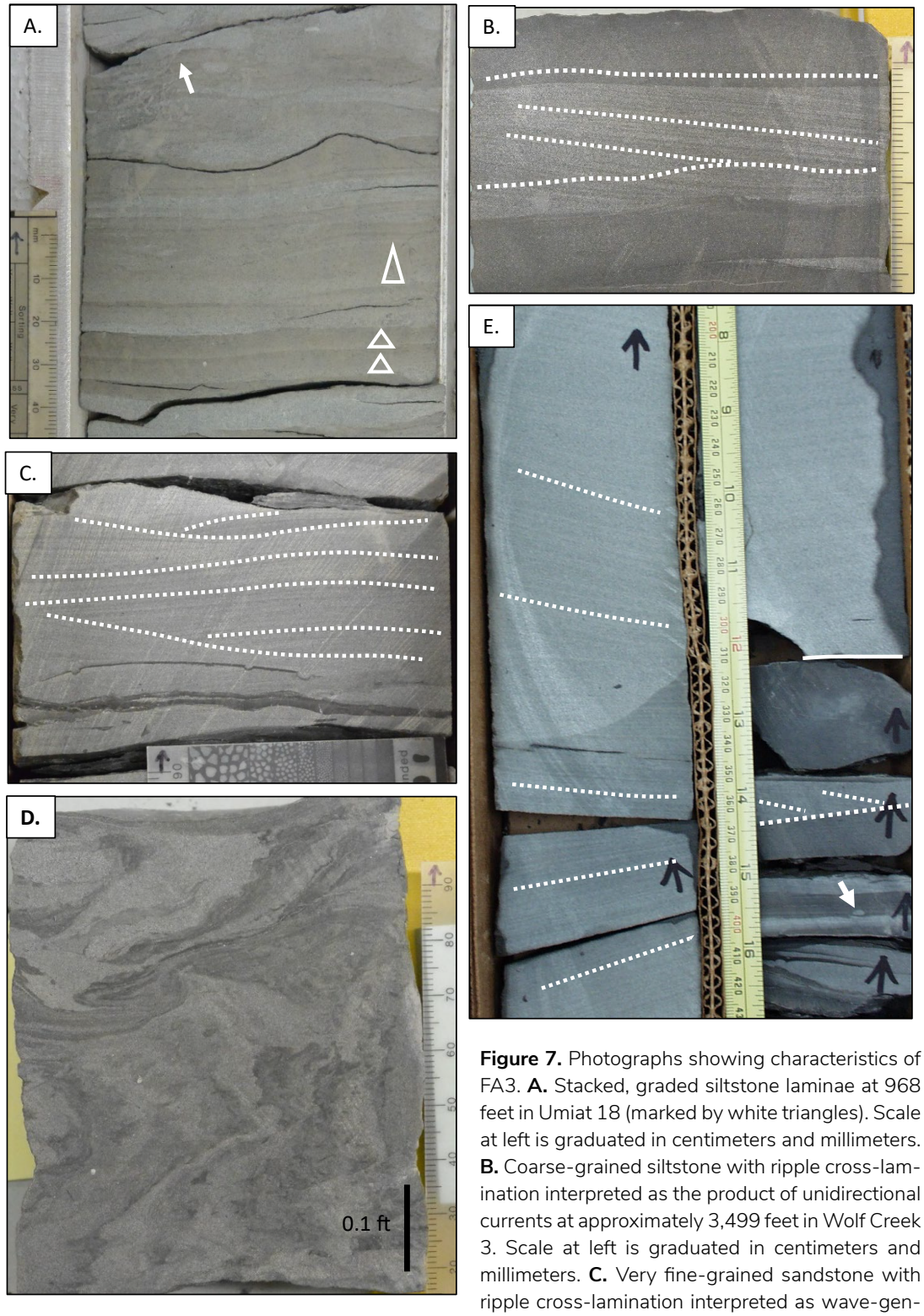

Figure 7. Photographs showing characteristics of FA3. **A.** Stacked, graded siltstone laminae at 968 feet in Umiat 18 (marked by white triangles). Scale at left is graduated in centimeters and millimeters. **B.** Coarse-grained siltstone with ripple cross-lamination interpreted as the product of unidirectional currents at approximately 3,499 feet in Wolf Creek 3. Scale at left is graduated in centimeters and millimeters. **C.** Very fine-grained sandstone with ripple cross-lamination interpreted as wave-generated at 2,692.7 feet in Wolf Creek 3. Grain size card is 5 cm wide. **D.** Soft-sediment deformed siltstone and darker colored mudstone at 3,305 feet in Wolf Creek 3. Scale at left is graduated in centimeters and millimeters. **E.** Plane lamination in a sandstone bed at approximately 3,595 feet in Square Lake 1. Note the low-angle dip of laminations and the gradual change in dip direction from the base of the photograph to the top in the core to the left of the yellow tape measure. These dip changes are attributed to HCS. The core to the right of the tape measure (above solid white line) is a sandstone with very subtle changes in lamina dip angles, which are also attributed to HCS. Yellow tape measure is graduated in inches (right side) and centimeters (left side).

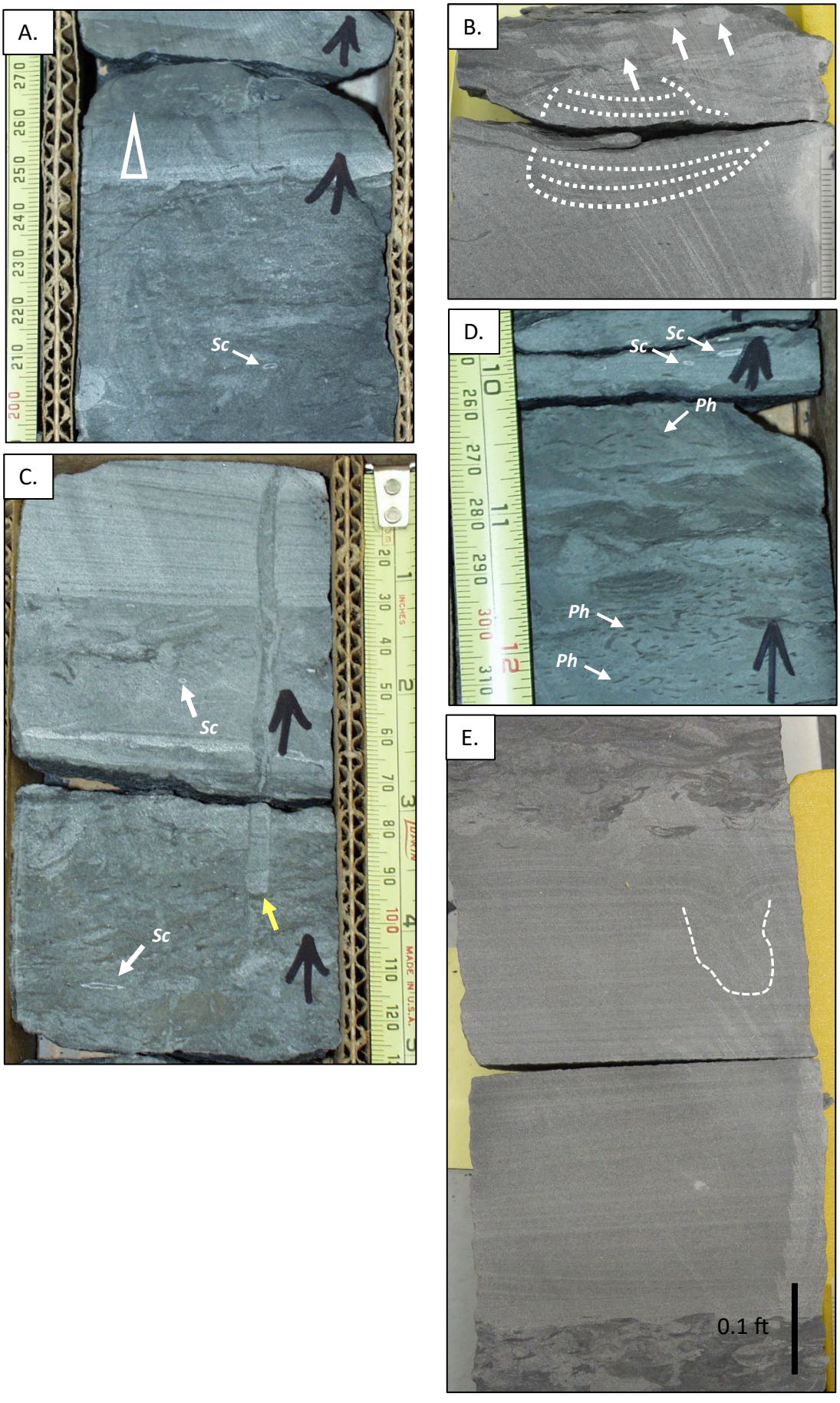
A.
Sc
B.
D.
Sc
Sc
Ph
Ph
Ph
C.
Sc
Sc
E.
0.1 ft

successions (see Scott and Fisher, 1969; Galloway and Hobday, 1996; Bhattacharya, 2006). In these wells, FA3 is classified as undifferentiated offshore transition—prodelta. In the Umiat 18 and Grandstand 1 cores, FA3 lacks abundant wave-generated structures and includes elements more typically ascribed to river-dominated prodelta successions and are shown as prodelta deposits.

In cores from Wolf Creek 3 and Square Lake 1, the abundance of sedimentary structures attributable to deposition under upper flow regime conditions and waning oscillatory flows suggest storm-related deposition (tempestites) between fairweather and maximum storm wave base in offshore transition and wave-influenced prodelta settings (Walker and Plint, 1992; Reading and Collinson, 1996). Thin beds resembling Bouma Ta, Tab, and Tac suggest deposition from thin, concentrated density flows, whereas Tbc and Tc beds suggest deposition from dilute turbidity currents (hyperpycnal flows?), with both flow types emanating directly from distant distributary channels (Mulder and others, 2003; Bhattacharya and MacEachern, 2009; Olariu and others, 2010), or originating from the failure of distributary mouth bars (Bhattacharya, 2006). Interbedded mudstone was deposited during the waning stages of storm events and from plumes of suspended fine-grained sediment discharged from deltaic distributaries. During ensuing fairweather conditions, burrowing organisms colonized muddy substrates, resulting in pervasive disruption of original depositional fabrics.

In contrast to offshore transition-prodelta deposits in the Wolf Creek 3 and Square Lake 1 wells, FA3 in Umiat 18 and Grandstand 1 includes coarse silt and very fine-grained sand deposited from density underflows that emanated from distributaries during flood events as frontal splays and, possibly, hyperpycnal flows that resemble dilute turbidites, and are interpreted as prodelta deposits (Galloway and Hobday, 1996; Mulder and others, 2003). The high sediment supply and freshwater flux created a high-stress environment which suppressed the activity of burrowing organisms (MacEachern and others, 2005). Wave-formed sedimentary structures are not common in FA3 in cores from these wells and bioturbation is more variable than in the Wolf Creek 3 and Square Lake 1 cores, which is consistent with deposition in more river-dominated prodelta settings (sheets 4 and 5).

Facies association 4 – Shoreface—Delta Front

Description – Facies association 4 (FA4) consists of sandier-upward successions up to 88 feet thick that typically start with thinly interbedded mudstone and very fine-grained sandstone, grading up-section to amalgamated light tan to light gray, very fine- to fine-grained sandstone. Mudstone is gray to dark gray and ranges from unbioturbated to pervasively bioturbated (figs. 9A–B). The narrow range of grain

Figure 8, previous page. Core photographs showing bioturbation in FA3 in cores from Wolf Creek 3 and Square Lake 1. **A.** Moderately to highly bioturbated mudstone at 3,902 feet in Square Lake 1, Note pervasive bioturbation in mudstone and the solitary *Schaubcylindrichnus* burrow (white Sc). Discontinuous black streaks visible in vicinity of the Schaubcylindrichnus burrow are *Phycosiphon* burrows. Note also normal size grading in the fine-grained sandstone near the top of the photograph (white triangle). Tape measure graduated in centimeters. **B.** *Teichichnus* burrow in ripple cross-laminated sandstone at 2,183.5 feet in Wolf Creek 3. Scale at right graduated in millimeters. **C.** Interbedded very fine-grained sandstone and intensely bioturbated mudstone at 3,217 feet in Square Lake 1. Sandstone is wave-ripple cross-laminated. Note the escape burrow extending from the mudstone upward through the overlying sandstone bed (yellow arrow marks base of burrow). Tape measure graduated in inches (right side) and centimeters (left side). **D.** *Phycosiphon (Ph)* and *Schaubcylindrichnus (S)* burrows in sandstone interbedded with dark gray mudstone at 3,221 feet in Square Lake 1. Note, most Phycosiphon burrows are unlabeled. Tape measure graduated in inches (right side) and centimeters (left side). **E.** Interbedded very fine-grained sandstone and mudstone at 3,302.5 feet in Wolf Creek 3. Mudstones are highly bioturbated (BI 3-4) and include irregular shaped patches of sandstone. The sandstone bed has sharp bounding contacts with mudstone – the lower contact is characterized by micro-relief due either to turbulent scour or loading, whereas the upper contact is highly disrupted due to burrowing organisms and the degree of bioturbation decreases abruptly downward in the sand bed (BI 2-3 to BI 0-1). The bioturbated upper mudstone likely records the near total disruption of the upper part of the sandstone bed. Note the re-burrowed burrow (outlined by dashed white line), and downward deflected laminations above it, near the right edge of the photo in the sandstone bed.

sizes present in sandstone makes identification of individual event beds in amalgamated successions difficult in some cores, unless mudstone rip-up clast lags or prominent scour surfaces associated with slight color changes are present (figs. 9C–D). Normally graded sandstone beds are common in the lower part of FA4, where they are interbedded with mudstone. Sandstone throughout the association most commonly include massive beds, beds with plane-parallel horizontal laminae, and low-angle dipping laminae, but cross-bedding and current- and wave-ripple cross-lamination are present locally. Mudstone rip-ups are common and locally sideritic (figs. 9C–D). Soft-sediment deformation is common in sandstone beds in the lower part of the association. Low-angle dipping laminae similar to low-angle laminations described in FA3, in which dip directions change gradually up and down the core are common and similarly attributed to HCS (figs. 10A–D). Macerated terrestrial plant debris is common and ranges from few fragments on parting surfaces to abundant debris covering these surfaces. Locally, laminae are accentuated by abundant macerated plant material and larger coalified fragments appear jumbled together in some beds. Broken and abraded *Ditrupa* and pelecypod fragments are locally common (fig. 11A). Bioturbation defines a mixed *Cruziana—Skolithos* ichnofacies, and ranges from sparse to intense (BI 1–5), decreasing progressively toward the top of the association, where it is generally absent to low (BI 0–2) in examples from distal settings, and is absent to sparse (BI 0–1) in more proximal settings. Recognizable ichnogenera include *Planolites* (fig. 11B), *Palaeophycus* (figs. 11C–D), *Schaubcylindrichnus (*fig. 9D*), and Macaronichnus* (fig. 11E); *Asterosoma* and *Teichichnus* are rare (fig. 11F). Escape traces are present locally as are re-burrowed burrows (figs. 11C–D). In some cores, notably Umiat 18, the plane-parallel laminations appear fuzzy and indistinct, resembling cryptobioturbation (MacEachern and others, 2005). FA4 is gradational above FA3 and is common in cores from Wolf Creek 3, Square Lake 1, Grandstand 1, and Umiat 18 (sheets 2–5).

Interpretation – In the Wolf Creek 3 and Square Lake 1 cores, FA4 includes facies elements common to both shoreface and delta front settings (Walker and Plint, 1992; Bhattacharya, 2006; Clifton, 2006), and is interpreted as a progradational storm wave-modified delta front succession. On the core descriptions, most examples of this association are labeled shoreface-delta front, unless there are clear facies criteria for interpreting the succession as a more typical high-energy shoreface (Walker and Plint, 1992; Ryer and Anderson, 2004; Clifton, 2006) or river-dominated delta front succession (Scott and Fisher, 1969; Bhattacharya and Walker, 1991; Ryer and Anderson, 2004; Bhattacharya, 2006).

FA4 in Wolf Creek 3 and Square Lake 1 includes abundant horizontal laminae interbedded with gently dipping laminae interpreted as HCS. The combination of both types of laminae in vertical succession within a single bed (Sl→Shcs) suggest event deposition from waning oscillatory flows associated with long-period storm waves (Duke and others, 1991). The abundance of trace fossils and sporadic occurrence of broken and abraded pelecypod shell fragments are common elements of high-energy shoreface successions.

Figure 9, next page. Photographs showing selected characteristics of FA4 in Wolf Creek 3 and Square Lake 1. **A.** Very fine-grained sandstone with thin mudstone interbeds in lower shoreface-distal delta front deposits at 2,034 feet in Wolf Creek 3. The disrupted mudstone laminae with patches of sandstone are likely a bioturbation fabric (BI 2–3). Note the *Palaeophycos* burrow *(Pa)*. Tape measure is graduated in centimeters (left side) and inches (right side). **B.** Very fine-grained sandstone with thin mudstone interbeds in lower shoreface-distal delta front deposits at 3,859.3 feet in Square Lake 1. Note *Planolites* burrows *(Pl)*. The base of the upper bed containing the *Planolites* burrow includes apparent load structures. Visible part of pencil is 0.28 feet long (85 cm). **C.** Plane-parallel, horizontal laminations in very fine-grained sandstone above a basal mudstone clast-rich layer at the base of a sandstone bed at 3,890.7 feet in Square Lake 1. Black line is one inch long (2.54 cm). **D.** Plane-parallel, horizontal laminations above and below a prominent scour surface (white dashed line) at 3,493 feet in Square Lake 1. Note the abundant sideritic mudstone rip-up clasts below the scour surface and scattered mudstone clasts resting on the surface. Note also the *Schaubcylindrichnus (Sc)* burrows. Tape measure graduated in inches.

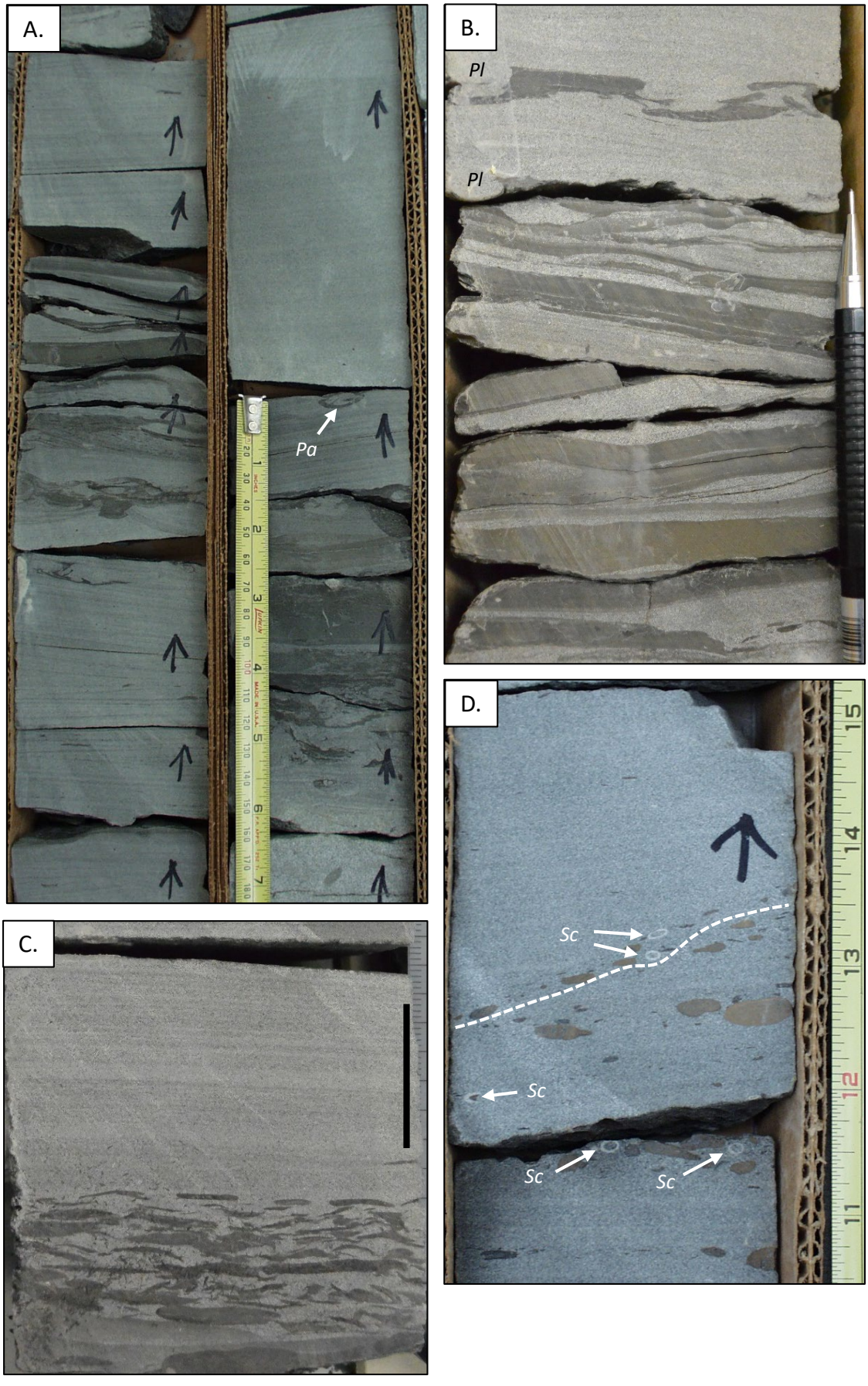
A.
Pa
B.
Pl
Pl
C.
D.
Sc
Sc
Sc
Sc

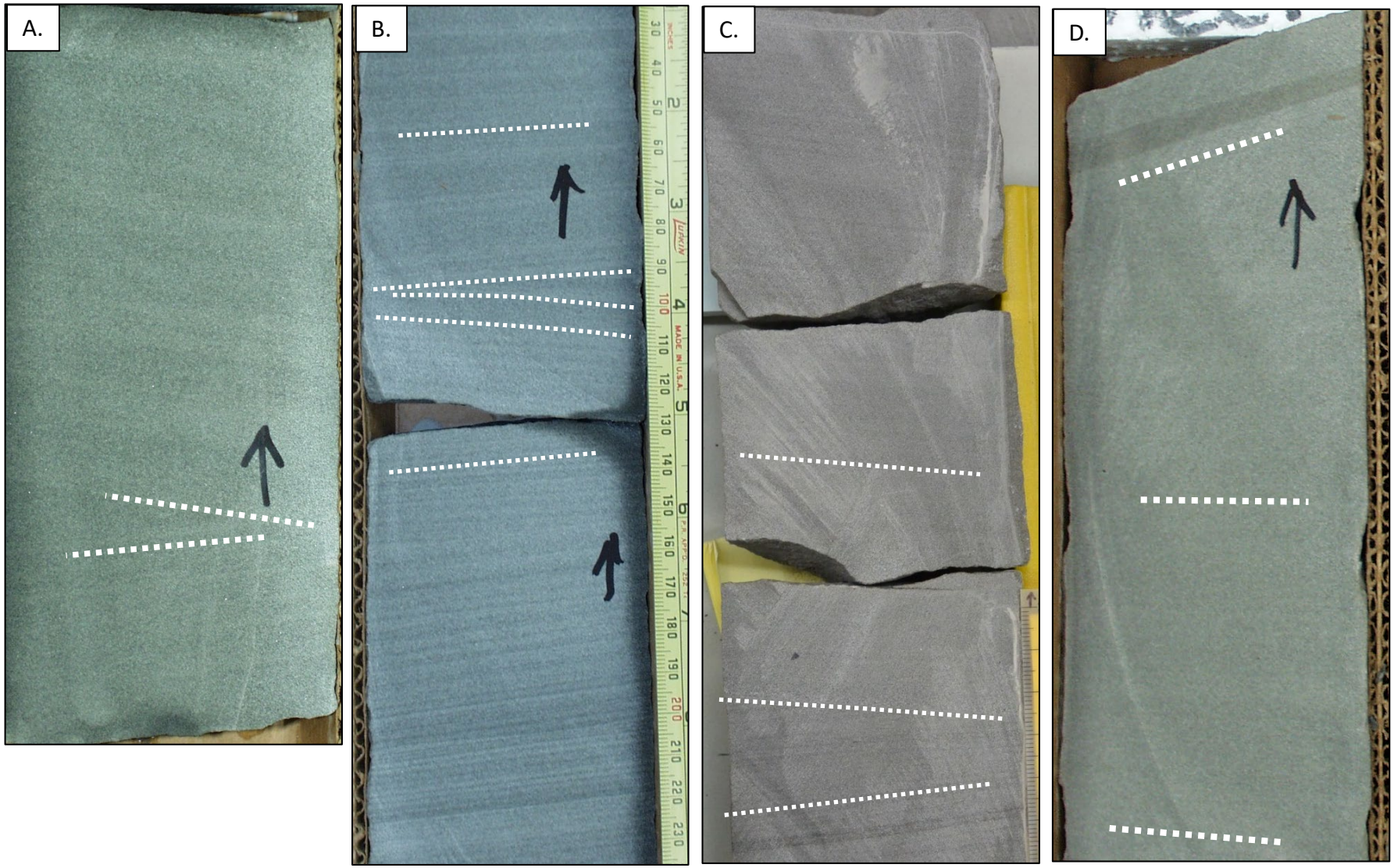

Figure 10. Photographs showing key features in amalgamated sandstone of FA4. Low-angle laminations at 3,872 feet (**A**) and 3,095.5 feet (**B**) in Square Lake 1. Low-angle laminations at 2,182 feet (**C**) and 2,156.5 feet (**D**) in Wolf Creek 3. Note the changes in dip direction (dotted white lines) in each photograph. These laminae are interpreted as HCS.

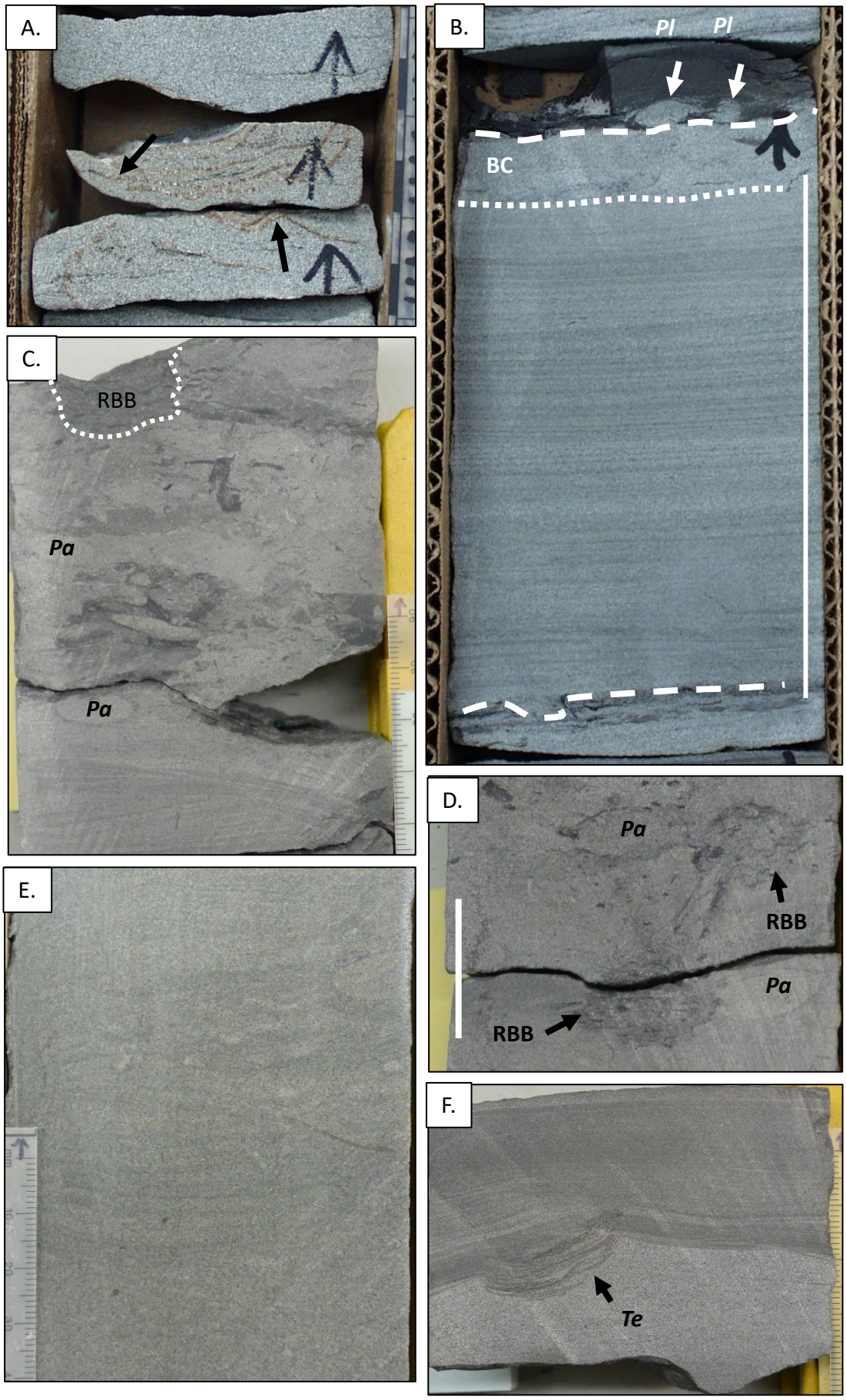
A.
B.
Pl
Pl
BC
C.
RBB
Pa
Pa
D.
Pa
RBB
Pa
RBB
E.
F.
Te

Bioturbation is most abundant in lower and middle shoreface settings where conditions are most suitable for preservation and tends to be absent or scarce in the more proximal reaches. These features, combined with the sporadic occurrence of abundant macerated plant debris (phytodetrital pulses of MacEachern and others, 2005), suggest deposition in a storm-wave influenced shoreface–delta front setting, with plant material transported to the depositional site by longshore currents from distant distributary channel mouths (sheets 2 and 3; LePain and Kirkham, 2001; LePain and others, 2017). Assuming this interpretation is correct, powerful storm waves shaped the nearshore marine setting during Nanushuk time at least in the southeastern part of the NPRA. Facies in Nanushuk outcrops south of Umiat include similar successions with abundant storm wave-generated sedimentary structures (HCS and swaley cross-stratification (SCS); LePain and others, 2009).

The absence of abundant wave-formed structures in the Umiat 18 and Grandstand 1 cores suggest that storm waves did not significantly impact this part of the Nanushuk coast when the cored successions were deposited, and that the delta front environment was more river-dominated overall than at the Wolf Creek 3 and Square Lake 1 locations. The sporadic occurrence of trace fossils (moderate to intense bioturbation locally) and the common presence of terrestrial plant material, sometimes in large quantities, are consistent with greater river influence (sheets 4 and 5; MacEachern and others, 2005).

Facies association 5 – Distributary Channel and Mouth bar

Description – Facies association 5 (FA5) consists of amalgamated very fine- to fine-grained sandstone successions ranging in thickness from approximately 7 feet to over 50 feet. Amalgamated sandstone includes abundant horizontal plane-parallel laminae, wave- and current-ripple cross-laminae, and macerated terrestrial plant debris (figs. 12A–C). Larger, coalified plant fragments are locally common (fig. 12D), as are trough cross-bedding (fig. 12E) and massive sandstone. Mudstone intraclasts and soft-sediment deformed beds are common (fig. 12F). Broken and abraded bivalve shell fragments (*Inoceramus*) aligned parallel to bedding are common near the tops of some coarsening-upward (CU) successions (fig. 13A). Bioturbation is absent to sparse (BI 0 to 2; fig. 13B), but is moderate to intense locally (fig. 13C). Some examples of FA5 grade down-section to interbedded mudstone and very fine-grained sandstone of FA3, while others grade down-section to amalgamated sandstones of FA4. FA5 has been tentatively identified in cores from Wolf Creek 3 (sheet 2, 2,661–2,673 feet, 2,330–2,359 feet, and 1,646–1,656 feet), Square Lake 1 (sheet 3, 1,716–1,723 feet and 1,657–1,694 feet), Umiat 18 (sheet 4, 777–833 feet), and possibly in Grandstand 1 (sheet 5, 829–837 feet).

The uppermost part of some CU successions consist of fine-grained sandstone overlying a scour surface (fig. 14A; sheet 2, scour surface 2,665 feet in Wolf Creek 3; sheet 3, scour surface inferred in gap between 1,694 feet and 1,695 feet in Square Lake 1). This sandstone includes abundant hori-

Figure 11, previous page. Photographs showing macrofossils and trace fossils in FA4. **A.** *Inoceramus* shell fragments (black arrows) in fine-grained sandstone at 1,849.5 feet in Square Lake 1. The grain size card along the right edge of the photograph is graduated in centimeters. **B.** Bioturbation fabric at 3,552 feet in Square Lake 1. The white dashed lines mark the base and top of a single sandstone event bed. The lower 90 percent of bed is largely undisturbed, whereas the upper part was thoroughly bioturbated after deposition (between white dotted and dashed lines). Note the mudstone drape with *Planolites* burrows (white arrows). White vertical line is 0.35 ft long. **C.** The bioturbated upper part of an event bed at 3,042.5 feet in Wolf Creek 3. Note the wave ripple cross-lamination in the unbioturbated part of the bed in lower part of image. Note *Palaeophycus* burrows (*Pa*) and re-burrowed burrow (RBB). **D.** Upper part of a sandstone bed at 3,034 feet in Wolf Creek 3. The upper 0.3 ft of the bed is highly to intensely bioturbated (BI 4–5). Note the *Palaephycus* burrows (*Pa*) and re-burrowed burrows (RBB). The white line is 1 inch. **E.** *Macaronichnus* burrows in amalgamated sandstone at 1,924 feet in Wolf Creek 3. **F.** *Teichichnus* burrow at the top of the current ripple-laminated sandstone bed at 3,376.7 feet in Wolf Creek 3.

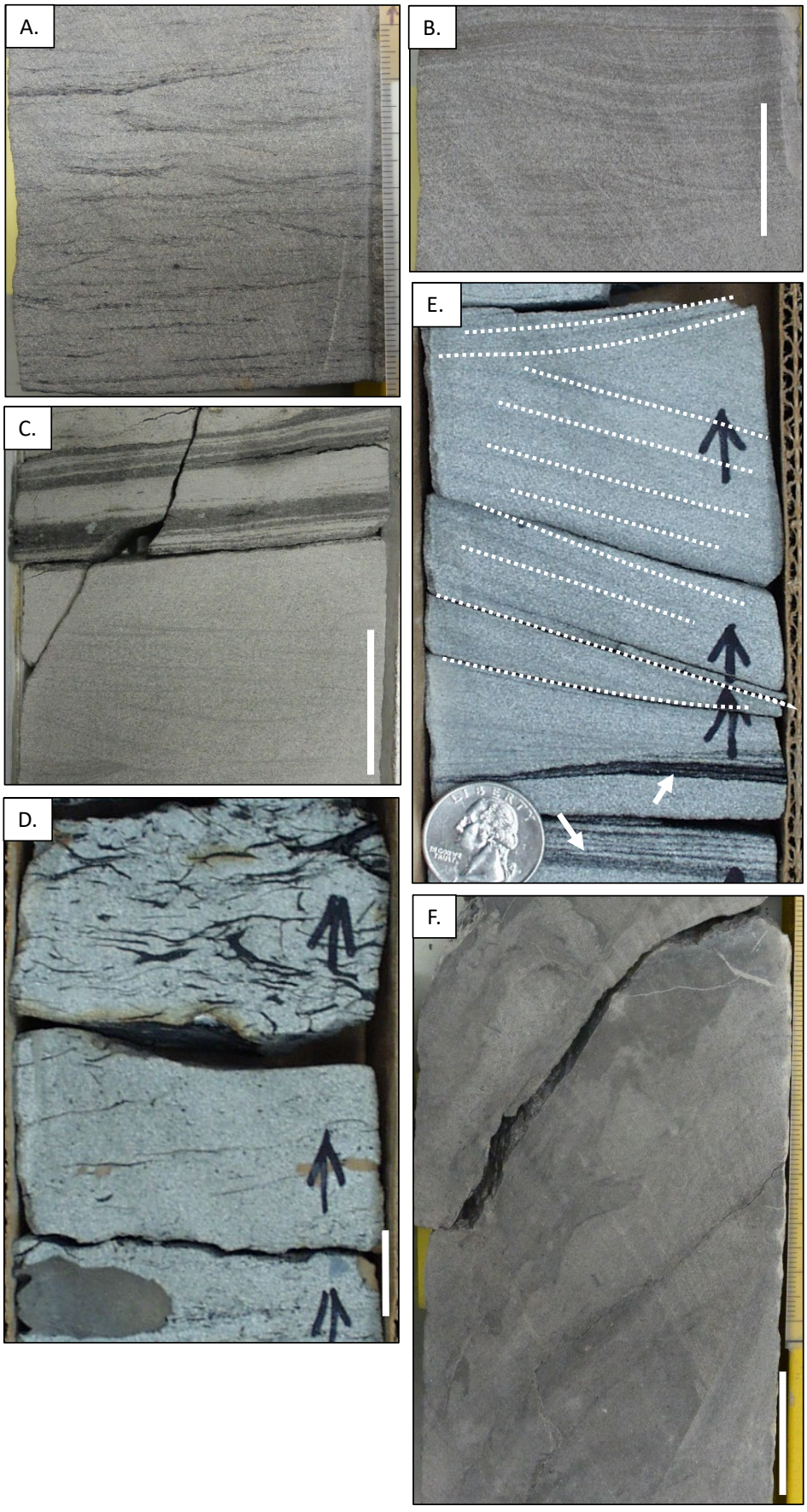

Figure 12. Photographs showing selected features of FA5 interpreted as distributary channel-mouth bar deposits. **A–B.** Wave-ripple cross-lamination at 2,333 feet and 2,113 feet in Wolf Creek 3, respectively, interpreted as mouth bar deposits reworked by fairweather waves. Dark colored laminae in A are rich in macerated plant fragments. Grain size card along the right side of A is graduated in millimeters and centimeters. White line in B is 0.08 feet long. **C.** Wave-ripple cross-lamination at 794 feet in Umiat 18. Note the dark colored carbonaceous laminae near top of image. White bar is 0.1 feet long. **D.** Large, coalified woody fragments at 2,116.5 feet in Wolf Creek 3. Note the sideritic mudstone rip-up clasts. White bar is 0.07 feet long. **E.** Trough cross-bedding in fine-grained sandstone at 2,116 feet in Wolf Creek 3. Some foreset laminae immediately above the quarter have a slight concave-upward geometry, which is consistent with trough cross-bedding. Note carbonaceous laminae near the quarter (white arrows). Quarter for scale. **F.** Soft-sediment deformed beds of siltstone (light colored lithology) and mudstone (darker lithology). Siltstone either foundered in a mudstone host due to a density contrast, or represents a small failure on the flank of a distributary mouth bar. White bar is 1 inch in length and scale on the grainsize card visible along the right edge of the image is graduated in millimeters and centimeters.

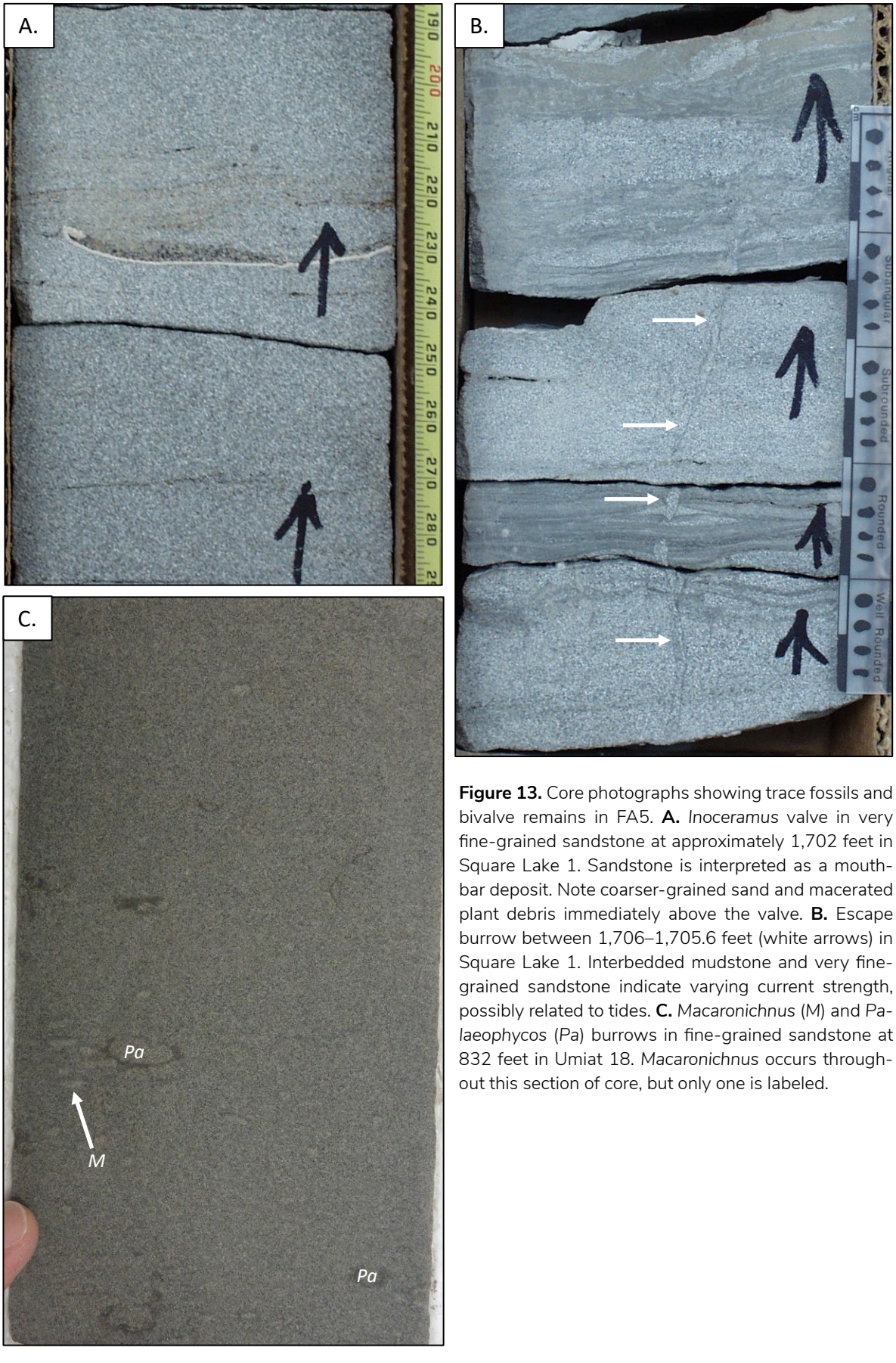

Figure 13. Core photographs showing trace fossils and bivalve remains in FA5. **A.** *Inoceramus* valve in very fine-grained sandstone at approximately 1,702 feet in Square Lake 1. Sandstone is interpreted as a mouth-bar deposit. Note coarser-grained sand and macerated plant debris immediately above the valve. **B.** Escape burrow between 1,706–1,705.6 feet (white arrows) in Square Lake 1. Interbedded mudstone and very fine-grained sandstone indicate varying current strength, possibly related to tides. **C.** *Macaronichnus* (*M*) and *Palaeophycos* (*Pa*) burrows in fine-grained sandstone at 832 feet in Umiat 18. *Macaronichnus* occurs throughout this section of core, but only one is labeled.

zontal plane-parallel laminae and cross-bedding (figs. 14B). Bivalve shell fragments (Square Lake 1, 1,694–1,674 feet) and possible pedogenic features are locally prominent. Bioturbation is typically absent (BI 0; fig. 14A–B), but some solitary traces are present locally (BI 1) and a few intervals are characterized by low (BI 2) to moderate bioturbation (BI 3). These successions are tentatively identified in Wolf Creek 3 (sheet 2, 2,661–2,665 feet), Square Lake 1 (sheet 3, 1,637–1,694 feet), and Umiat 18 (sheet 4, 777–796.8 feet). Where this sandstone is present, it rests erosionally above gradationally based deposits of FA5, or above either FA3 or FA4.

Interpretation – Most examples of FA5 in the studied cores are interpreted as distributary mouth bar deposits; the coarser-grained successions capping some examples of the association are interpreted as distal distributary channel deposits. Flow expansion and velocity reduction at the seaward end of distributary channels results in an abrupt decrease in flow capacity and competence, resulting in deposition of a bar deposit at the channel mouth, with subsequent

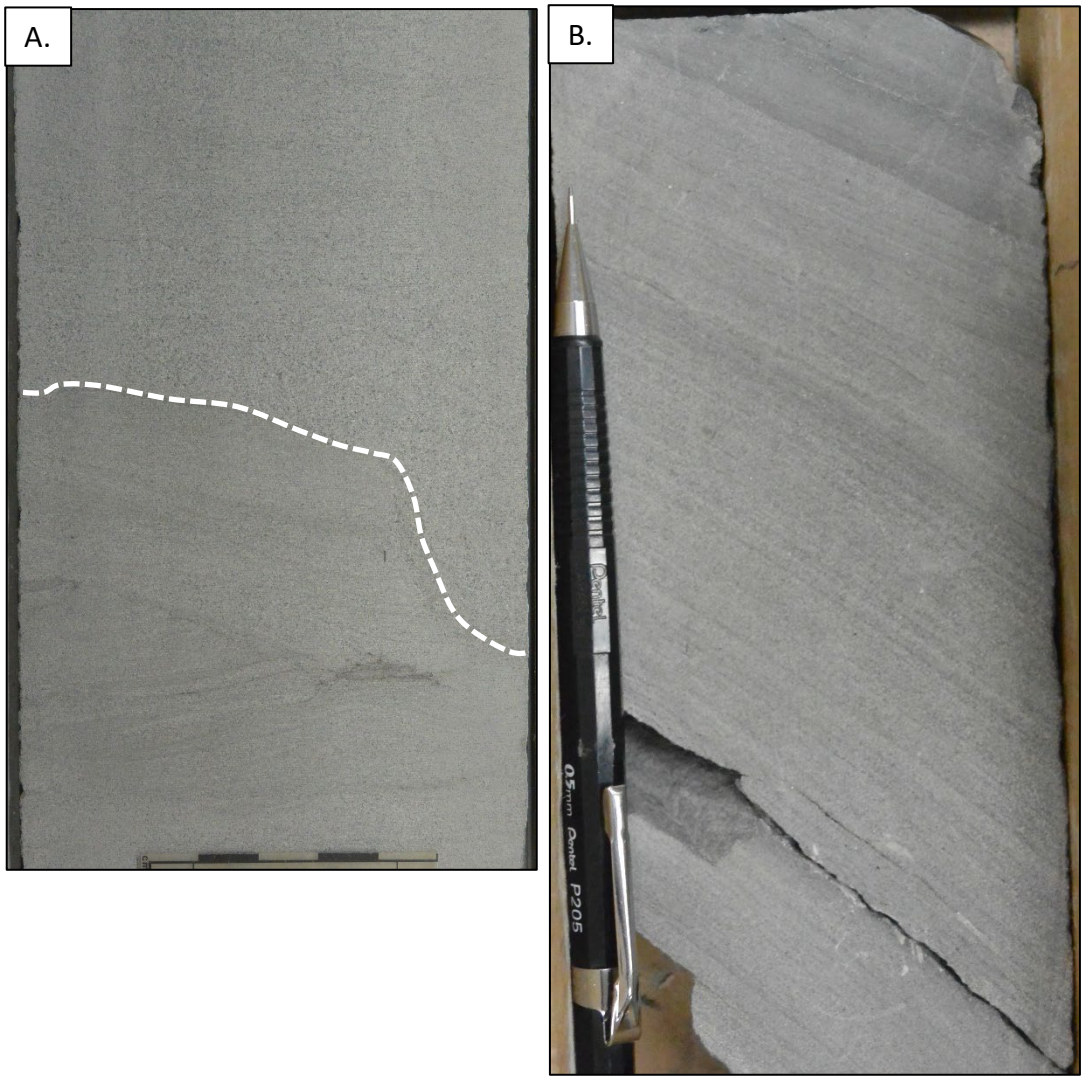

Figure 14. Core photographs showing sedimentary characteristics of FA5 interpreted as distributary channel deposits. **A.** Scour surface at 796.5 feet (dashed white line) truncating current ripple cross-laminae in Umiat 18. Scale at base of photograph graduated in centimeters. **B.** Foreset laminae associated with cross-bedding at 2,661.5 feet in Wolf Creek 3. Visible part of pencil is 0.43 feet long.

channel bifurcation around mouth bar deposits (Scott and Fisher, 1969). Mouth bar deposits are typically reworked by shoaling waves to form strike-elongated subaqueous sand bodies (Bhattacharya, 2006). In the resulting deposits mouth bar facies commonly dominate over distributary channel-fill facies and the two can be difficult to differentiate with confidence. For this reason, most examples of facies association

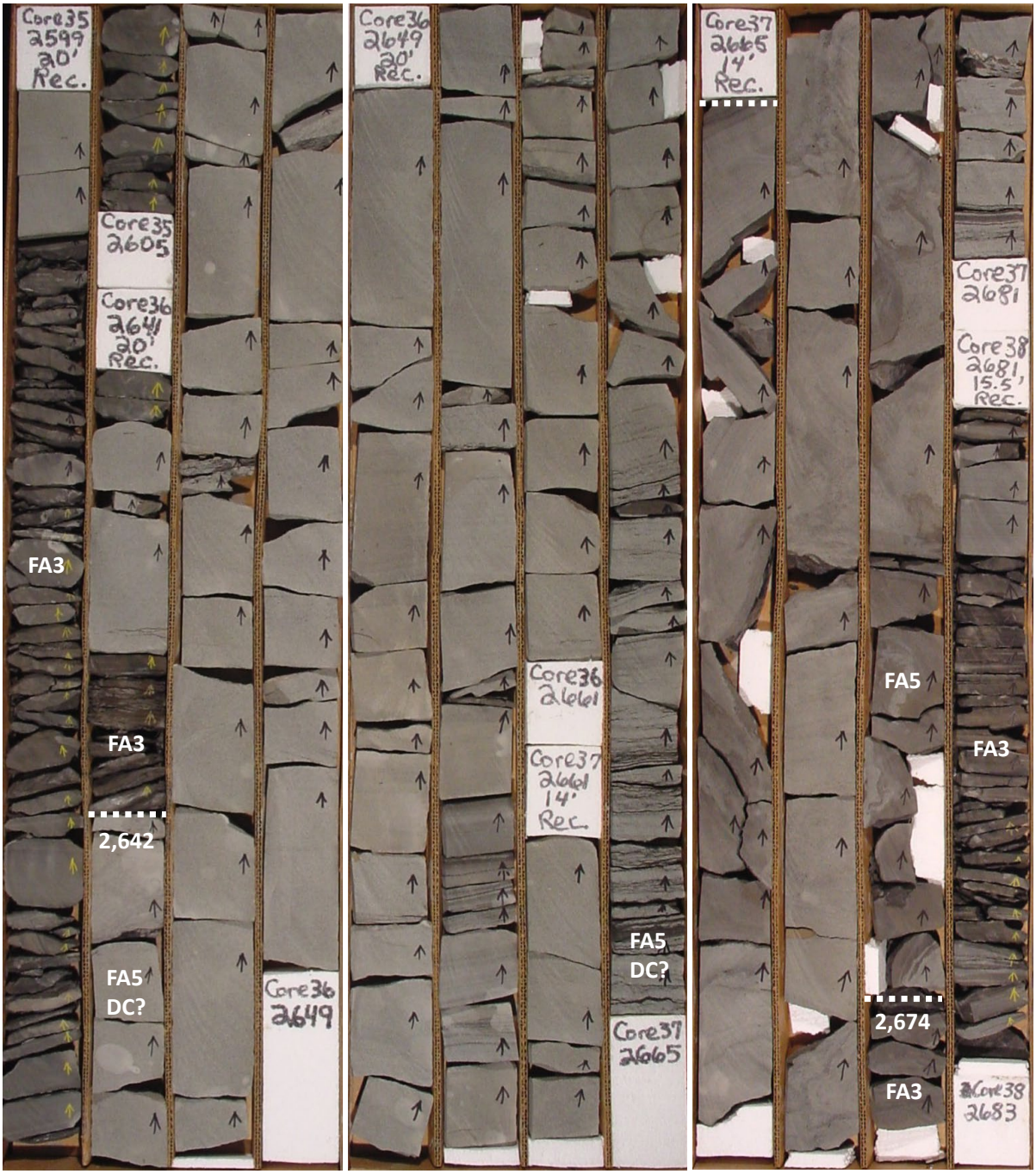

Figure 15. Core box photographs showing a continuously cored succession through FA5 from approximately 2,674 feet (lower white dashed line in second row of core from right) to 2,642 feet (upper white dashed line in second row of core from left) in Wolf Creek 3. Note the sandier-upward trend and soft-sediment deformation (deformed section between dashed white lines in core 37), interpreted as mouth bar deposits. The dark laminations immediately above the 2,665 foot mark in the box are carbonaceous mudstones at the base of a distributary channel-fill that extends up to 2,642 feet. The carbonaceous laminae above 2,665 feet may record a tidal influence. Each core row is 3.28 feet (1 meter) long. Core box photos modified from D'Agostino and Houseknecht (2002).

5 in the core descriptions include undifferentiated mouth bar and distributary channel deposits, with the exception of a few occurrences where these components are tentatively recognizable (fig. 15 and sheet 2, Wolf Creek 3, from 2,642 to 2,674 feet, 2,330 feet to 2,359 feet, 2,241 feet to 2,247 feet; fig. 16, sheet 3, Square Lake 1, from 1,715.5 feet to 1,722.5 feet and from 1,637 feet to 1,694 feet; sheet 4, Umiat 18, from 777 feet to 833.5 feet; sheet 5, Grandstand 1, 829 feet to 837 feet).

Facies Association 6 – Bayfill

Description – Facies association 6 (FA6) consists mainly of an irregular succession of brown to brown-gray mudstone and thinly interbedded siltstone and very fine- to fine-grained sandstone

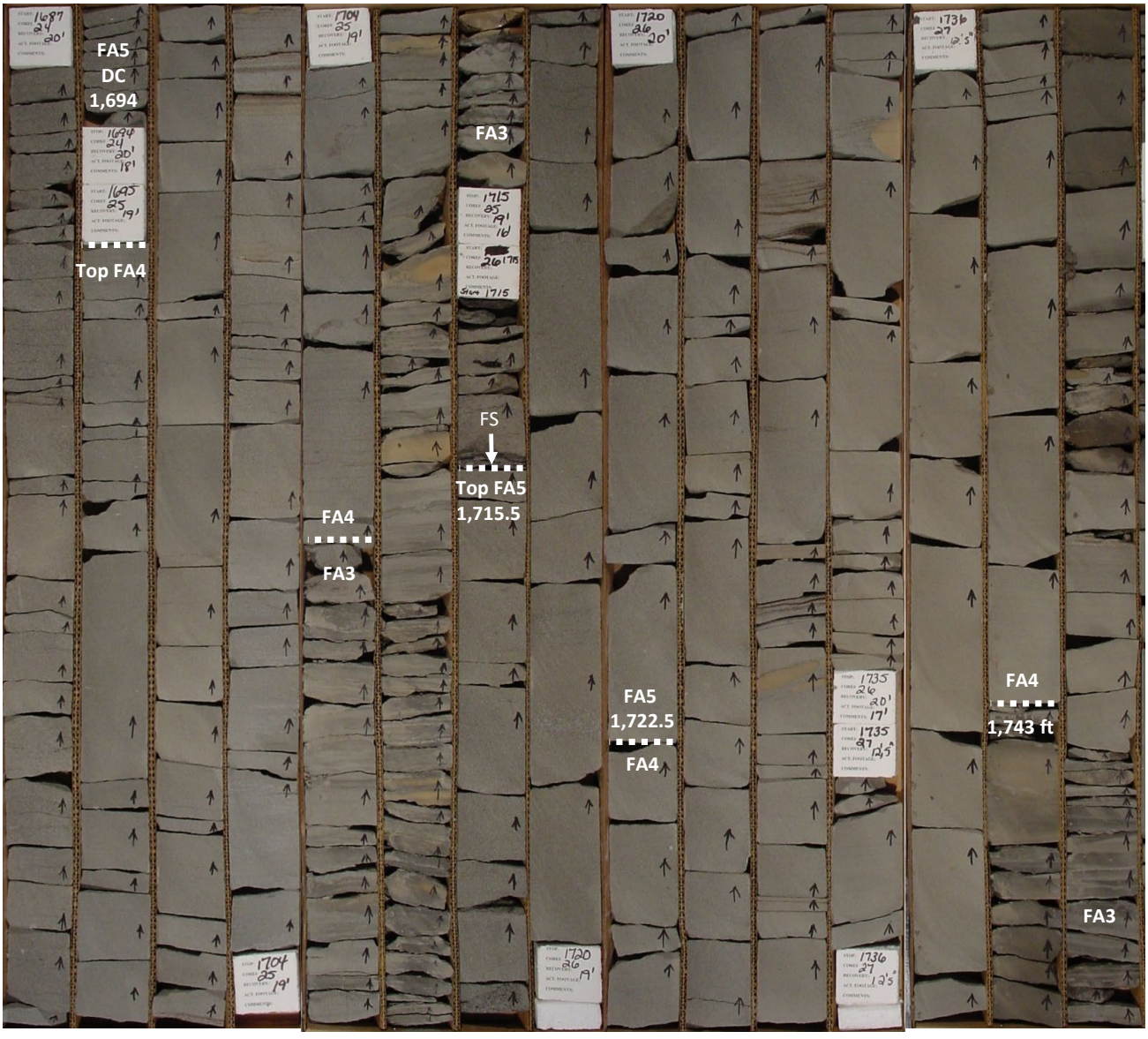

Figure 16. Core box photographs showing a continuously cored succession of FA3, FA4, and FA5 from approximately 1,743 feet to 1,637 feet in Square Lake 1. Core box photographs for this figure continue on next page. The oldest FA5 succession, interpreted as mouth bar deposits, grades upward from FA3 and lower very fine-grained sandstone of FA4 to upper very fine-grained sandstone of FA5 (contact at 1,722.5 feet), and is capped by a flooding surface at 1,715.5 feet (white dashed line labeled FS). The FA5 succession from 1,694 feet to 1,657 feet is interpreted as a distributary channel-fill succession (only 1,694 feet to 1,687 feet is shown in photograph). DC, distributary channel; MB, mouth bar. Each core row is 3.28 feet (1 meter) long. Core box photos modified from D'Agostino and Houseknecht (2002).

(fig. 17A–C). Mudstones appear massive to thinly laminated; macerated plant fragments are locally abundant and serve to accentuate laminations. Carbonaceous mudstone, high-ash coal stringers, and small coal clasts are present locally, as are rare small pieces of amber (sheet 3, Square Lake 1, 2,056 feet and 2,020 to 2,021.5 feet). Siltstone and sandstone beds range from less than 0.1 to approximately 1 foot thick and include horizontal, plane-parallel laminae, current and wave ripple

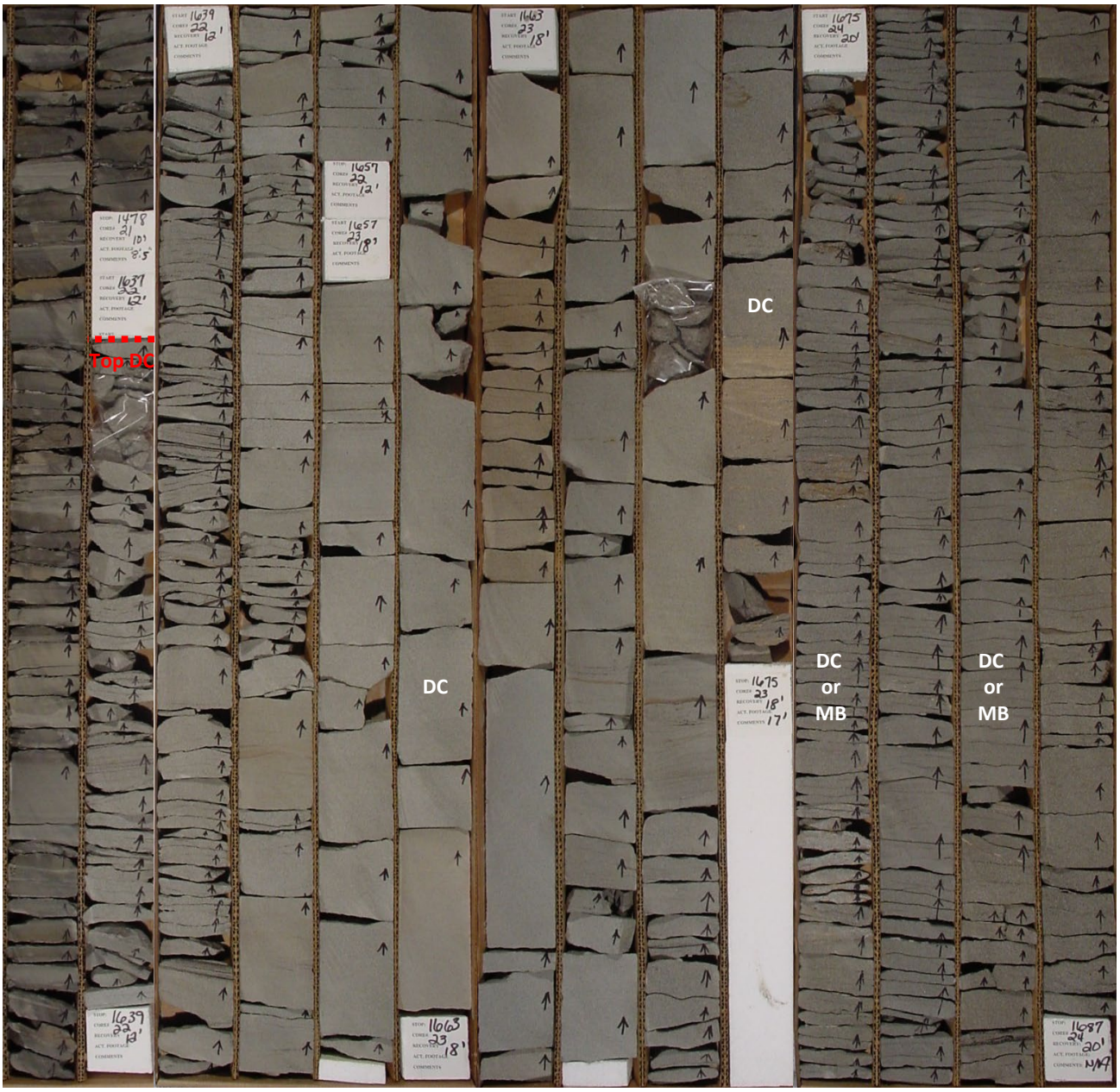

Figure 16, continued. Core box photographs showing a continuously cored succession of FA3, FA4, and FA5 from approximately 1,743 feet to 1,637 feet in Square Lake 1. Core box photographs for this figure continue on next page. The oldest FA5 succession, interpreted as mouth bar deposits, grades upward from FA3 and lower very fine-grained sandstone of FA4 to upper very fine-grained sandstone of FA5 (contact at 1,722.5 feet), and is capped by a flooding surface at 1,715.5 feet (white dashed line labeled FS). The FA5 succession from 1,694 feet to 1,657 feet is interpreted as a distributary channel-fill succession (only 1,694 feet to 1,687 feet is shown in photograph). DC, distributary channel; MB, mouth bar. Each core row is 3.28 feet (1 meter) long. Core box photos modified from D'Agostino and Houseknecht (2002).

cross-laminae (figs 17B-C), and soft-sediment deformation features (fig. 17D); massive textures are also common (fig. 17A). Bioturbation is highly variable, ranging from absent (BI 0) to intense (BI 5-6) in mudstone and sandstone (figs. 18A−C). Trace fossils include *Schaubcylindrichnus*, *Teichnichnus* (fig. 18A−B), and *Phycosiphon* (fig. 18C). One bed at approximately 1,645.5 feet in Wolf Creek 3 includes irregular, carbonaceous mud-filled vertical structures of uncertain affinity that may be rhizoliths (fig. 18D). Where FA6 rests above FA4 or FA5, the contact is typically sharp (fig. 19; sheet 2, Wolf Creek 3, 1,887 feet; sheet 4, Umiat 18, 777 feet; sheet 5, Grandstand 1, 829 feet, though bayfill interpretation is questionable). Cores 33 (below 1,886 feet) through 43 in Square Lake 1 are interpreted as FA6; the interval between cores 43 and 44 was not cored, but cuttings suggest the contact is sharp (sheet 3, Square Lake 1, 2,852−3,027 feet).

The irregular successions described above are interrupted locally by sand-dominated successions. Two varieties are recognized: 1. Sharp-based fining-upward successions up to five feet thick (sheet 2, Wolf Creek 3, 1,571–1,576 feet; sheet 3, Square Lake 1, 2,020–2,032 feet); and 2. Gradational coarsening-upward successions up to 15 feet thick (sheet 2, Wolf Creek 3, 1,716–1,726 feet and 1,645.5–1,656 feet; sheet 3, Square Lake 1, 1,912.5–1,928.5 feet). Sandstone in both varieties include horizontal, plane-parallel laminae and ripple cross-laminae. The geometry of ripple cross-laminae suggests reworking of sand by small waves. HCS, or possibly SCS, is present in some coarsening-upward successions (sheets 2 and 3).

Interpretation –The irregular succession characteristic of most examples of FA6 resembles interdistributary bay deposits documented in the central Appalachians by Horne and others (1978), the Dunvegan Formation by Bhattacharya and Walker (1991), and the Ferron Sandstone Member of the Mancos Shale by Ryer and Anderson (2004). Interdistributary bay deposits account for most of the cored Nanushuk Formation in the Wainwright 1 well in the western NPRA (LePain and Decker, 2016) and are common in outcrop to the south (LePain and others, 2009). Thin sandstone interbeds up to 1 foot thick represent overbank splay deposits. The sharp-based fining-upward sandstone and gradational coarsening-upward sandstone successions are interpreted as crevasse channel-fills and crevasse delta-front deposits, respectively (Elliot, 1974). The latter includes distributary mouth bar deposits associated with crevasse channels. Highly variable bioturbation is attributed to varying water salinity owing to frequent incursions of fresh floodwaters from nearby distributary channels. Highly bioturbated muddy sandstones with low diversity trace fossil assemblages are consistent with this interpretation (Pemberton and Wightman, 1992).

STRATIGRAPHIC ORGANIZATION AND IMPLICATIONS FOR DELTA STYLE

Analysis of facies stacking patterns in vertical sections provides important insights on depositional environments and their migration patterns through time. The graphic core descriptions for Wolf Creek 3, Square Lake 1, Grandstand 1, and Fish Creek 1, as portrayed in sheets 1–3 and 5, are not readily suitable for this type of analysis due to the non-uniform scale at which they were drafted. The scale of the cored intervals is uniform, but the scale in thick, uncored intervals is compressed, resulting in the false impression that the succession penetrated in the wells includes more sand than is actually present. Collins (1959a, 1959b) and Robinson (1958) do not provide process-response sedimentologic analyses and their graphic logs provide only lithologic information. Adding to the challenge is the absence of modern log suites for these four wells—only spontaneous potential (SP) and resistivity (short and long normal) logs are available—and the fact that some sands in each well were not cored (see Collins, 1959a, plate 32; and Collins, 1959b, plates 29 and 30). To help overcome these issues, sheet 6 shows simplified versions of the core descriptions drafted at a uniform scale. Umiat 18 is included on sheet 6 for comparison.

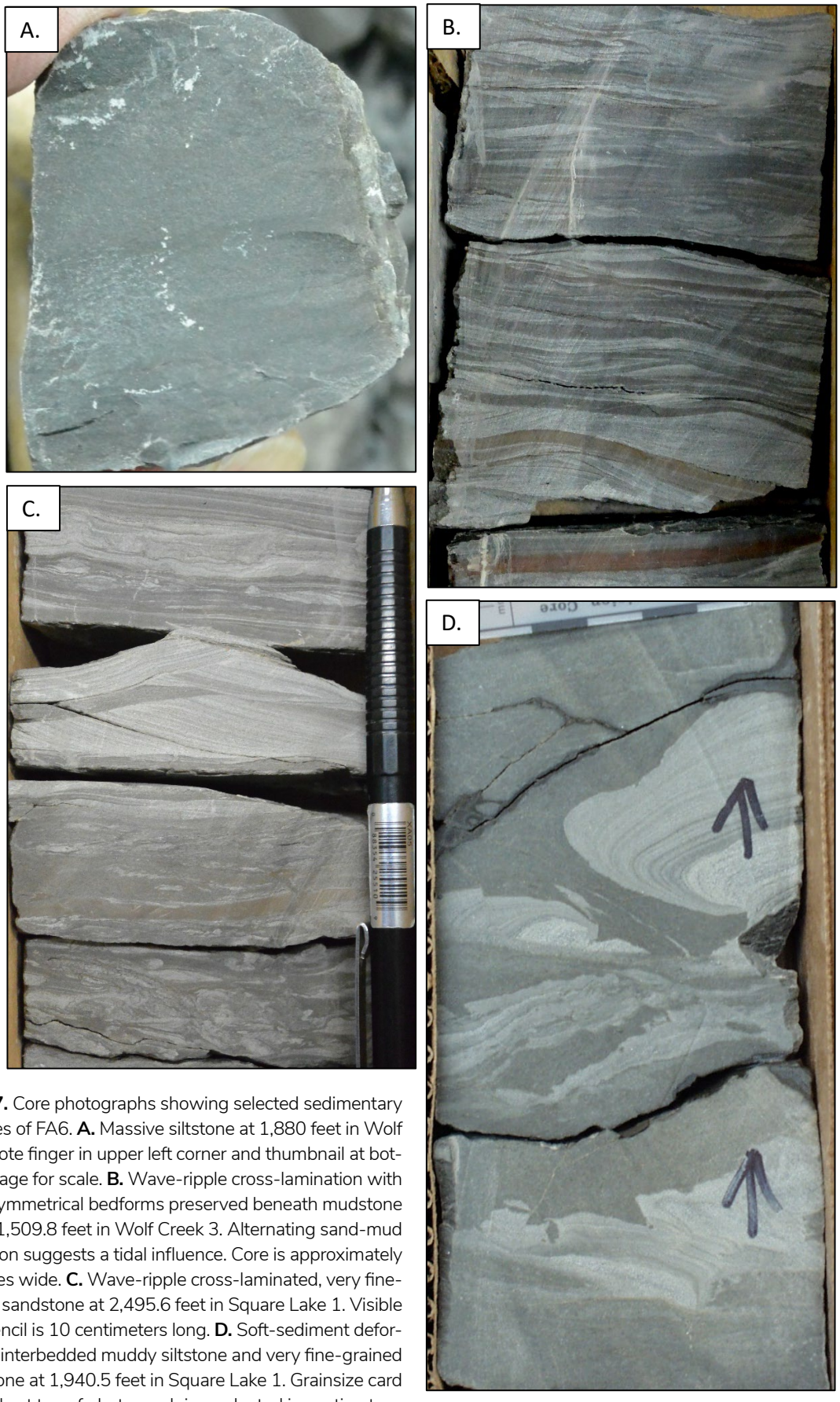

Figure 17. Core photographs showing selected sedimentary features of FA6. **A.** Massive siltstone at 1,880 feet in Wolf Creek 3. Note finger in upper left corner and thumbnail at bottom of image for scale. **B.** Wave-ripple cross-lamination with nearly symmetrical bedforms preserved beneath mudstone drapes at 1,509.8 feet in Wolf Creek 3. Alternating sand-mud deposition suggests a tidal influence. Core is approximately 2.25 inches wide. **C.** Wave-ripple cross-laminated, very fine-grained sandstone at 2,495.6 feet in Square Lake 1. Visible part of pencil is 10 centimeters long. **D.** Soft-sediment deformation in interbedded muddy siltstone and very fine-grained sandstone at 1,940.5 feet in Square Lake 1. Grainsize card visible at top of photograph is graduated in centimeters.

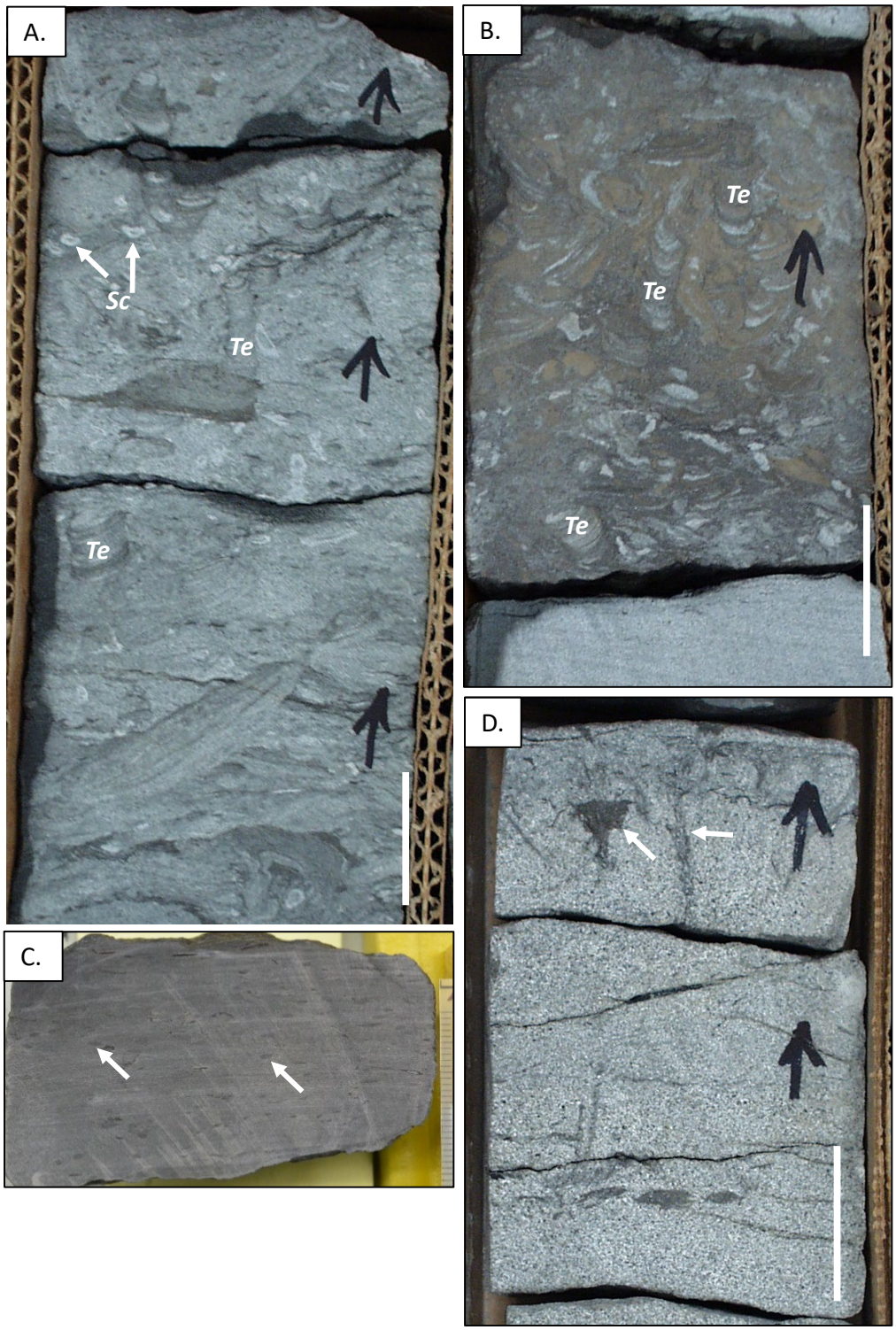

Figure 18. Core photographs showing bioturbation in FA6. **A.** Highly to intensely bioturbated (BI 4–5) muddy sandstone at 2,497.5 feet in Square Lake 1. Several examples of *Schaubcylindrichnus* (Sc) and *Teichichnus* (T) are present. White line is 1 inch long. **B.** Highly to intensely bioturbated muddy sandstone (BI 4–5) with many *Teichichnus* (T) burrows at 2,498 feet in Square Lake 1. White line is 1 inch long. **C.** Mudstone with abundant *Phycosiphon* burrows (white arrows point to a few examples) at 1,731 feet in Wolf Creek 3. Absence of visible bleached halo around traces suggests these might be *Helminthopsis* burrows instead of *Phycosiphon*. Scale along the right edge of the photograph is graduated in millimeters. **D.** Fine-grained sandstone with discrete vertical burrows at 1,645.5 feet in Wolf Creek 3, including features interpreted as rhizoliths. Funnel-shaped trace (white arrow on left side of image) is filled with carbonaceous mudstone. This piece of core appears to be missing in the split archived at the Alaska Geologic Materials Center. White line is 1 inch long.

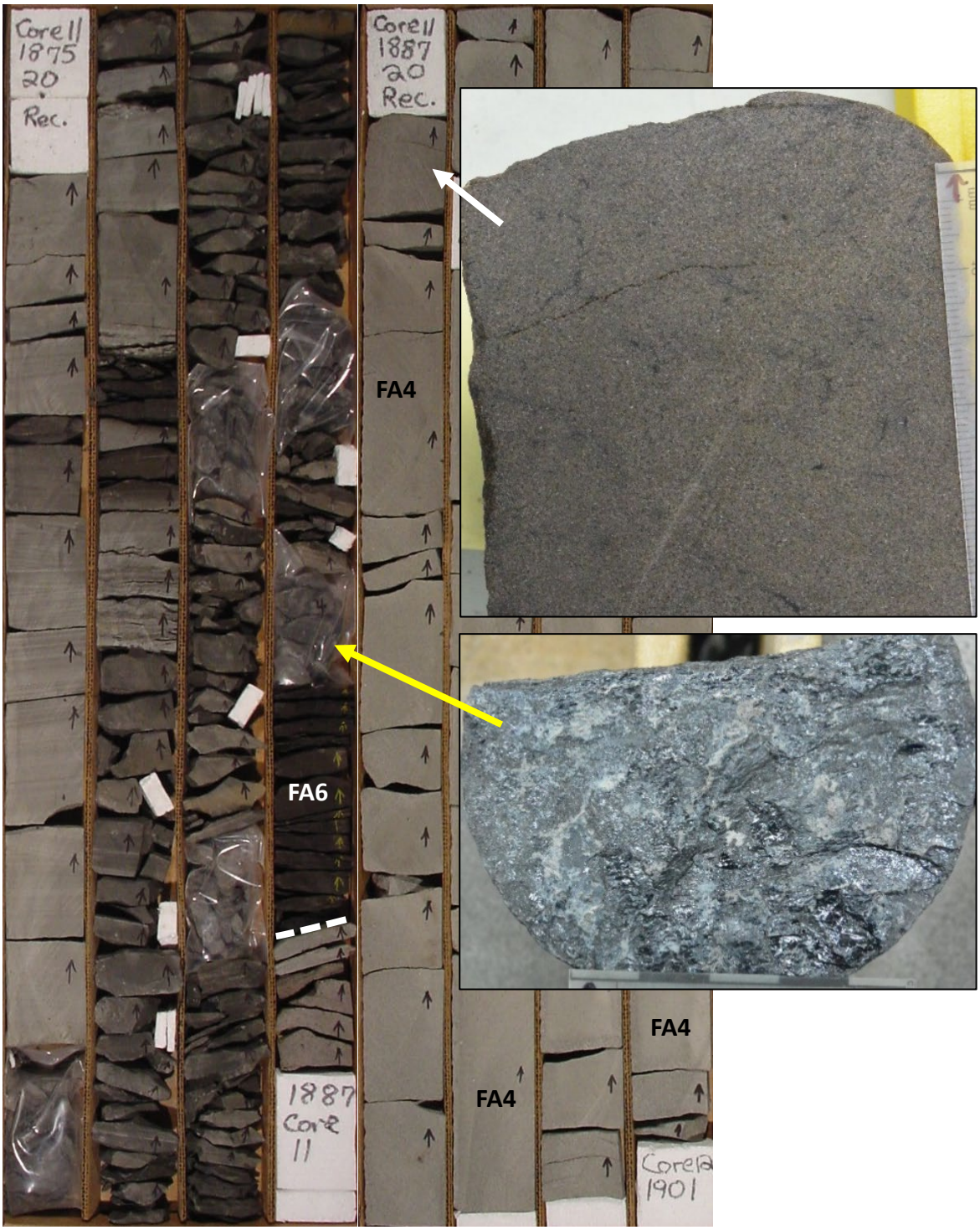

Figure 19. Core box photograph showing part of the splits of cores 11 and 12 from Wolf Creek 3 archived at the USGS Core Research Center. Inset photos taken of core archived at the Alaska Geologic Materials Center. Note the contact between sandstone of FA4 and carbonaceous mudstone with coal stringers of FA6 above 1,887 feet (dashed white line). The upper inset photo shows sandstone at the top of FA4 (white arrow) with irregular-shaped wisps of carbonaceous mudstone imparting a mottled appearance resembling a pedogenic fabric. If correct and the fabric is pedogenic, FA4 was emergent prior to burial beneath FA6. Grainsize card along right side of image is graduated in millimeters and centimeters. Lower inset photograph shows a coaly stringer at base of FA6 and immediately above sandstone of FA4 (yellow arrow). Note edge of grain size card graduated in centimeters at base of photo. Core box photograph from D'Agostino and Houseknecht (2002). Each row in core box photograph is 3.28 feet long (1 meter).

Despite the lack of gamma ray logs for the older wells, the SP log response can usually be tied to lithologies in the studied cores with some confidence, allowing use in the uncored intervals, along with cuttings descriptions (Collins, 1959a, 1959b; Robinson, 1958) and the overall stratigraphic context relative to nearby cored intervals, to infer lithologies, facies, and their stacking patterns.

Fish Creek 1

Using Bird's (1988) formation top, the Fish Creek 1 well penetrated approximately 1,220 feet of Nanushuk strata, with the cored intervals consisting entirely of distal shelf deposits of FA2, and 2,910 feet of the Torok Formation, with the cored intervals consisting mostly of unbioturbated slope deposits of FA1 (sheets 1 and 6). The bioturbated mudstone (BI 2–3) in core 42 is in the upper part of the Torok Formation, based on the formation top at 4,110 feet TVD (Bird, 1988), and it represents the first definitive occurrence of visible bioturbation in core. The bioturbation and light color of this mudstone contrast sharply with the dark brown-gray to gray, unbioturbated clay shale and mudstone in cores 43 through 75, interpreted as slope deposits (sheet 1), suggesting the upper 90 to 100 feet of the Torok Formation includes distal shelf deposits (topset Torok, see Houseknecht and Schenk, 2001). The absence of bioturbation fabrics in FA1 (cores 43–75), with the sole exception of possible sparse bioturbation in core 57 (sheet 1), is consistent with the observation of Houseknecht and Schenk (2001) that bioturbation is rare in slope deposits of the Torok. Thus, the Fish Creek 1 well penetrated a thick, progradational succession of slope mudstone overlain by a thinner succession of distal shelf deposits. Slope deposits in this well correspond to prominent clinoform reflectors on seismic sections (Houseknecht and others, 2008; Houseknecht, 2019). According to Weimer (1987, his fig. 6), approximately the lower 1,200 feet of the Fish Creek 1 well (5,800–7,020 feet TVD) consists of lower slope deposits involved in the Fish Creek slide. No evidence of disrupted bedding was noted in cores 63 to 75, indicating the part of the slide block penetrated by the well includes relatively coherent stratigraphy. The prominent left deflection on the SP log starting around 4,110 feet suggests the presence of a sandy succession up to 40 feet thick at the base of the Nanushuk Formation (sheet 6, approximately 4,110–4,070 feet), possibly associated with a sea level lowstand.

Umiat 18

The graphic core description and gamma ray log for Umiat 18 define three progradational parasequences from a depth of approximately 1,150 feet to 777.8 feet (labeled Kn1 through Kn3 on sheet 4). Note the lower part of Kn1 was not cored and the down-hole extent and lithological character are inferred from the gamma ray log (sheets 4 and 6; uncored part of Kn1 is shown with a dashed red line). The gamma log suggests at least two additional sandier-upward parasequences between approximately 1,420 to 1,150 feet (dashed red lines on left side of gamma ray log, sheet 4) that are likely part of the Nanushuk Formation. These five parasequences define a progradational succession with each successively younger parasequence recording deposition in more proximal settings. In the cored interval, each parasequence consists, in ascending order, of heterolithic deposits of FA3 grading up-section to amalgamated sandstones of FA4 (sheet 4). In Umiat 18, FA3 and FA4 in Kn1 and Kn2 define shoaling-upward prodelta to delta front successions capped by sharp marine flooding surfaces. FA3 is inferred to comprise the lower, uncored part of Kn1. The two sandier-upward parasequences recognizable on the gamma ray log below Kn1 are interpreted as the distal expression of delta front cycles/shingles comprising the lower 250–300 feet of the Nanushuk Formation. The cored succession below 777.4 feet records deposition of delta lobes that were influenced more by riverine processes than by shoaling waves (river-dominated).

The upper 67.4 feet of the cored interval is a mudstone-dominated succession that appears different than the prodelta successions at the base of Kn2 and Kn3 and different than the bayfill succes-

sions interpreted in the Wolf Creek 3 and Square Lake 1 cores (sheet 4). The flooding surface at approximately 777.4 feet overlies bioturbated sandstone at the top of a sand body in Kn3 interpreted as a distributary channel-fill. This surface is overlain by a little over six feet of interbedded light gray mudstone and bioturbated (BI 2–3) fine-grained sandstone that is, in turn, overlain by approximately 21 feet of brown-gray, massive to finely laminated mudstone that is unbioturbated (BI 0), except for a thin interval from approximately 761.8 feet to 762.2 feet that is moderately bioturbated (BI 3). Delicate, thin-walled, disarticulated, monospecific pelecypod valves are present at discrete intervals in the mudstone below the bioturbated interval, but are not abundant (fig. 20A); similar pelecypod valves are abundant above the bioturbated interval, between 761.3 feet and 759.0 feet (fig. 20B). Most of the pelecypod shells are oriented parallel to bedding and many shells are oriented convex side up and many others convex side down. The mudstone interval above the friable sandstone (top at 749.5 feet) is highly to intensely bioturbated (BI 4–5?) and includes abundant *Helminthopsis* (or *Phycosiphon*) burrows. The interbedded mudstone and sandstone above the flooding surface from 777.4–768 feet are interpreted to record reworking of underlying distributary channel-fill, mouth bar, and delta-front successions that were present nearby. The unbioturbated mudstone interval records deposition in a setting that was inhospitable to a burrowing infauna, possibly due to an oxygen deficiency, or brackish water, or both. The thin-walled shell material suggests a low energy setting where it originated and minimal transport to the depositional site by low-energy currents capable of moving the valves without destroying the delicate shell material. The depositional setting is provisionally interpreted as an interdistributary bay (bayfill) that was initially characterized by either anoxic bottom conditions and/or brackish water. If this interpretation is correct, the surface shown on sheet 4 at 777.4 feet is not a flooding surface, but merely represents a facies contact in a normal progradational succession from distributary channel deposits (FA5) to overlying interdistributary bayfill deposits (FA6).

Wolf Creek 3

Wolf Creek 3 spudded in a thin mantle of unconsolidated deposits, penetrated the top of the Nanushuk Formation at a depth of 30 feet (below top of Kelly bushing; Collins, 1959b), and reached total depth in the upper part of the Torok Formation at 3,760 feet (Bird, 1988). Based on Bird's (1988) formation top, the preserved thickness of Nanushuk in this well is 3,545 feet (sheets 2 and 6). The absence of a younger bedrock formation above the Nanushuk indicates an unknown thickness of strata in the upper part of the unit is missing due to uplift and erosion. The 47 cores cut from the well are distributed throughout the lower 2,100 feet of the formation and uppermost Torok. Cores and the SP log document an aggradational-progradational stack of marine parasequences at least 1,635 feet thick (cores 46 through lower part of core 11) that grade upward to interbedded marine and marginal marine facies in the upper 412 feet of the cored succession (cores 11 through 1). The marine parasequences in cores 46 through the lower part of 11 contain abundant features commonly associated with storm-influenced lower to middle shoreface and delta front environments, including possible HCS, wave ripple cross-lamination, unidirectional current indicators, graded beds, mudstone rip-up clasts, small- and large-scale soft sediment deformation structures, abundant macerated terrestrial plant fragments and larger coalified material, and a locally abundant and diverse suite of trace fossils representing widespread bioturbation by a mixed *Cruziana-Skolithos* ichnofacies assemblage. Many of these features are associated with discrete event beds, including classic shallow marine storm deposits (Walker and others, 1983; Duke and others, 1991) and the deposits of density underflows that emanated from distributary channels (frontal splays and/or hyperpycnites; Myrow and Southard, 1996; Mulder and others, 2003; Bhattacharya and MacEachern, 2009). Collectively, these features suggest the interval from approximately 3,522 feet to 1,887 feet represents a progradational succession of storm wave influenced delta lobes composed of

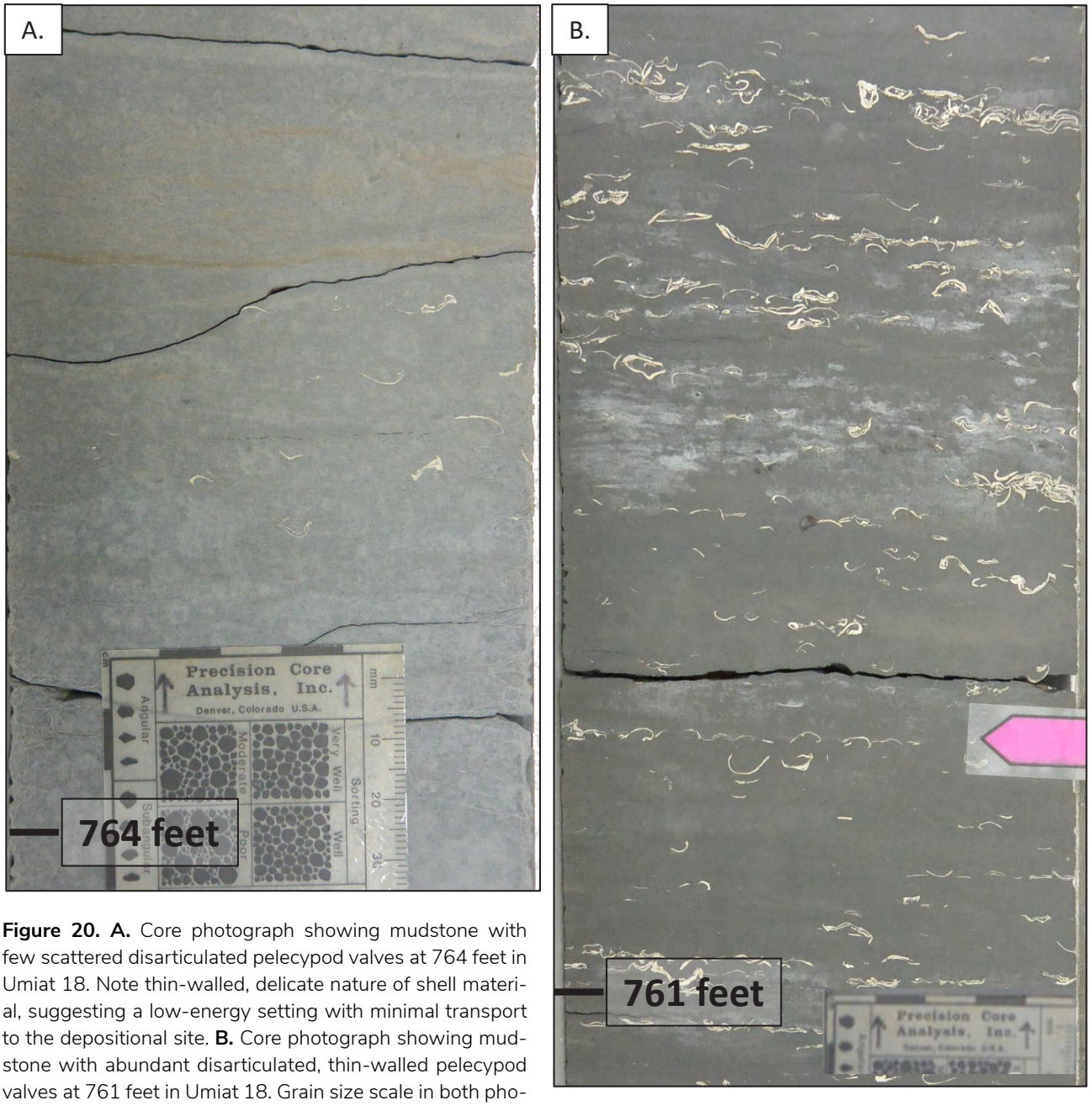

Figure 20. A. Core photograph showing mudstone with few scattered disarticulated pelecypod valves at 764 feet in Umiat 18. Note thin-walled, delicate nature of shell material, suggesting a low-energy setting with minimal transport to the depositional site. **B.** Core photograph showing mudstone with abundant disarticulated, thin-walled pelecypod valves at 761 feet in Umiat 18. Grain size scale in both photographs graduated in millimeters and centimeters.

a repeating stack of FA3, FA4, and FA5 that gradually become more proximal up-section (sheet 2; fig. 21, see caption for additional discussion).

The SP log and cuttings suggest the flooding surfaces bounding these parasequences are not represented in most of the cores (sheet 6). Most of the lower parasequences consist of offshore transition to lower shoreface–distal delta front deposits and their associated flooding surfaces most likely mark an unknown thickness of sandy strata removed through wave ravinement processes associated with ongoing subsidence and transgressive reworking of abandoned delta lobes (cf. Penland and others, 1988). In all of these parasequences, even though only captured in a few cores, the flooding surface represents an abrupt relative sea level rise. A notable exception to this pattern, is documented in core 11, where carbonaceous mudstone interpreted as bayfill facies rests on a brown-gray, fine-grained sandstone with a mottled appearance suggestive

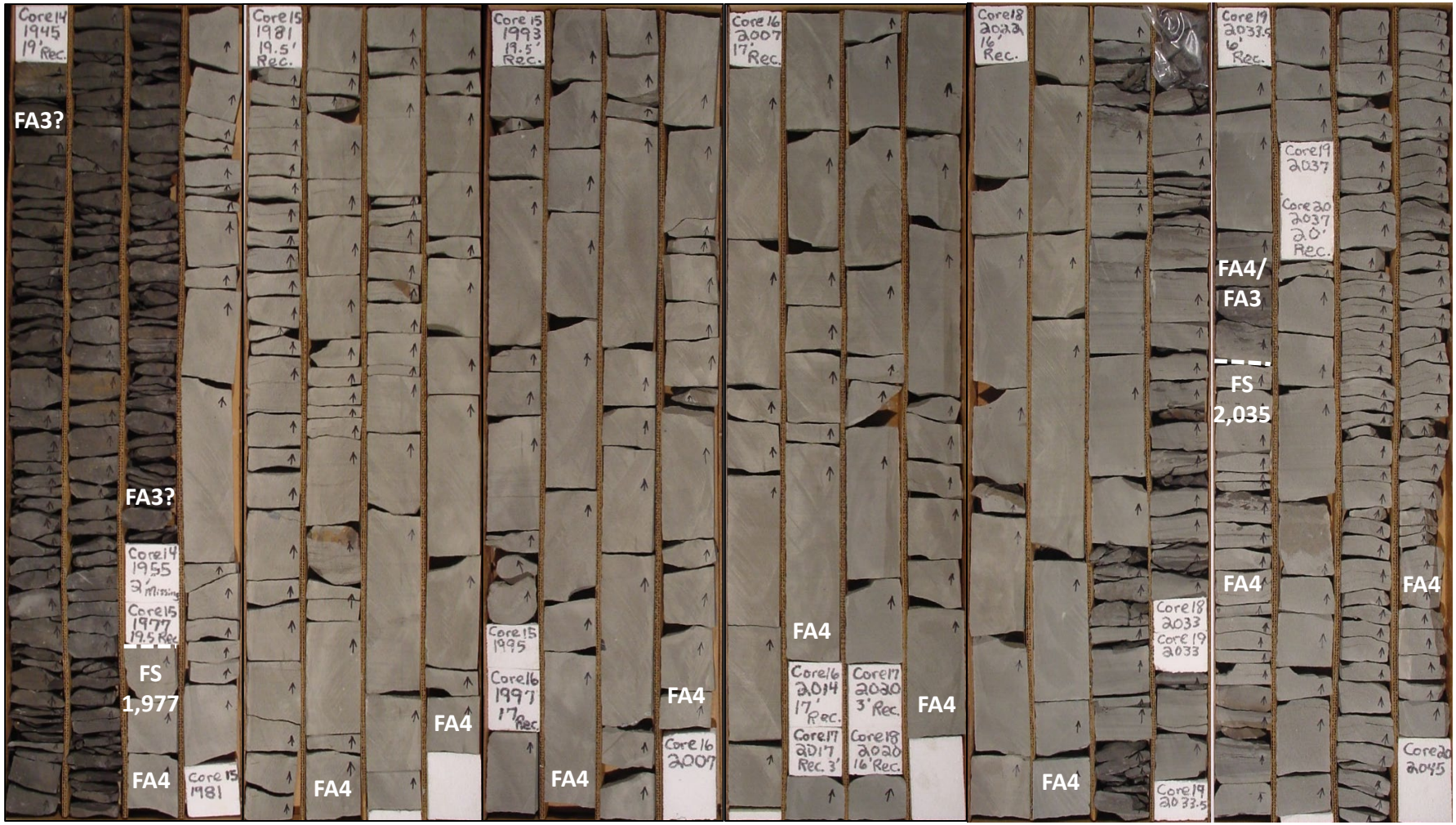

Figure 21. Core box photograph showing the lower part of core 14 (1,945 feet) through the upper part of core 20 (2,045 feet) in Wolf Creek 3. The upper part of core 20 includes amalgamated sandstone of FA4 overlain by a flooding surface at 2,035 feet. This surface is overlain by a thin interval of FA3 or the distal expression of FA4 that grades upward to amalgamated sandstone of FA4 by approximately 2,028 feet. A flooding surface is inferred in the interval between 1,955 feet and 1,977 feet, but that interval is not present in the preserved cores and this surface is shown in the photograph at 1,977 feet. The overlying bioturbated mudstone is tentatively interpreted as offshore transition-prodelta deposits of FA3, but could represent bayfill deposits of FA6, in which case the prominent facies change from sandstone to mudstone shown at 1,977 feet represents uninterrupted shoreline-lower delta plain progradation. Each core row is 3.28 feet (1 meter) long. Core box photos modified from D'Agostino and Houseknecht (2002).

of pedogenic processes (fig. 19). If correctly interpreted, this contact is not a flooding surface, but instead represents an exposure surface and the contact between sandy shorezone or beach berm facies and backshore mudstone in a normal regressive succession. This has been observed at several locations in outcrop to the south and southeast (LePain and others, 2009; LePain and others, 2021a; LePain and others, 2021b).

Square Lake 1

A complete thickness of the Nanushuk Formation was penetrated in Square Lake 1 where, based on Bird's (1988) formation top, the unit is 2,310 feet thick (sheets 3 and 6). The 44 cores cut in the formation are distributed throughout this thickness and document an aggradational–progradational–retrogradational stacking pattern. Despite the lack of robust age control, the retrogradational part of the Nanushuk in Square Lake 1 is likely correlative with the Ninuluk Formation of former usage (Cenomanian age). Core 67, the deepest core in the well, includes bioturbated mudstone with few thin beds of bioturbated very fine-grained sandstone of the distal shelf association (FA2; sheet 3, topset Torok). Based on core, cuttings descriptions (Collins, 1959b), and the SP log, the well penetrated a thick stack of offshore transition–shoreface/delta front parasequences from approximately 3,978 feet to 2,683 feet (repetitious facies stacking pattern of FA2/FA3 to FA4). Cores over this depth interval (cores 66 through 43) contain abundant features commonly associated with storm–wave–influenced lower to middle shoreface environments (HCS, wave ripple cross-lamination, and a widespread, high degree of bioturbation), and some features commonly found in river-dominated deltaic successions (graded beds, abundant macerated terrestrial plant fragments, convolute beds, and unidirectional current indicators). As such, this succession is interpreted as a series of storm-wave-modified delta lobes similar to the succession documented in Wolf Creek 3. Figure 22 shows cores 66 through 61, which include the lowest well-defined parasequence captured in core – note the possible presence of HCS, abundant horizontal laminae, wave ripple cross-laminae, and mudstone rip-up clasts, all of which are common features in high-energy, storm wave-influenced shoreface settings. Cores, cuttings, and the SP log motif from cores 66 through 46 (3,918 to 3,087 feet) are consistent with a progradational stack of sandier-upward parasequences typical of a prograding series of storm wave-influenced delta lobes (sheets 3 and 5).

The sandy succession in cores 45 and 44 has a slight coarsening-upward grain size trend, is thoroughly bioturbated but includes some preserved remnants of wave ripple cross-laminae, which are consistent with deposition in a lower energy, lower to middle shoreface setting (FA4) or an abandoned distributary mouth bar (FA5). An alternative interpretation based on the SP log response through this interval (3,066 feet to 3,027 feet), although not favored, is that it represents the fill of an abandoned distributary channel (FA5). A flooding surface is inferred at the top of core 44, or in the uncored interval between 2,970 and the top of the core. Cuttings and the SP log through the overlying uncored interval indicate a succession of interbedded clay shale, siltstone, and minor sandstone, possibly similar to the lithologies in core 43. Fine-grained lithologies in core 43 are moderately to highly bioturbated, indicating deposition in a marine setting interpreted as distal bayfill (FA6). Facies deposited on the seaward side of an interdistributary bay open to the sea could be similar, and indistinguishable, from facies deposited in a distal shelf setting. Given the overall context, we favor the distal bayfill interpretation.

Core 42 through the lower 10 feet of core 33 (from approximately 2,683 feet to 1,886 feet) penetrate a succession of interbedded mudstone, siltstone, and sandstone (sheet 3). Mudstone is generally moderately to highly bioturbated (BI 3 to 5), but locally is sparsely bioturbated (BI 1) with only slightly disrupted horizontal laminations. Abundant carbonaceous plant material on parting surfaces in core 40, thin accumulations of carbonaceous claystone (or high-ash coal) in cores 38 and 37, including possible rhizoliths in core

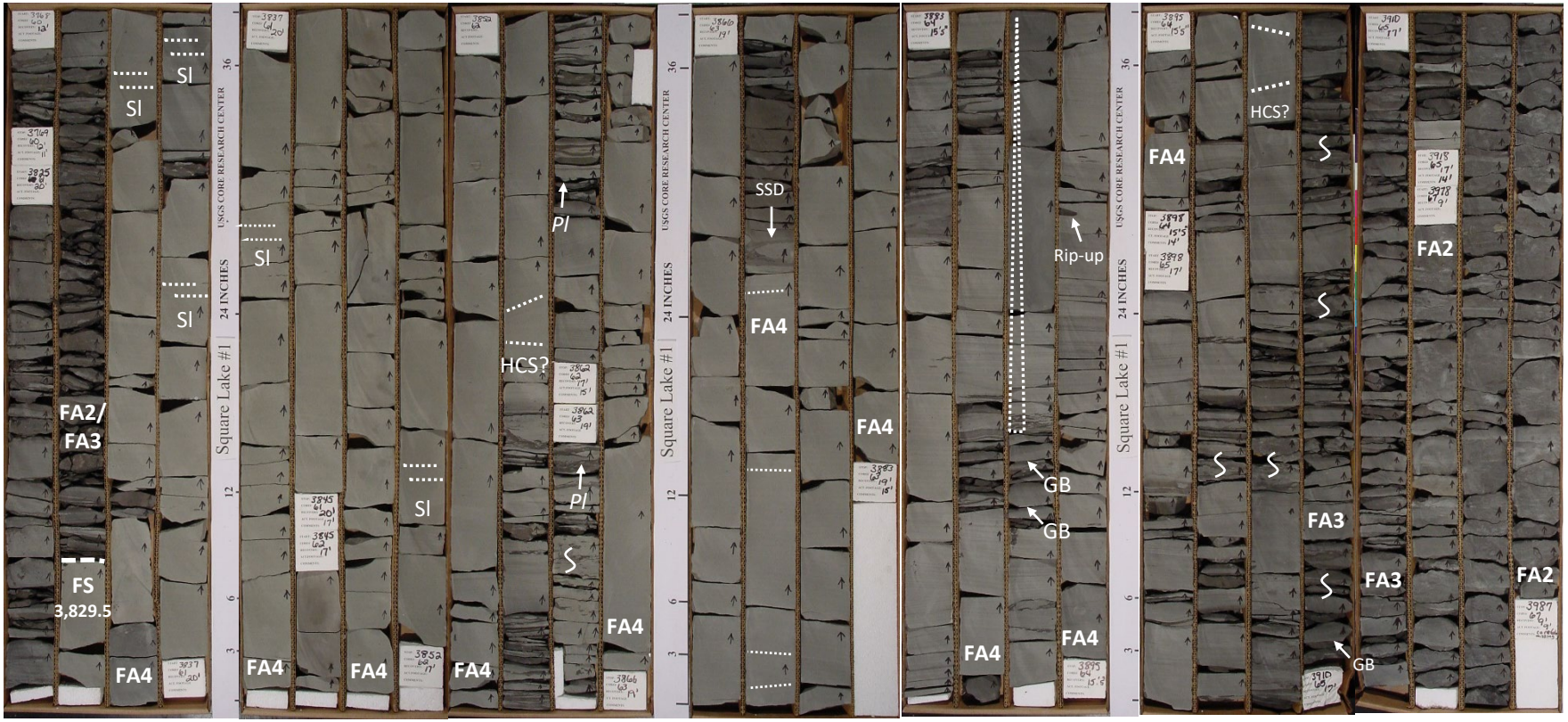

Figure 22. Core box photographs from Square Lake 1 showing the sandier-upward succession from 3,918 feet to approximately 3,829.5 feet, illustrating the gradual change up–section from FA3 to FA4. Note the interval from 3,910 feet to 3,918 feet is core 66 and is mislabeled as core 65 in these boxes (USGS split). The lower nine feet of core 67 consist of FA2. The vertical stacking pattern records progradation of a storm-wave-influenced delta lobe. The heavy white dashed line denotes the flooding surface at the top of the parasequence at 3,829.5 feet. Note the possible HCS, abundant horizontal laminations (SI), thin graded beds (GB with white arrow pointing to base of bed), thick graded bed shown with white dashed triangle, soft-sediment deformation (SSD), and *Planolites* burrows (PI). Bioturbation shown by white curvilinear line, as defined on Sheets 1–5. Each core row is 3.28 feet (1 meter) long. Core box photos modified from D'Agostino and Houseknecht (2002).

37, suggest deposition in a lower delta plain bayfill setting (FA6). Abundant very fine- to fine-grained sandstone in thin to medium, solitary beds (sheet 3, cores 41 and 38) distributed in random order, and similar beds arranged in both coarsening- and fining-upward successions (sheet 3, cores 35 and 34 from approximately 1,931 feet to 1,912.5 feet, and core 37 from 2,032 feet to 2,020 feet, respectively) record deposition as overbank splays, small crevasse deltas, and abandoned crevasse channels, respectively (Elliot, 1974). The latter two emanated from distributary channels through breaches in flanking levees inferred to be nearby. The degree of bioturbation in the sandstone ranges from absent (BI 0) to moderate (BI 3) and recognizable traces suggest a low to moderate diversity assemblage consistent with deposition in an interdistributary bay setting (FA6), with salinities ranging from near normal marine to brackish due to episodic incursions of fresh water during floods (Bhattacharya, 2006).

The quartz-chert pebble lag at approximately 1,886 feet in core 33 marks a dramatic change in facies stacking pattern (fig. 23 and sheet 3). The lag rests on an erosion surface that truncates bayfill facies and is overlain by shoreface–delta front deposits. The origin of the pebble lag is unclear—it could represent a remnant of coarser-grained material that bypassed the site during the falling stage and early lowstand systems tracts, or a transgressive lag deposited on a sequence boundary. In the former scenario, the lag rests on a regressive surface of marine erosion and in the latter, the lag rests on a composite surface consisting of a sequence boundary that was modified during the ensuing transgression (ravinement). The latter is the favored interpretation (LePain and Kirkham, 2001; LePain and others, 2018), but good quality seismic data are needed to determine which is correct. The few feet of interbedded fine-grained sandstone and mudstone immediately above the pebble lag is sparsely bioturbated and includes wave ripple cross-lamination (in sandstone); the amalgamated sandstone package from 1,884–1,841 feet (upper part of core 33 and continuing in cores 32 and 31) includes abundant horizontal laminae and conspicuous broken and abraded pelecypod fragments of the genus *Inoceramus* (fig. 23). The SP log response through this interval is barrel-shaped (sheet 6). The succession below the pebble lag is interpreted as highstand deposits and above as a shoreface-delta-front succession associated with a subsequent lowstand of relative sea level (or forced regression during falling relative sea level).

LePain and others (2009) recognized two sharp-based shoreface successions in the upper 190 feet of the Nanushuk at Ninuluk Bluff, located approximately 30 miles south of Square Lake 1, that they interpreted as forming during falling stage systems tracts. Available data are insufficient to allow correlation of the pebble lag at 1,886 feet in Square Lake 1 to the outcrop at Ninuluk Bluff. A similar surface has not been identified in the Wolf Creek 3 well, located approximately 14 miles to the southwest of Square Lake 1, where the corresponding succession may have been removed due to uplift and erosion on the Wolf Creek anticline (Mull and others, 2005).

The remaining Nanushuk cores from Square Lake 1 (sheet 3, cores 30 to 22; SP log shown on sheet 6) document a stack of parasequences comprised of offshore transition/distal prodelta (FA3), shoreface-delta front (FA4), and mouthbar deposits (FA5). Very fine- and fine-grained sandstone with few broken *Inoceramus* shells in core 24 is interpreted as proximal mouth bar-distributary channel-fill deposits (FA5). Closely spaced carbonaceous-rich laminae between 1,728–1,726 feet in core 26 suggest possible tidal influence. Robust age control is not available for this interval, but some sandstone appears tuffaceous, as seen in the upper part of the Nanushuk (Cenomanian) in outcrops along the Colville River.

Grandstand 1

Grandstand 1 spudded in a mantle of unconsolidated deposits, penetrated the top of the Nanushuk Formation at a depth of 110 feet (below top of Kelly bushing), and reached total depth in the Torok Formation at 3,939 feet (Robinson,

1958). Based on facies criteria observed in core, the Torok—Nanushuk contact is placed in the depth interval between cores 44 and 45 (fig. 24; sheet 5, 2,712 feet to 2,926 feet), which is slightly deeper than Robinson's (1958) placement of the contact at 2,650 feet, and significantly deeper than Bird's (1988) placement at 1,070 feet. Core 45 consists of unbioturbated silty clayshale dipping approximately 20 degrees that is interpreted as slope deposits that were involved in a mass-wasting event (FA1; fig. 24). Core 44 consists of moderately to highly bioturbated silty clayshale and interbedded lightly bioturbated siltstones interpreted as distal shelf deposits (FA2). Core 46 includes sparsely bioturbated silty clayshale of FA1 and is the only core below core 44 that includes visible bioturbation. All deeper cores (core 47 to 52) are devoid of visible bioturbation and record deposition in a slope setting with conditions unfavorable to burrowing infaunas. Core 46 may record a sea level lowstand during which a low diversity, burrowing infauna colonized part of the upper slope. The

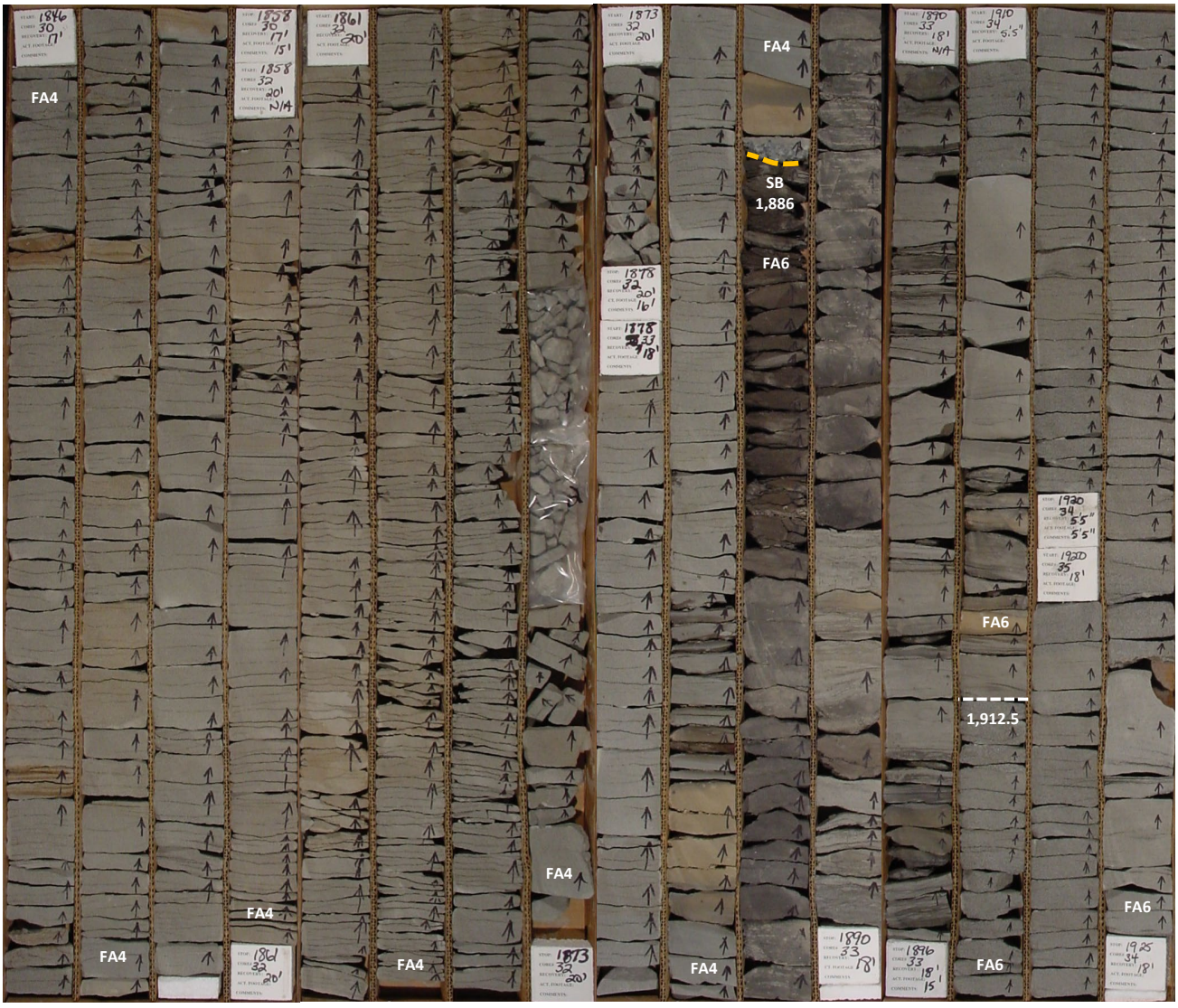

Figure 23. Core box photographs from Square Lake 1 showing bayfill deposits (FA6) truncated by an erosion surface at 1,886 feet marked by a chert-quartz pebble lag. This surface is interpreted as a sequence boundary (SB) that was subsequently modified during transgression. The overlying shoreface—delta front succession that extends to the top of core 31 (1,841 feet, not shown in this figure) is interpreted as a lowstand deposit unrelated to the pebble lag (or related to forced regression during a subsequent episode of falling relative sea level). Core 31 is mislabeled in photograph as core 30. Each core row is 3.28 feet (1 meter) long. Core box photographs modified from D'Agostino and Houseknecht (2002).

Figure 24. Core box photographs from Grandstand 1 showing slope (FA1) deposits of the Torok Formation in core 45 and distal shelf deposits (FA2) of the Nanushuk Formation in cores 44 through 42. Note the dip of strata in core 45 and the absence of bioturbation fabrics. These features suggest deposition in a slope setting that experienced occasional mass-wasting events. Note the bioturbated appearance of cores 44 through 42, which is interpreted to indicate deposition in a distal shelf setting, below storm wave base. Each core row is 3.28 feet (1 meter) long. Core box photographs modified from D'Agostino and Houseknecht (2002).

slope setting at this location was prone to small- to moderate-sized mass-wasting events manifesting as rotational slump blocks (cores 52, 50, 49, 47, and 45; fig. 25). Smaller scale soft-sediment deformation is evident in some of these cores (fig. 25, white arrows). Core 45's position between bioturbated mudstones in cores 46 and 44, and a short stratigraphic distance below our placement of the Nanushuk–Torok contact, leaves open the possibility that it represents a shelf-edge failure.

The shallower cores from Grandstand 1 record an aggradational-progradational stack of distal shelf, prodelta, shoreface-delta front, delta front, and bayfill deposits. Core 21 is tentatively interpreted as mouthbar deposits of FA5, and cores 20 and 19 as distributary channel deposits, also of FA5. Core 10 from 829 feet to approximately 833.3 feet is interpreted as mouth bar deposits, but the prominent scour surface suggests this interval could be a thin distributary channel-fill succession. The retrogradational package present in the cored succession in the upper part of the Nanushuk in Square Lake 1 is not present in the cores from Grandstand 1, possibly due to uplift and erosion associated with the Grandstand anticline. Overall, the cored succession below a depth of 791 feet consists of a stack of deltaic parasequences that record deposition in more river-dominated settings than documented in the Wolf Creek 3 and Square Lake 1 cores.

RESERVOIR POTENTIAL

The sandier-upward parasequences captured in the studied cores represent episodes of shorezone-nearshore progradation punctuated by marine flooding surfaces. In accordance with Walter's Law, progradation of a single storm wave-influenced delta lobe should produce a sandier-upward succession consisting of the following facies associations, in ascending order, offshore transition—prodelta (FA3), shoreface—delta front (FA4), capped by the most shoreline proximal deposits, depending on position along the coastline. Capping associations can include distributary mouth bar (FA5), distributary channel-fill (FA5), and a variety of off-channel axis deposits, including spit, foreshore, eolian dune, and bayfill facies (FA6). Foreshore and eolian dune facies have not been recognized in the studied cores, and spit deposits would be difficult to recognize in a single one-dimensional core. In all of the wells, with the exception of Fish Creek 1, older, more distal parasequences lack these proximal caps and the sandier-upward successions are truncated by marine flooding surfaces that are overlain by muddy distal shelf or offshore transition deposits (FA2 or FA3, respectively). In more proximal settings, some sandier-upward parasequences culminate in distributary mouth bar-channel deposits (FA5) that are truncated by marine flooding surfaces and overlain by offshore transition-prodelta deposits (FA3). In a few cores from the most proximal settings in Wolf Creek 3, Square Lake 1, and Grandstand 1, the most proximal parasequences are capped by muddy bayfill deposits (FA5) resting on sandstones with poorly developed rhizoliths.

Sandier-upward deltaic parasequences represent attractive stratigraphic traps, with overlying muddy facies potentially providing an effective reservoir topseal. Shorezone facies associations overlain by muddy sealing facies could comprise leaky traps if connected to a distributary channel capable of serving as a conduit for continued up-dip migration of hydrocarbons. Erosion associated with transgressive reworking at the top of distal parasequences and many of the more proximal parasequences resulted in top-truncated shoreline-delta lobe shingles in which the upper part of progradational successions is missing. If erosion removed a

Figure 25, next page. Core box photographs from Grandstand 1 showing slope (FA1) deposits of Torok Formation in cores 49 through 45. Note the dip of strata in all cores and the absence of bioturbation fabrics. These features suggest deposition in a slope setting that experienced occasional mass-wasting events manifested here as rotated slump blocks. Note smaller-scale soft-sediment deformation in core 49 (white arrows). Each core row is 3.28 feet (1 meter) long. Core box photographs modified from D'Agostino and Houseknecht (2002).


Core44
2717
Core45
2926
20' Rec.
Core45
2932
20'
Rec.
Core49
3730
12' Rec.
Core49
3733
12' Rec.
Core45
2946
Rec.
Core46
3170
19.5 Rec
Core45
2932
Core46
3171
Core49
3733
Core49
3742
Core50
3902
8' Rec.

significant thickness of section, it is possible that thinner distributary channel-fills were completely removed, thereby eliminating one of the primary conduits for stratigraphic trap leakage. The amount of section removed by wave ravinement during transgression varies from inches to over 130 feet (Kraft and others, 1987, Nummedal and Swift, 1987), with an estimated average ranging from 32–66 feet in the Cretaceous Western Interior (Bhattacharya and Willis, 2001; Bergman and Walker, 1988). The low end of this average range is potentially enough to completely remove a distributary channel-fill, thus eliminating a potential conduit for leakage. A 97-foot-thick sandstone body consisting of at least two amalgamated channel-fills was documented in the Nanushuk in the Wainwright 1 well (LePain and Decker, 2016). The high end of the average range of section removed by transgressive ravinement is not enough to remove the entire thickness of a composite channel-fill of similar thickness, but the high end of the overall range documented by Kraft and others (1987) and Nummedal and Swift (1987) would remove the entire thickness of the composite channel in the Wainwright 1 well. The stratigraphic trap potential of delta lobes near the base of the formation, combined with available data that suggests Torok slope deposits represent effective hydrocarbon carrier beds (Hayba and others, 2002), makes them highly attractive exploration targets from the central part of the NPRA to the terminal Nanushuk shelf margin east of the Colville River. Recent discoveries at Willow, West Willow, and Pikka demonstrate the stratigraphic trap potential of Nanushuk lowstand shelf-margin deltas (Houseknecht, 2019). Shoreface and delta front parasequences in highstand settings overlain by transgressive mudstone could also represent attractive exploration targets if conduits for up-dip leakage of fluids are absent and the deposits have access to charge. An outcropping bed of friable sandstone in the upper part of the Nanushuk at Rooftop Ridge, southeast of Umiat, emits a light hydrocarbon odor demonstrating at least some access to charge in highstand deposits at that location (RR next to blue square on fig. 1; LePain and others, 2021).

ACKNOWLEDGMENTS

The former staff at the U.S. Geological Survey's Core Research Center, particularly Bill Linenberger and Bill Whitus, laid out the Square Lake 1 and Wolf Creek 3 cores during visits in the Fall of 2000 and early Winter of 2001. Kurt Johnson, Jean Riordan, Alexandra Busk, and Walter Zimmerman laid out splits of these cores and the Fish Creek 1, Grandstand 1, and Umiat 18 cores at the Alaska Geologic Materials Center (GMC) during several visits between 2017 and 2019. Our work on the Nanushuk Formation, both in outcrop and in core, has benefited significantly from work on the formation by former U.S. Geological Survey geologists Florence Rucker Collins, Florence Robinson (Weber), Ken Bird, Thomas Ahlbrandt, Curtis Huffman, James Fox, and Cornelius Molenaar, and from more recent work on the formation by David Houseknecht. Nina Harun (Alaska Division of Geological & Geophysical Surveys) and Dr. Bill Morris (ConocoPhillips, retired) reviewed the manuscript and provided valuable suggestions for its improvement. We gratefully acknowledge the efforts of all these individuals. Funding was provided over the past 22 years by an industry consortium comprised of various companies, including Anardarko Petroleum, BP Exploration, Chevron USA Production Company, ConocoPhillips (and ARCO), Encana, Eni, Oil Search, PetroCanada, Pioneer Resources, Shell Western Exploration and Production, TotalFinaElf, and Unocal; some of these companies no longer exist. Additional funding was provided by the U.S. Geological Survey and the State of Alaska.

REFERENCES

Ahlbrandt, T.S., Huffman, A.C., Fox, J.E., Pasternack, I., 1979, Depositional framework and reservoir-quality studies of selected Nanushuk Group outcrops, North Slope, Alaska, *in* Ahlbrandt, T.S., ed., Preliminary Geologic, Petrologic, and Paleontologic Results of the Study of Nanushuk Group Rocks, North Slope, Alaska: U.S. Geological Survey Circular 794, p. 14–31.

Alaska Oil and Gas Conservation Commission, Umiat 18 Well History, accessed July 16, 2021. http://aogweb.state.ak.us/WebLink/DocView.aspx?id=71628&searchid=ddc3d3fe-0b7f-46d8-bf97-69f2576b972a&dbid=0

Bergman, K.M., and Walker, R.G., 1988, Formation of Cardium erosion surface E5, and associated deposition of conglomerate: Carrot Creek field, Cretaceous Western Interior Seaway, Alberta, *in* James, D.P., and Leckie, D.A., eds., Sequences, Stratigraphy, Sedimentology: Surface and Subsurface: Canadian Society of Petroleum Geologists Memoir 15, p. 15–24.

Bhattacharya, J.P., 2006, Deltas, *in* Posamentier, H.W., and Walker, R.W., eds. Facies Models Revisited: SEPM Special Publication 84, p. 237–292.

Bhattacharya, J.P., and Giosan, L., 2003, Wave-influenced deltas: geomorphological implications for facies reconstruction: Sedimentology, v. 50, p. 187–210.

Bhattacharya, J.P., and MacEachern, J.A., 2009, Hyperpycnal rivers and prodeltaic shelves in the Cretaceous Seaway of North America, Journal of Sedimentary Research, v.79, p. 184–209.

Bhattacharya, J., and Walker, R.G., 1991, Facies and facies successions in river- and wave-dominated depositional systems of the Upper Cretaceous Dunvegan Formation, northwestern Alberta: Bulletin of Canadian Petroleum Geology, p. 165–191.

Bhattacharya, J.P., and Willis, B.J., 2001, Lowstand deltas in the Frontier Formation, Powder River Basin, Wyoming: Implications for sequence stratigraphic models: AAPG Bulletin, v. 85, p. 261–294.

Bird, K.J., 1988, Alaskan North Slope stratigraphic nomenclature and data summary for government-drilled wells, *in* Gryc, G., ed., Geology and Exploration of the National Petroleum Reserve in Alaska, 1974 to 1982: U.S. Geological Survey Professional Paper 1399, p. 314–353.

Bird, K.J., and Molenaar, C.M.,1992, The North Slope foreland basin, Alaska, *in* Macqueen, R.W., and Leckie, D.A., eds., Foreland Basins and Fold Belts: AAPG Memoir 55, p. 363–393.

Boyd, R., Dalyrymple, R., and Zaitlin, B.A., 1992, Classification of clastic coastal depositional environment: Sedimentary Geology, v. 80, p. 139–150.

Brown, L.F., and Fisher, W.L., 1969, Delta systems in other basins, *in* W. L. Fisher, L. F. Brown, Jr., A. J. Scott, and J. H. McGowen, eds., Delta Systems in the Exploration for Oil and Gas: Texas Bureau of Economic Geology, p. 67–78.

Clifton, H.E., 2006, A reexamination of facies models for clastic shoreline, *in* Posamentier, H.W., and Walker, R.W., eds. Facies Models Revisted: SEPM Special Publication 84, p. 293–337.

Collins, F.R., 1959a, Fish Creek Test Well 1, *in* Robinson, F.M., and Collins, F.R., eds., Core Test, Sentinel Hill Area, and Test Well, Fish Creek Area, Alaska: U.S. Geological Survey Professional Paper 305-I, p. 501-521, 1 plate.

———1959b, Test wells, Square Lake and Wolf Creek Areas: U.S. Geological Survey Professional Paper 305-H, 484 p., 2 plates.

D'Agostino, S.L., and Houseknecht, D.W, 2002, Core Photographs–Digital Archive, *in* Houseknecht, D.W., ed., National Petroleum Reserve–Alaska (NPRA) Core Images and Well Data: U.S. Geological Survey Digital Data Series, DDS-75, Disk 4.

Decker, P.L., LePain, D.L., Wartes, M.A., Gillis, R.J., Mongrain, J.R., Kirkham, R.A., and Shellenbaum, D.P., 2009, Sedimentology, stratigraphy, and subsurface expression of upper Cretaceous strata in the Sagavanirktok River area, east-central North Slope, Alaska: Alaska Division of Geological & Geophysical Surveys, 3 sheets. https://doi.org/10.14509/30156

Droser, M.L., and Bottjer, D.J., 1986, A semiquantitative field classification of ichnofabric: Journal of Sedimentary Petrology, v. 56, p. 558–559.

Duke, W.L., Arnott, R.W.C., and Cheel, R.J., 1991, Shelf sandstones and hummocky cross-stratification—New insights on a stormy debate: Geology, v. 19, p. 625–628.

Elliott, T., 1974, Interdistributary bay sequences and their genesis: Sedimentology, v. 21, p. 611–622.

Galloway, W.E., and Hobday, D.K., 1996, Terrigenous Clastic Depositional Systems: Springer-Verlag, Berlin, 489 p.

Hayba, D.O., Bird, K.J., and Garrity, C.P., 2002, Subsurface oil and gas indications in and adjacent to the NPRA, *in* Houseknecht, D.W., ed., National Petroleum Reserve—Alaska (NPRA) Core Images and Well Data: Digital Data Series DDS–75, Disk 3.

Helmold, K.P., and LePain, D.L., 2021, Sedimentary petrology, reservoir quality, and provenance of Albian–Cenomanian Nanushuk Formation sandstone, NPRA test wells, Umiat 18, and measured outcrop sections, central North Slope, Alaska *in* LePain, D.L., and Helmold, K.P., eds., Sedimentology and Reservoir Quality of the Nanushuk Formation (Albian-Cenomanian) in Cores from the National Petroleum Reserve–Alaska and Adjoining State Lands to the South: Alaska Division of Geological & Geophysical Surveys Report of Investigation 2021-4B. https://doi.org/10.14509/30728

Herriott, T.M., Wartes, M.A., Decker, P.L., Gillis, R.J., Shellenbaum, D.P., Willingham, A.L., and Mauel, D.J., 2018, Geologic map of the Umiat-Gubik area, central North Slope, Alaska: Alaska Division of Geological & Geophysical Surveys Report of Investigation 2018-6, 55 p., 1 sheet, scale 1:63,360. http://doi.org/10.14509/30099

Horne, J.C., Ferm, J.C., Caruccio, F.T., and Baganz, B.P., 1978, Depositional models in coal exploration and mine planning in Appalachian region: AAPG Bulletin, v. 62, p. 2,379–2,411.

Houseknecht, D.W., 2019, Petroleum systems framework of significant new oil discoveries in a giant Cretaceous (Aptian-Cenomanian) clinothem in Arctic Alaska: AAPG Bulletin, v. 103, p. 619–652.

Houseknecht, D.W., Bird, K.J., and Schenk, C.J., 2008, Seismic analysis of clinoform depositional sequences and shelf-margin trajectories in Lower Cretaceous (Albian) strata, Alaska North Slope: Basin Research, 11 p.

Houseknecht, D.W., and Schenk, C.J., 2001, Depositional sequences and facies in the Torok Formation, National Petroleum Reserve–Alaska (NPRA), *in* Houseknecht, D.W., ed., NPRA Core Workshop: Petroleum Plays and Systems in the National Petroleum Reserve–Alaska, p. 179–199.

Huffman, A.C., Ahlbrandt, T.S., Bartsch-Winkler, S., 1988, Sedimentology of the Nanushuk Group, North Slope, *in* Gryc, G., ed., Geology and Exploration of the National Petroleum Reserve in Alaska, 1974 to 1982: U.S. Geological Survey Professional Paper 1399, p. 281–298.

Huffman, A.C., Ahlbrandt, T.S., Pasternack, I., Stricker, G.D., and Fox, J.E., 1985, Depositional and sedimentologic factors affecting the reservoir potential of the Cretaceous Nanushuk Group, central North Slope, Alaska, *in* Huffman, A.C., ed., Geology of the Nanushuk Group and Related Rocks, North Slope, Alaska: U.S. Geological Survey Bulletin 1614, p. 61–74.

Kraft, J.C., Chrzastowski, Belnap, D.F., Toscano, M.A., and Fletcher, C.H., 1987, The transgressive barrier-lagoon coast of Delaware: Morphostratigraphy, sedimentary sequences and responses to relative rise in sea level, *in* Nummedal, D., Pilkey, O.H., and Howard, J.D., eds., Sea-Level Fluctuation and Coastal Evolution: SEPM Special Publication No. 41, p. 129–143.

Lease, R.O., and Houseknecht, D.W., 2017, Timing of Cretaceous shelf margins in the Colville basin, Arctic Alaska: AAPG Pacific Section Annual Meeting, Anchorage, Alaska, May 21–24, 2017; accessed January 12, 2021. http://www.search0anddiscovery.com/abstracts/pdf/2018/90302ps/abstracts/ndx_lease.pdf

LePain, D.L., and Decker, P.L., 2016, Lithofacies analysis of the Wainwright #1 continuous core, western Arctic Slope, Alaska: Transition from lower to upper delta plain environments in the Albian-Cenomanian Nanushuk Formation, *in* LePain, D.L., Stratigraphic and reservoir quality studies of continuous core from the Wainwright #1 coalbed methane test well, Wainwright, Alas-

ka: Alaska Division of Geological & Geophysical Surveys Report of Investigation 2016-3-2, p. 5-35, 1 sheet. http://doi.org/10.14509/29656

LePain, D.L., Decker, P.L., and Helmold, K.P., 2018, Brookian core workshop: Depositional setting, potential reservoir facies, and reservoir quality in the Nanushuk Formation (Albian-Cenomanian), North Slope, Alaska: Alaska Division of Geological & Geophysical Surveys Miscellaneous Publication 166, 58 p. https://doi.org/10.14509/30137

LePain, D.L., Helmold, K.P., Wartes, M.A., and Decker, P.L., 2017, Depositional setting and potential reservoir facies in the Nanushuk Formation (Albian-Cenomanian), Brookian topset play, North Slope, Alaska: AAPG Pacific Section Meeting, 21-24 May, 2017, Anchorage, AK, Program and Abstracts, p. 74.

LePain, D.L., and Kirkham, Russell, 2001, Potential reservoir facies in the Nanushuk Formation (Albian-Cenomanian), central North Slope, Alaska: Examples from outcrop and core, *in* Houseknecht, D.W., ed., NPRA core workshop: Petroleum plays and systems in the National Petroleum Reserve in Alaska: SEPM Core Workshop 21, p. 19–36.

LePain, D.L., Kirkham, R.A., and Montayne, Simone, 2021a, Measured stratigraphic section, Nanushuk Formation (Albian–Cenomanian), Nanushuk River (Rooftop Ridge), Alaska: Alaska Division of Geological & Geophysical Surveys Preliminary Interpretive Report 2021-5, 8 p., 1 sheet. https://doi.org/10.14509/30744

LePain, D.L., Harun, N.T., and Kirkham, R.A., 2021b, Measured stratigraphic section, lower Nanushuk Formation (Albian), Arc Mountain anticline, Nanushuk River, Alaska: Alaska Division of Geological & Geophysical Surveys Preliminary Interpretive Report 2021-6, 15 p., 1 sheet. https://doi.org/10.14509/30762

LePain, D.L., McCarthy, P.J., and Kirkham, R.A., 2004, Outcrop expression of sequence boundaries in the Albian–Cenomanian Nanushuk Formation, central North Slope, Alaska: AAPG 2004 Annual Convention Abstract Volume, p. A82.

———2009, Sedimentology and sequence stratigraphy of the middle Albian-Cenomanian Nanushuk Formation in outcrop, central North Slope, Alaska: Alaska Division of Geological & Geophysical Surveys Report of Investigation 2009-1 v. 2, 76 p., 1 sheet. http://doi.org/10.14509/19761

MacEachern, J.A., Bann, K.L., Bhattacharya, J.P., and Howell, C.D., 2005, Ichnology of deltas: Organism responses to the dynamic interplay of rivers, waves, storms, and tides, *in* Giosan, L., and Bhattacharya, J.P., eds., River Deltas—Concepts, Models, and Examples: SEPM Special Publication 83, p. 49–85.

Molenaar, C.M., 1982, Umiat field, an oil accumulation in a thrust-faulted anticline, North Slope Alaska: Rocky Mountain Association of Geologists, v. 2, p. 537–548.

Mulder, T., and Alexander, J., 2001, The physical character of subaqueous sedimentary density flows and their deposits: Sedimentology, v. 48, p. 269–299.

Mulder, T., Syvitski, J.P.M., Migeon, S., Faugeres, J.C., and Savoye, B., 2003, Marine hyperpycnal flows: initiation, behavior and related deposits: Marine and Petroleum Geology, v. 20, p. 861–882.

Mull, C.G., Houseknecht, D.W., Pessel, G.H., and Garrity, C.P., 2005, Geologic map of the Ikpikpuk River Quadrangle, Alaska: U.S. Geological Survey Scientific Investigations Map 2817-B, 1 sheet, scale 1:250,000.

Mull, C.G., 1985, Cretaceous tectonics, depositional cycles, and the Nanushuk Group, Brooks Range and Arctic Slope, Alaska, *in* Huffman, A.C., ed., Geology of the Nanushuk Group and related rocks, North Slope, Alaska: U.S. Geological Survey Bulletin 1614, p. 7–36.

Myrow, P.M., and Southard, J.B., 1996, Tempestite deposition: Journal of Sedimentary Research, v. 66, p. 875–887.

Nelson, P.H., and Kibler, J.E., 2001, Porosity and permeability data and plots for the National Petroleum Reserve–Alaska, *in* Houseknecht, D.W., ed., National Petroleum Reserve–Alaska (NPRA) Core Images and Well Data: U.S. Geological Survey Digital Data Series, DDS-75, Disk 3.

Nummedal, D., and Swift, D.J.P., 1987, Transgressive stratigraphy at sequence-bounding unconformities: Some principles derived from Holocene and Cretaceous examples, *in* Nummedal, D., Pilkey, O.H., and Howard, J.D, eds., Sea-Level

Fluctuations and Coastal Evolution: SEPM Special Publication No. 41, p. 241–260.

Olariu, C., Steel, R.J., and Petter, A.L., 2010, Delta-front hyperpycnal bed geometry and implications for reservoir modeling: Cretaceous Panther Tongue delta, Book Cliffs, Utah: AAPG Bulletin, v. 94, p. 819–845.

Pemberton, S.G., and Wightman, D.M., 1992, Ichnological characteristics of brackish water deposits, in Applications of ichnology to petroleum exploration; a core workshop: SEPM Core Workshop 17, p. 141–167.

Penland, S., Boyd, R., and Suter, J.R., 1988, transgressive depositional systems of the Mississippi delta plain: A model for barrier shoreline and shelf sand development: Journal of Sedimentary Petrology, v. 58, v. 932–949.

Reading, H.G. and Collinson, J.D., 1996, Clastic Coasts. Sedimentary Environments: Processes, Facies and Stratigraphy. Blackwells, Cornwall, p. 154–231.

Reed, J.C., 1958, Exploration of Naval Petroleum Reserve No. 4 and adjacent areas, northern Alaska, 1944-53; Part 1, History of the exploration: U.S. Geological Survey Professional Paper 301, 192 p., 2 sheets, scale 1:1,000,000.

Robinson, F.M., 1958, Test well, Grandstand area, Alaska: U.S. Geological Survey Professional Paper 305-E, p. 317–339, 1 sheet.

Ryer, T.A., and Anderson, P.B., 2004, Facies of the Ferron Sandstone, east-central Utah, *in* Chidsey, T.C., Adams, R.D., and Morris, T.H., eds., Regional to Wellbore Analog for Fluvial-Deltaic Reservoir Modeling: The Ferron Sandstone of Utah: AAPG Studies in Geology 50, p. 59–78.

Scott, A.J., and Fisher, W.L., 1969, Delta Systems and Deltaic Deposition, *in* Fisher, W.L., Brown Jr., L.F., Scott, A.J., and McGowen, J.H., eds., Delta Systems in the Exploration for Oil and Gas: Texas Bureau of Economic Geology, p.10–29.

Shimer, G.T, McCarthy, P.J., and Hanks, C.L., 2014, Sedimentology, stratigraphy, and reservoir properties of an unconventional, shallow, frozen petroleum reservoir in the Cretaceous Nanushuk Formation at Umiat field, North Slope, Alaska: AAPG Bulletin, v. 98, no. 4, p. 631–661.

Taylor, A.M., and Goldring, R., 1993, Description and analysis of bioturbation and ichnofabric: Journal of the Geological Society of London, v. 150, p. 141–148.

Walker, R.G., Duke, W.L., and Leckie, D.A. 1983, Hummocky stratification: Significance of its variable bedding sequences: Geological Society of America Bulletin, v. 94, p. 1,245–1,249.

Walker, R.G., and Plint, A.G., 1992, Wave- and storm-dominated shallow marine systems, *in* Walker, R.G., and James, N.P., eds., Facies Models: A Response to Sea Level Change: Geoscience Canada, p. 219–238.

Weimer, P., 1987, Seismic stratigraphy of three areas of lower slope failure, Torok Formation, northern Alaska, *in* Tailleur, I., and Weimer, P., eds., Alaskan North Slope Geology: Bakersfield, Society of Economic Paleontologists and Mineralogists, Pacific Section, p. 481–496.

Wilson, F.H., Hults, C.P., Mull, C.G., and Karl, S.M., 2015, Geologic map of Alaska: U.S. Geological Survey Scientific Investigations Map 3340, 196 p., 2 sheets, scale 1:1,584,000. https://alaska.usgs.gov/science/geology/state_map/interactive_map/AKgeologic_map.html

CHAPTER B: SEDIMENTARY PETROLOGY, RESERVOIR QUALITY, AND PROVENANCE OF ALBIAN–CENOMANIAN NANUSHUK FORMATION SANDSTONE, NPRA TEST WELLS, UMIAT 18, AND MEASURED OUTCROP SECTIONS, CENTRAL NORTH SLOPE, ALASKA

Kenneth P. Helmold[1] and David L. LePain[2]

INTRODUCTION

Hydrocarbon discoveries announced between 2015 and 2018 that are associated with stratigraphic traps in the Nanushuk Formation on the North Slope of Alaska have spurred renewed interest in exploration of the Colville basin. These discoveries form two roughly parallel fairways: a western trend that includes the Willow and West Willow oil accumulations and an eastern trend comprising the Pikka, Narwhal, and Horseshoe oil accumulations (fig. 1). Recoverable resources are estimated to be more than 300 million barrels at Willow and West Willow, and 500 to 1200 million barrels at Pikka, Narwhal, and Horseshoe (Houseknecht, 2019).

Exploration drilling in the area dates back nearly three quarters of a century to the U.S. Navy's Pet-4 exploration program that was conducted from 1944 to 1953 in the Naval Petroleum Reserve No. 4, currently known as the National Petroleum Reserve-Alaska (NPRA; Robinson and Collins, 1959). The Pet-4 program included detailed geologic field mapping that led to the documentation of numerous oil seeps. As part of this program, 45 shallow core tests and 36 shallow test wells were drilled to evaluate the petroleum potential of Cretaceous strata in the area (Gryc, 1988). Among the early wells are the U.S. Navy Fish Creek test well 1 (spudded May 17, 1949), U.S. Navy Square Lake test well 1 (spudded January 26, 1952), U.S. Navy Grandstand test well 1 (spudded May 1, 1952), and U.S. Navy Wolf Creek test well 3 (spudded August 20, 1952)—for simplicity, these wells will hereafter be referred to as Fish Creek 1, Square Lake 1, Grandstand 1, and Wolf Creek 3. Grandstand 1 is located outside of NPRA to the southeast but was drilled as part of the Pet-4 program and is considered an NPRA well for this report. The four wells were drilled by Arctic Contractors under contract to the U.S. Navy. Square Lake 1, Grandstand 1, and Wolf Creek 3 were drilled on anticlines (Robinson, 1958; Collins, 1959), whereas Fish Creek 1 was drilled near a surface oil seep (Robinson and Collins, 1959). The presence of oil seeps also led the Navy to drill eleven wells on a shallow faulted anticlinal structure in the southeastern portion of NPRA which resulted in discovery of the Umiat field in 1946 (see Herriott and others, 2018). Linc Energy recently (2013–2014) drilled two additional wells at Umiat. One of these, the Umiat 18 (spudded March 10, 2013) successfully cored through the Nanushuk Formation with 100 percent recovery. The core was saturated with oil, but the well would not flow even after extensive production testing.

The Alaska Division of Geological & Geophysical Surveys (DGGS) and Alaska Division of Oil & Gas (DOG) have studied conventional cores from the four NPRA test wells and the Umiat 18 exploration well. The sedimentology of the cores is documented by LePain (2021 [this volume]). As a parallel study, this report documents the sedimentary petrology and reservoir quality of the Nanushuk siltstone and sandstone encountered in the wells. To augment the subsurface data, petrographic analyses of Nanushuk sandstone collected over several years from measured outcrop sections on the central North

[1]Alaska Division of Oil & Gas, 550 W. 7th Ave., Suite 800, Anchorage, AK 99501-3560; helmold@alaskan.com
[2]Alaska Division of Geological & Geophysical Surveys, 3354 College Rd., Fairbanks, Alaska 99709-3707.
david.lepain@alaska.gov

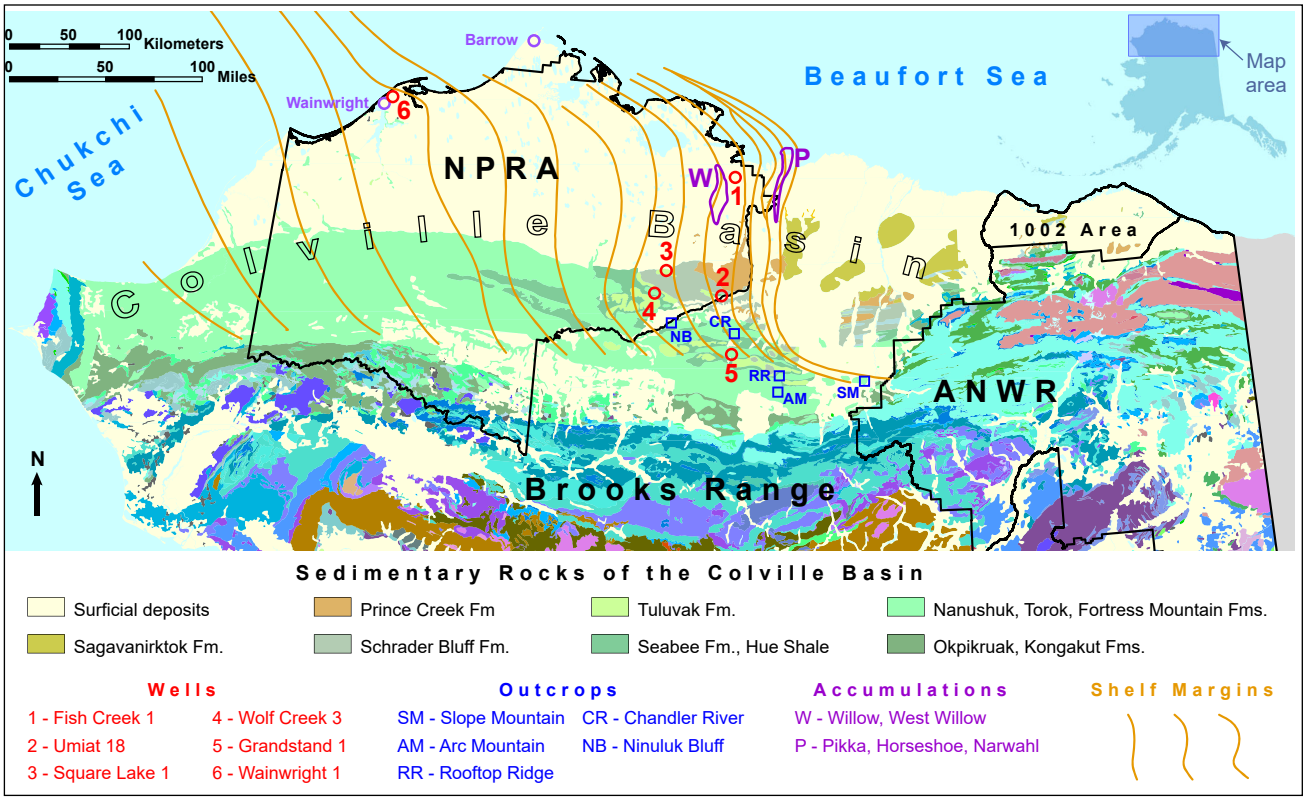

Figure 1. Geologic map of northern Alaska (from Wilson and others, 2015) showing the location of cored wells and measured outcrop sections addressed in this report. Red circles correspond to wells: 1–Fish Creek 1, 2–Umiat 18, 3–Square Lake 1, 4–Wolf Creek 3, 5–Grandstand 1, 6–Wainwright 1; blue squares indicate outcrop sections: SM–Slope Mountain, AM–Arc Mountain, RR–Rooftop Ridge, CR–Chandler River, NB–Ninuluk Bluff. Purple ovals show the locations of the Willow and West Willow (W) and Pikka, Horseshoe, and Narwahl (P) accumulations. Orange lines delineate the approximate locations of Nanushuk lowstand shelf margins (from Houseknecht, 2019).

Slope were incorporated in this study. They proved useful in deciphering the provenance of Nanushuk sandstone. These sedimentologic and petrographic data will advance the understanding of factors that influence hydrocarbon exploration for undiscovered Nanushuk resources.

REGIONAL FRAMEWORK

The Nanushuk Formation outcrops in a belt 30–50 km wide and roughly 650 km long in the northern foothills of the Brooks Range (fig. 1). It consists of a thick succession of marine, transitional, and nonmarine strata of Albian to Cenomanian age (fig. 2) deposited in the asymmetrical Colville foreland basin. The Nanushuk includes a lower, dominantly marine succession of shale, siltstone, and sandstone deposited in shelf, deltaic, and shoreface settings. The lower unit is gradationally overlain by a dominantly nonmarine succession of mudstone, coal, sandstone, and conglomerate deposited in lower delta plain and alluvial settings (Huffman and others, 1985; Mull and others, 2003; LePain and others, 2009). Together these units form a thick regressive package punctuated by higher-frequency marine transgressions resulting from channel avulsion and subsidence of the abandoned delta lobes (LePain and others, 2009) and episodic pulses of basin subsidence (Molenaar, 1985). The uppermost beds of the Nanushuk in the northern part of the outcrop belt and in some wells (Square Lake 1) consist of a Cenomanian mixed marine, marginal-marine, and nonmarine succession deposited during a regional transgressive episode. The transgression culminated in termination of fluvial and deltaic deposition and the re-establishment of widespread marine shelf conditions

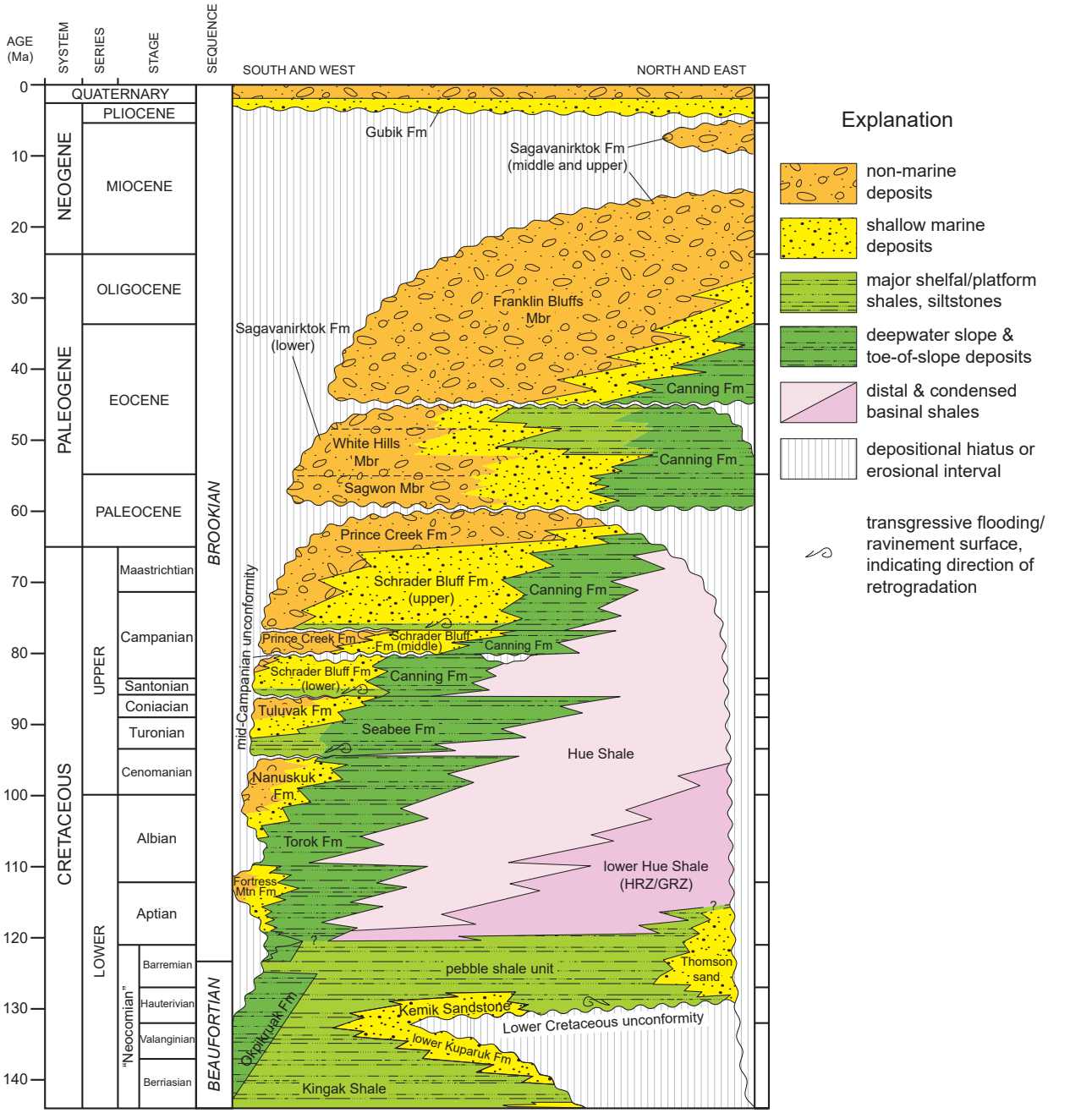

Figure 2. Chronostratigraphic column for the Colville basin, Alaska, showing the stratigraphic position of the Nanushuk Formation; revised from Mull and others (2003), Garrity and others (2005), Decker (2010), and Gillis and others (2014). Abbreviations as follows: Fm = Formation; Mbr = Member; Mtn = Mountain; HRZ = Highly radioactive zone; GRZ = Gamma-ray zone.

throughout the central and western North Slope, and deposition of the Turonian Seabee Formation (Molenaar, 1985; LePain and others, 2009).

Regional studies suggest Nanushuk deposition occurred in two large deltaic complexes separated by the north–south-trending Meade arch (Ahlbrandt and others, 1979; Huffman and others, 1985). The Corwin delta complex (fig. 3) is west of the arch and was interpreted to be the product of a river-dominated system (Ahlbrandt and others, 1979; Huffman and others, 1985). It was sourced from a large drainage basin that extended west of

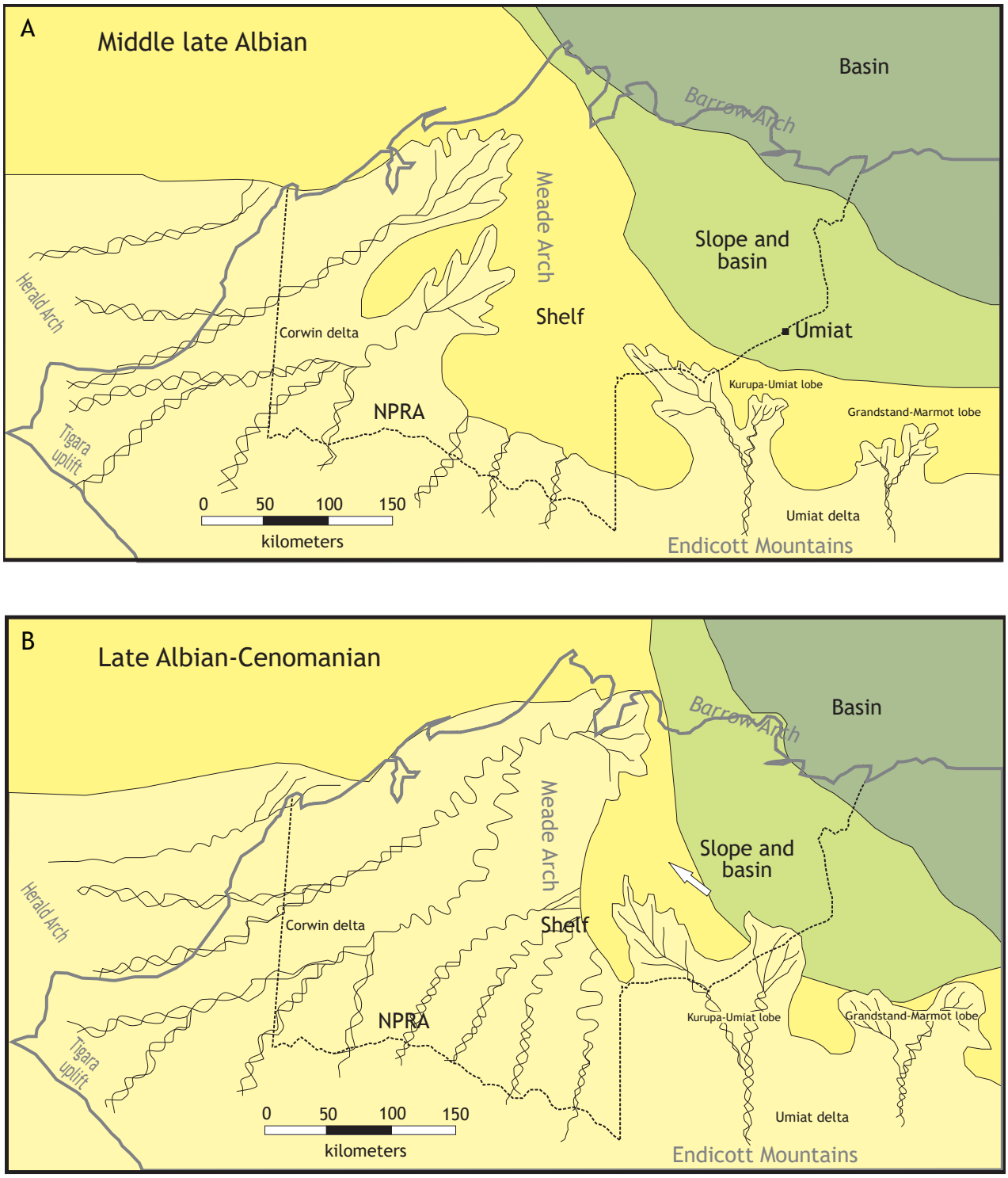

Figure 3. Paleogeographic reconstruction of the central and western Colville basin during (**A**) middle to late Albian time and (**B**) late Albian to Cenomanian time. Diagrams show schematic representation of the Corwin delta west of the Meade Arch and the Umiat delta, including the Kurupa–Umiat and Grandstand–Marmot lobes, east of the arch. Modified from LePain and others (2009) and Huffman and others (1985).

present-day Arctic Alaska (Molenaar, 1985). East of the arch, the Umiat delta complex is comprised of a western Kurupa–Umiat lobe and an eastern Grandstand–Marmot lobe (fig 3). These lobes were recognized as river-dominated systems with a greater degree of wave influence (Ahlbrandt and others, 1979; Huffman and others, 1985) and have been reinterpreted as wave-modified to wave-dominated deltas (LePain and Kirkham, 2001; LePain and others, 2009). They were fed by north-flowing rivers draining smaller catchment areas in the ancestral Brooks Range to the south and southwest (Huffman and others, 1985; LePain and others, 2009). Early Cretaceous uplift of the Brooks Range resulted in clastic detritus shed into the foreland basin from southern sources. The resulting deposits include the deepwater to nonmarine Fortress Mountain Formation, deepwater turbidites of the Torok Formation, and coeval shallow marine to nonmarine strata of the Nanushuk Formation. Some Nanushuk detritus was also probably recycled from the slightly older Fortress Mountain Formation, which was likely sourced exclusively in the ancestral Brook Range to the south (Molenaar and others, 1988; Crowder, 1989; Wartes, 2008). The Torok and Nanushuk Formations collectively represent the transition from an underfilled to an overfilled basin (LePain and others, 2009), with Nanushuk strata eventually over-topping the rift shoulder (Barrow arch) in the late Albian (Molenaar, 1985). The collective Nanushuk deltaic deposits, along with coeval slope and basinal deposits of the Torok Formation, fill the western portion of the Colville basin (Houseknecht and Schenk, 2001; Houseknecht and others, 2008).

Initial work on the petrology of these deltaic systems by Bartsch-Winkler (1979, 1985), Bartsch-Winkler and Huffman (1988), and Johnsson and Sokol (2000) emphasized mineralogy, reservoir quality, provenance, and petroleum potential. Reservoir quality of the Nanushuk sandstone was previously investigated by Fox (1979), Fox and others (1979), Reifenstuhl and Loveland (2004), and Shimer and others (2014).

DATASETS AND METHODS

Two datasets were utilized for this report: modal data and routine core analyses (RCA). The modal data were obtained by point counting existing thin sections from the four 1950's-vintage U.S. Navy test wells that are archived at the Alaska Geological Materials Center (GMC) in Anchorage and more recent vintage (2013) thin sections from the Umiat 18 conventional cores. To aid the assessment of provenance, modal data were also obtained from thin sections collected from five outcrop sections in the central North Slope. The routine core analyses consist largely of legacy data for conventional cores from the four U.S. Navy test wells (Robinson, 1958; Collins, 1959; Robinson and Collins, 1959), a small secondary dataset from Grandstand 1, and more recent (2013) analyses of Umiat 18 conventional cores that were commissioned by Linc Energy. The routine core analyses for Umiat 18 were performed by Weatherford Laboratories and obtained from the Linc Energy data archivist. Recent analyses of petrophysical properties (porosity, permeability, grain density) are available for many of the outcrop samples.

Modal Analyses

GMC's thin-section collection was mined for existing thin sections from the four U.S. Navy test wells that covered the stratigraphic intervals described by LePain (2021 [this volume]). Initial cursory examination of 111 thin sections—21 from Fish Creek 1, 23 from Square Lake 1, 41 from Grandstand 1, and 26 from Wolf Creek 3—revealed they are of widely varying quality and of different vintages. Many of the older thin sections are not impregnated with blue-dyed epoxy, a procedure that is currently accepted as standard protocol to aid in the recognition of porosity. Other thin sections are severely plucked or wedged rendering them unsuitable for further analysis. The extent and quality of staining also are highly variable. Only a few thin sections are stained for K-feldspar and virtually none for carbonate minerals. Sixty-six thin sections that are impregnated with blue-dyed epoxy and which

display minimal plucking or wedging were deemed of acceptable quality for more detailed analysis: 10 from Fish Creek 1, 13 from Square Lake 1, 26 from Grandstand 1, and 17 from Wolf Creek 3. They are listed in appendix A.

Forty-one thin sections from the Umiat 18 conventional cores were obtained from Linc Energy. They are of high quality and are both impregnated with blue-dyed epoxy and stained for carbonates; a small subset is also stained for plagioclase. Thirty-eight of the thin sections were deemed suitable for modal analysis; they are listed in appendix A. The three samples that were not analyzed consist of mudstone and are too fine grained to point count.

Modal analyses of the 104 samples were performed by Michael D. Wilson of Wilson & Associates. He counted a minimum of 300 points using the traditional (non-Gazzi–Dickinson) point-counting method (Ingersoll and others, 1984; Decker and Helmold, 1985) to determine the composition of the framework (detrital grains) and intergranular (matrix, cement, porosity) components. The modal analyses are presented in two formats: (1) raw counts by Wilson (app. B), and (2) standardized hierarchical categories originally devised by Decker (1985) and subsequently modified by the senior author to include additional categories (app. C). All interpreted data, plots, and tables in this report are based on the Decker–Helmold system. Summaries of the modal data, standard petrologic parameters, and ternary ratios are presented in appendix D, and petrographic ratios used to construct ternary diagrams are listed in appendix E.

Wilson conducted a second count of 200 grains (including matrix) for grain size. A complete listing of the grain-size data in both millimeter and ϕ (phi) units is presented in appendix F. The original composition and grain-size files provided by Wilson and a file containing the composition data in Decker–Helmold format are available from the DGGS website (https://doi.org/10.14509/30728).

To facilitate provenance determination, this report also includes existing modal analyses of fifty Nanushuk thin sections from the DGGS/DOG petrographic database. The represented samples had been collected over a period of several years from five measured outcrop sections on the central North Slope: 15 from Slope Mountain, 10 from Arc Mountain, 3 from Rooftop Ridge, 5 from Chandler River, and 17 from Ninuluk Bluff. The thin sections are of high quality and are impregnated with blue-dyed epoxy and stained for carbonates. The modal analyses were performed by Michael D. Wilson shortly after the samples were collected following the procedure outlined above but have not previously been published. The analyses are detailed in appendices A–F.

Routine Core Analyses

Contemporary studies of sandstone reservoir quality routinely utilize thin sections made from trim ends of core plugs destined for routine core analyses. This ensures good correlation between petrologic parameters (detrital grain composition, cement abundance, rock texture) and reservoir rock properties (porosity, permeability, grain density). This study utilizes two disparate sets of routine core analyses: legacy data dating back to 1959 that do not meet the above criteria, and more recent data circa late 1980's and 2013 that do. Available core analyses of the four test wells date back to the original evaluations of the cores by the U.S. Geological Survey (Collins, 1959; Robinson and Collins, 1959), and consist of measurements of permeability to air and porosity under ambient conditions. Very few of the thin sections point counted for this study have corresponding measurements of porosity and permeability in the legacy RCA data. The sampling depths for porosity and permeability are reported to the nearest foot, while the locations of the thin sections are typically recorded to the nearest tenth or hundredth of a foot. As a result, it cannot be ascertained whether RCA data acquired at any given depth are from the same piece of rock used to make the thin sections. Discrepancies of as little as one tenth of a foot are enough to call into question the degree of correlation between the RCA and point-count data. Further, some of the thin sections are

rectangular in shape, suggesting they were not cut from cylindrical RCA plugs that have a round cross section. Appendix G lists a total of 240 analyses have been compiled from Fish Creek 1 (2 analyses), Square Lake 1 (54 analyses), Grandstand 1 (123 analyses), and Wolf Creek 3 (61 analyses).

Routine core analyses from the late 1980's are available for 14 samples from the Grandstand 1 well. These data consist of measurements of permeability to air and porosity under ambient conditions (app. G). The data were obtained from plugs cut from the core stored at the Alaska Geological Materials Center (GMC), which at the time was in Eagle River, AK. Unfortunately, modal analyses of thin section cut from the analyzed plugs are not available for publication.

For the Umiat 18 well, Linc Energy provided routine core analyses of 72 samples that were performed by Weatherford Labs in 2013 (app. G). These measurements include permeability to air and calculated Klinkenberg equivalent values, and porosity measured under a net confining stress of 300 psi and under ambient conditions. Because the Umiat thin sections were cut from the analyzed core plugs there is good correlation between the petrographic and routine core datasets.

Analyses of petrophysical properties (porosity, permeability, grain density) performed by Weatherford Laboratories are available for 38 central North Slope outcrop samples (app. G). These measurements include air permeability, calculated Klinkenberg values, ambient porosity, and porosity under a net confining stress of 400 psi.

To integrate data from both the legacy and recent routine core analyses in scatter plots and discussions, the rudimentary measurements of permeability to air and ambient porosity are utilized throughout this report.

PETROLOGIC FACIES

Grouping samples into petrologic facies (petrofacies) helps summarize data, decipher trends, and describe groups with similar characteristics. Samples from the five NPRA wells were assigned to petrofacies with the aid of DataDesk, a statistical software application produced by Data Description, Inc. (Velleman, 1998). Due to the lack of correlation between the modal and routine core data (see above), these two datasets were analyzed independently. Variables describing texture (e.g., grain size, sorting) and composition (e.g., grain types, matrix, cement) were amassed into one database; while variables describing reservoir quality (e.g., porosity, permeability, burial depth) were compiled into a second database.

Evaluation of rock texture and composition ascertained from detrital modes reveals natural grouping of the data based on grain size. Similar trends in mineralogy versus grain size (e.g., chert vs grain size) were observed for all five NPRA wells. As a result, the modal data were grouped into three petrofacies based on grain size: siltstone petrofacies (21 samples), very-fine-grained sandstone petrofacies (36 samples), and fine-grained sandstone petrofacies (47 samples). Two medium-grained sandstones (Umiat 18, 769 ft measured depth and Grandstand 1, 902 ft measured depth) were included in the fine-grained sandstone petrofacies to avoid having a group based only on two samples. Their average grain sizes—1.93 phi (0.26 mm) for Umiat 18 and 1.90 phi (0.27 mm) for Grandstand 1—are close to the 2.0 phi (0.25 mm) lower boundary of medium-grained sand, so their inclusion in the fine-grained sandstone petrofacies is easily justified. To assess how the composition of these petrofacies compare to Nanushuk sandstone across the North Slope, data from 30 exploration and test wells (table 1) are included in the ternary plots for comparison (fig. 4) and are hereafter referred to as regional Nanushuk data. The petrology and reservoir quality of Nanushuk sandstone in one of these wells, the USGS Wainwright test well 1 (Wainwright 1 in table 1), is documented in Helmold (2016) and is highlighted throughout the text and figures of this report were relevant.

Evaluation of reservoir quality (porosity, permeability, burial depth) reveals natural grouping

Table 1. Exploration and test wells for which point-count data are available for Nanushuk sandstone. These 30 wells comprise the regional Nanushuk data addressed in this report.

Ord	Operator	Well	API	Top Zone (feet)	Base Zone (feet)	N	Erosion (feet)
1	Arco	Alpine 1	50103202110000	4046.00	4535.00	4	1176
2	US Navy	Barrow Core Test 1	50023100050000	169.00	194.00	6	2725
3	Arco	Big Bend 1	50287200110000	1100.00	2840.00	9	8002
4	Husky	E Simpson 2	50279200070000	2387.00	2398.00	9	1785
5	Arco	Fiord 2	50103202010000	4828.00	4828.00	1	844
6	Arco	Hunter A	50103204050000	3625.00	3652.00	7	2068
7	Husky	Inigok 1	50279200030000	2632.00	3081.90	7	3223
8	US Navy	Knifeblade 1	50119100120000	312.00	1490.00	6	6777
9	BP	Kuparuk Unit 1	50287100180000	5529.00	5930.00	9	7090
10	Sinclair	Little Twist Unit 1	50287100220000	942.00	3611.00	4	8895
11	US Navy	Meade 1	50163100020000	1795.00	2950.00	2	4560
12	Arco	Nanuk 2	50103203320000	4796.00	4828.00	3	1381
13	US Navy	Oumalik Test 1	50119100050000	916.00	2758.30	17	4711
14	ConocoPhillips	Putu 2A	50103207630100	4293.40	4361.25	10	1531
15	Husky	Seabee 1	50287200070000	270.00	2120.00	7	6564
16	ConocoPhillips	Tinmiaq 2	50103207300000	3311.00	3766.50	45	1650
17	ConocoPhillips	Tinmiaq 6	50103207310000	2450.00	3824.00	56	1418
18	US Navy	Topagoruk 1	50279100330000	302.00	2097.00	10	2748
19	BP	Trailblazer A1	50103203640000	2972.00	3454.00	4	1402
20	BP	Trailblazer H1	50103203690000	2760.00	3090.00	3	1525
21	Texaco	Tulugak 1	50057200010000	1460.00	2540.00	4	8030
22	Husky	Tunalik 1	50301200010000	3288.00	5560.60	3	3036
23	Union	Tungak Ck 1	50207200020000	3067.00	4661.00	10	4979
24	US Navy	Umiat Test 1	50287100010000	1335.00	2996.00	6	6614
25	US Navy	Umiat Test 2	50287100020000	413.00	969.00	4	6469
26	US Navy	Umiat Test 7	50287100070000	834.00	1370.00	5	6543
27	US Navy	Umiat Test 8	50287100080000	507.00	711.00	2	6374
28	US Navy	Umiat Test 11	50287100110000	2048.00	3004.00	37	6301
29	USGS	Wainwright 1	50301200030000	181.15	1501.45	48	2762
30	US Navy	Wolf Ck 2	50119100090000	2511.00	3520.00	20	7071

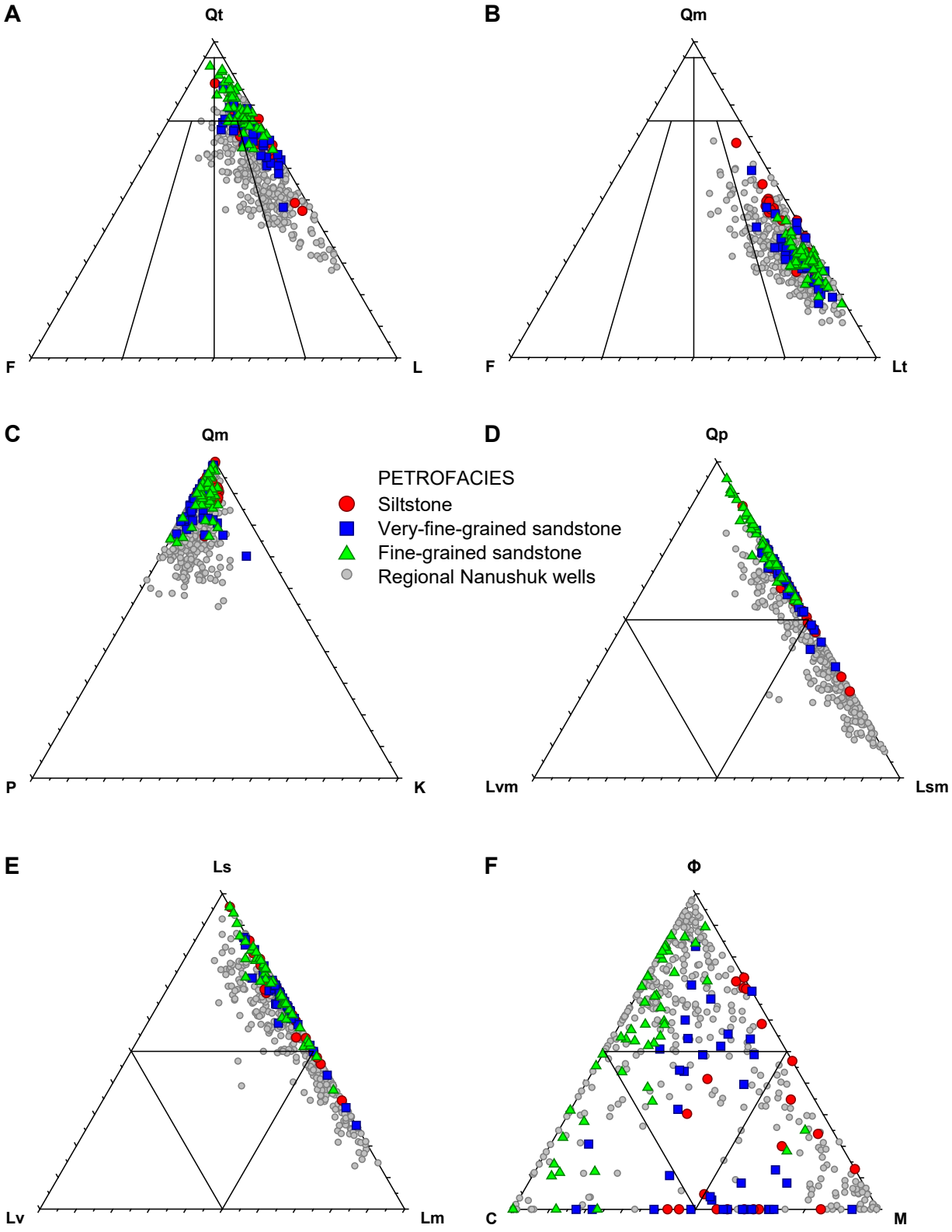

Figure 4. Ternary diagrams showing composition of Nanushuk sandstone. The data were obtained via the traditional point-counting method in which phaneritic rock fragments are classified by their lithology (for example, granite, diorite, gabbro, gneiss). Colored symbols represent petrofacies from the five NPRA wells in this study; gray circles represent regional Nanushuk wells (table 1). See table 2 for explanation of grain and intergranular parameters used in the diagrams. (**A**) QtFL diagram; (**B**) QmFLt diagram; (**C**) QmPK diagram; (**D**) QpLvmLsm diagram; (**E**) LsLvLm diagram; (**F**) ΦCM diagram.

of the data by well. Sandstone in wells that have undergone deeper burial tend to have lower porosity and permeability. As a result, data in plots illustrating trends in reservoir quality are coded by well.

To summarize, this report groups samples differently depending on the type of data under discussion: diagrams dealing with mineral composition (e.g., ternary plots) are coded by grain size, those dealing with reservoir quality are coded by well.

Siltstone Petrofacies

The siltstone petrofacies is represented by 21 samples typically consisting of laminated siltstone with a variable matrix content. The samples have an average modal composition of $Qt_{71}F_4L_{25}$, $Qm_{41}F_4Lt_{55}$, $Qm_{91}P_6K_3$, $Qp_{57}Lvm_0Lsm_{43}$ (fig. 4, app. E, table 2), and a plagioclase/total feldspar (P/F) ratio of 0.71. The average grain size (fig. 5, app. F) of the siltstone is 0.047 mm (coarse silt), with an average Folk sorting (Folk, 1974) of 1.78 (poor). The siltstone framework composition is somewhat different from the sandstone largely due to the difference in grain size (see section on petrologic trends). Monocrystalline quartz (Qm) and polycrystalline quartz (Qp) are the two most abundant detrital grains, averaging 37 percent and 15 percent of the framework fraction, respectively (fig. 6). Feldspar is a minor framework component (average 4 percent), consisting of roughly equal proportions of plagioclase and K-feldspar. The lithic fraction consists largely of chert (average 13 percent), phyllite/schist (average 11 percent), detrital carbonate (average 6 percent), and shale/mudstone (average 4 percent). Volcanic rock fragments (VRFs) and quartzite are minor lithic components. Micas (average 3 percent) and organic material (average 3 percent) are more abundant

Table 2. Classification of grain and intergranular parameters used in ternary diagrams (fig. 4).

A. Quartzose grains

Qm = Monocrystalline quartz

Qp = Polycrystalline quartz (including chert)

Qt = Total quartzose grains (Qm + Qp)

B. Feldspar grains

P = Plagioclase

K = Potassium feldspar

F = Total feldspar grains (P + K)

C. Lithic grains

Ls = Sedimentary rock fragments (including chert)

Lv = Volcanic rock fragments

Lm = Metamorphic rock fragments

Lp = Plutonic rock fragments

Lsm = Sedimentary and metasedimentary rock fragments

Lvm = Volcanic and metavolcanic rock fragments

L = Lithic grains (Ls + Lv + Lm + Lp)

Lt = Total lithic grains (L + Qp)

D. Intergranular components

Φ = Total porosity

C = Total cement

M = Matrix + clay laminae/burrows

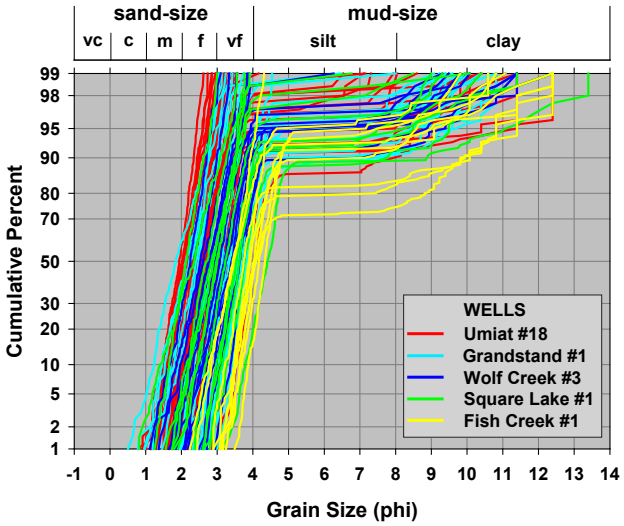

Figure 5. Cumulative probability plots of grain size by well; each line represents an individual sample. Sediment with a normal (Gaussian) distribution plot as a straight line; tails to the right indicate a significant mud (silt and clay) fraction. The value of the 50th percentile indicates the median grain size, while sorting is denoted by the slope of the line.

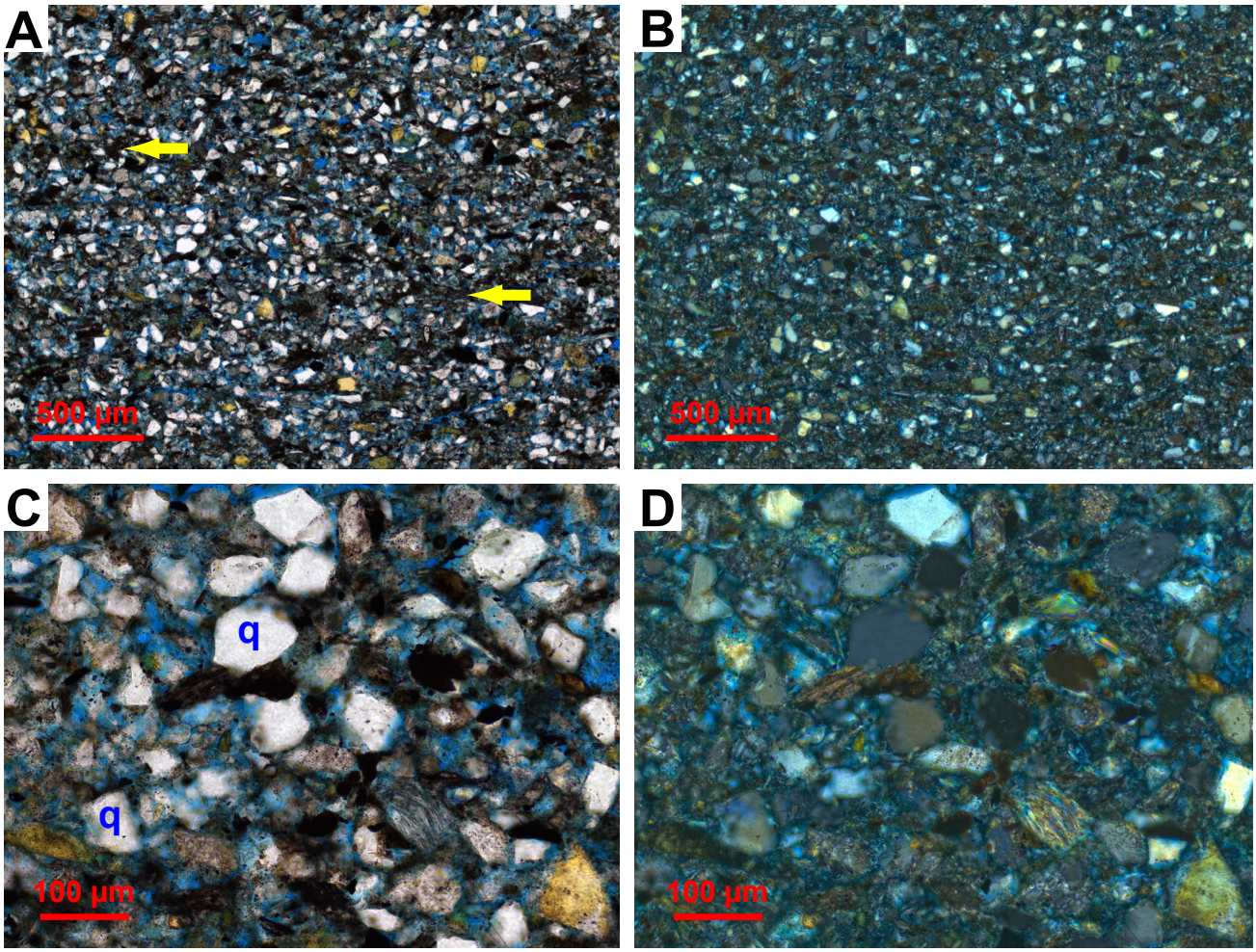

Figure 6. Photomicrographs of siltstone petrofacies. (**A**) General view of siltstone showing an abundance of detrital clay (arrows). Plane-polarized light; Fish Creek 1, 3,025.9 ft. (**B**) Same view as A. Crossed polars; Fish Creek 1, 3,025.9 ft. (**C**) Detailed view of siltstone in which the framework fraction consists largely of monocrystalline quartz (q). Plane-polarized light; Fish Creek 1, 3,025.9 ft. (**D**) Same view as C. Crossed polars; Fish Creek 1, 3,025.9 ft.

than in the sandstones, due to their hydrodynamic equivalence with the finer detritus.

Thin-section porosity averages 6.3 percent but varies widely between samples (0–19 percent). Detrital clay matrix is a prominent intergranular component (average 11 percent) that negatively impacts reservoir quality, particularly permeability. Quartz cement is negligible in all samples, but carbonate cement is present in a few samples (0–14 percent of bulk rock, average 3 percent). Intergranular volume (IGV), which is defined as the sum of intergranular porosity, intergranular cement, and depositional matrix (Szabo and Paxton, 1991; Paxton and others, 2002) and is an indicator of degree of compaction, ranges from 13 to 33 percent suggesting a wide range in compaction resulting from large differences in maximum burial depths (see discussion of reservoir quality).

Very-Fine-Grained Sandstone Petrofacies

The very-fine-grained sandstone petrofacies is represented by 36 litharenites with an average modal composition of $Qt_{70}F_5L_{25}$, $Qm_{31}F_5Lt_{64}$, $Qm_{86}P_{11}K_3$, $Qp_{62}Lvm_0Lsm_{38}$ (fig. 4, app. E, table 2), and plagioclase/total feldspar (P/F) ratio of 0.86. Their average grain size (fig. 5, app. F) is 0.088 mm (upper very fine), with an average Folk sorting (Folk, 1974) of 1.33 (poor). Monocrystalline and polycrystalline

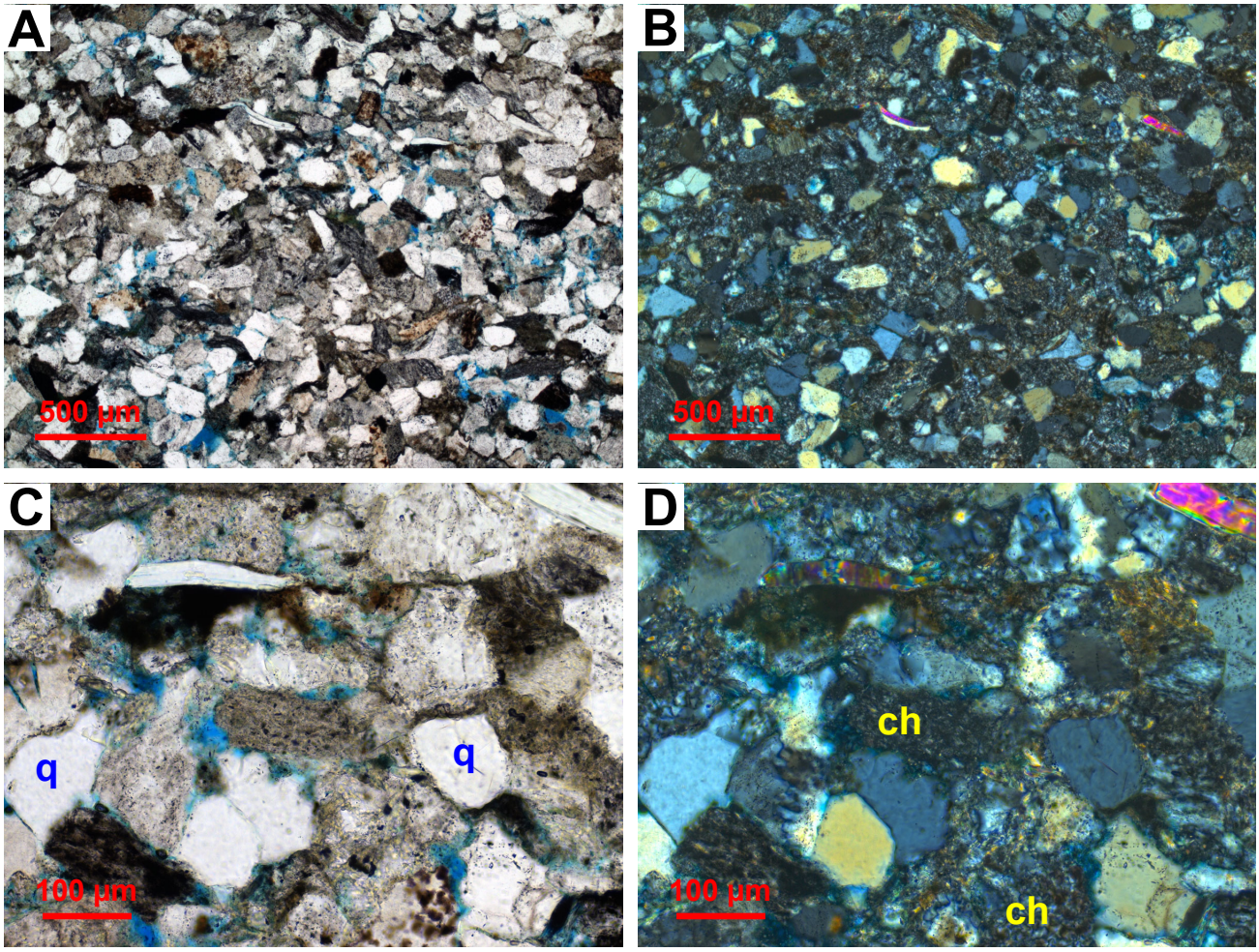

Figure 7. Photomicrographs of very fine-grained sandstone petrofacies. (**A**) General view showing a moderately compacted framework lacking significant cement. Plane-polarized light; Square Lake 1, 3,058 ft. (**B**) Same view as A. Crossed polars; Square Lake 1, 3,058 ft. (**C**) Detailed view of sandstone showing abundance of monocrystalline quartz (q). Plane-polarized light; Square Lake 1, 3,058 ft. (**D**) Same view as C. Note chert grains (ch). Crossed polars; Square Lake 1, 3,058 ft.

quartz are the two dominant framework components, averaging 29 percent and 17 percent of the framework fraction, respectively (fig. 7). Feldspar is a minor framework component, averaging 4 percent plagioclase and 1 percent K-feldspar. Lithic detritus consists largely of chert (20 percent), phyllite/schist (13 percent), detrital carbonate (4 percent), shale/mudstone (4 percent), and quartzite (2 percent). Organic matter (3 percent) and micas (2 percent) are accessory detrital components.

Thin-section porosity averages 4 percent and like the siltstone petrofacies exhibits substantial inter-sample variability (0–19 percent). Quartz (average 1 percent) and carbonate (average 3 percent) are minor cements in most samples, but carbonate cement ranges up to 10 percent in a few samples. Kaolinite occurs in trace quantities as a patchy, pore-filling cement. Detrital matrix ranges from 1 to 11 bulk percent (average 5 percent) and is locally concentrated along diffuse laminae. Intergranular volume (IGV) ranges from 8 to 26 percent (average 13 percent) suggesting the samples have undergone a range of compaction from moderate to significant.

Fine-Grained Sandstone Petrofacies

The fine-grained sandstone petrofacies is represented by 47 chert-rich litharenites with an average modal composition of $Qt_{79}F_4L_{17}$, $Qm_{30}F_4Lt_{66}$,

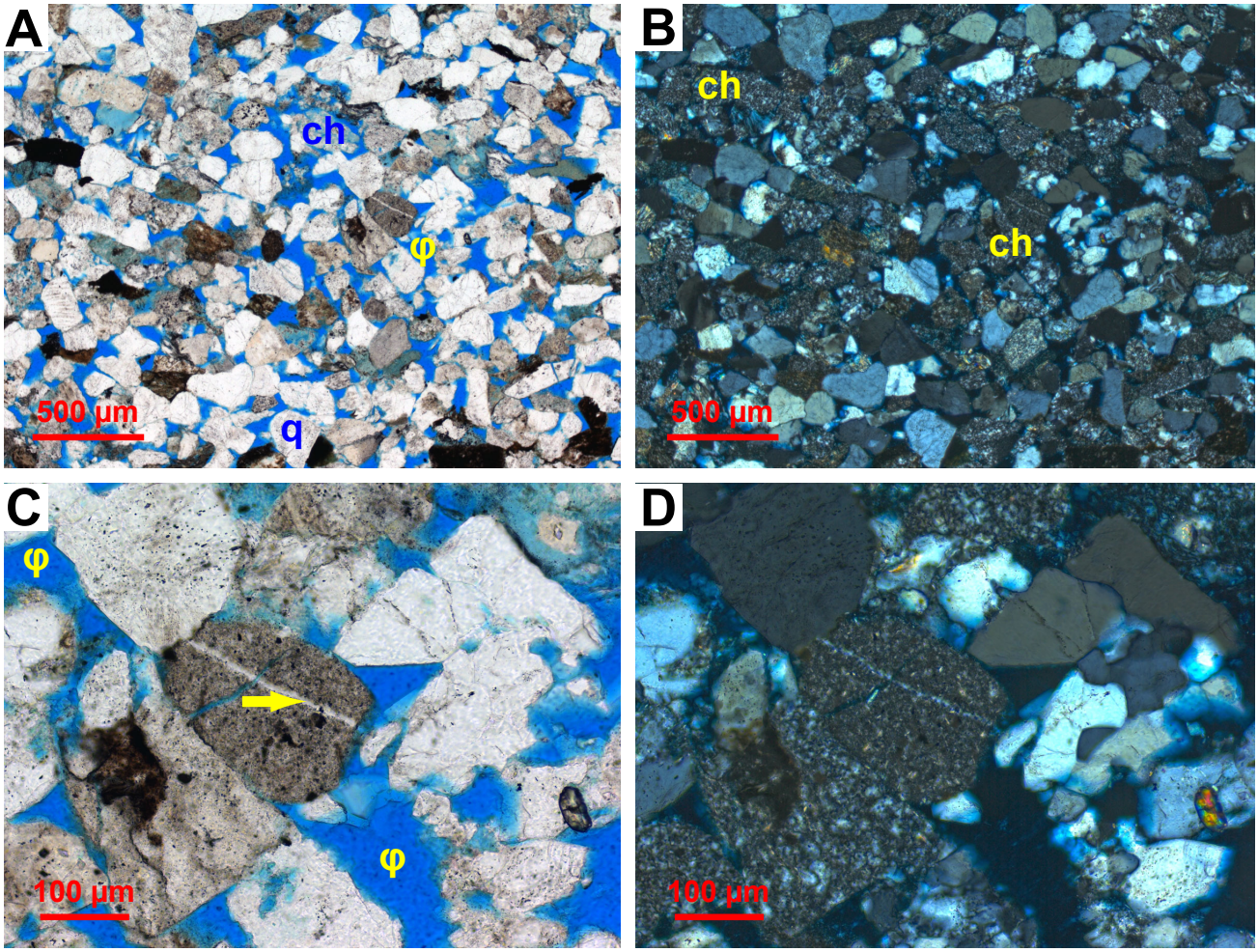

Figure 8. Photomicrographs of fine-grained sandstone petrofacies. (**A**) General view showing abundance of quartz (q) and chert (ch) which is best seen under crossed polars. Note abundant intergranular pores (ϕ). Plane-polarized light; Umiat 18, 803.05 ft. (**B**) Same view as A showing abundant chert grains (ch). Crossed polars; Umiat 18, 803.05 ft. (**C**) Detailed view showing common intergranular pores (ϕ). Note fractured chert grain with quartz veinlet (arrow). Plane-polarized light; Umiat 18, 803.05 ft. (**D**) Same view as C. Crossed polars; Umiat 18, 803.05 ft.

$Qm_{89}P_9K_1$, $Qp_{74}Lvm_0Lsm_{26}$ (fig. 4, app. E, table 2), and plagioclase/total feldspar (P/F) ratio of 0.77. The average grain size (fig. 5, app. F) is 0.186 mm (upper fine), with an average Folk sorting (Folk, 1974) of 0.67 (moderate). Chert and monocrystalline quartz (Qm) with dominantly straight to slightly undulose extinction are the two dominant framework components, each averaging 29 percent of the framework fraction (fig. 8). Chert is largely of the common microcrystalline variety, although micaceous-argillaceous and micro-porous chert also occur. Polycrystalline quartz (Qp) averages 17 percent of the detrital framework and consists of grains with 2–5 crystals (plutonic and high-rank metamorphic provenance) and grains with more than 5 crystals (low-rank metamorphic provenance; Basu and others, 1975; Blatt and others, 1980; Blatt, 1982; Boggs, 2009). Feldspar comprises roughly 4 percent of the framework with plagioclase—some of which exhibit minor to moderate dissolution—more abundant than K-feldspar. Lithic fragments (excluding chert) comprise approximately 17 percent of the rock framework, consisting of phyllite/schist, quartzite, and detrital carbonate. Micas, heavy minerals, and dispersed organic grains occur in trace amounts.

Thin-section porosity averages 9.2 percent, and like the other petrofacies, exhibits substantial

inter-sample variability (0–20 percent). Quartz (average 3 percent) and carbonate (average 3 percent) are minor cements in most samples, but carbonate cement ranges up to 35 percent in a few samples. Kaolinite is a patchy, pore-filling cement that occurs in trace quantities. The samples exhibit a wide range of IGV (1–39 percent, average 17 percent) suggesting the five wells experienced substantial differences in compaction.

GRAIN-SIZE TRENDS

The Nanushuk siltstone and sandstone in the five NPRA wells exhibit a positive correlation between chert content and grain size (correlation coefficient of -0.76), with the fine-grained sandstone averaging 24 percent (whole rock) chert while the siltstone averages over 10 percent (fig. 9A). It should be noted that because grain size is given in phi (ϕ) which is defined as $-\log_2(\text{grain size}_{mm})$, a positive correlation between variables (e.g., chert content increases with increasing grain size) is reported as a negative value of the Pearson product-moment correlation coefficient (r). To best display the relationship between chert content and grain size, the ordinate (chert content) on the cross-plot (fig. 9A) is displayed using a logarithmic scale with a corresponding increase of r to -0.80. A similar trend was noted in Nanushuk siltstone and sandstone in the Wainwright 1 test well (Helmold, 2016). The regional, subsurface Nanushuk sandstone samples (gray dots in fig. 9A, table 1) display a similar, although weaker, correlation suggesting the grain size versus chert relationship may be characteristic of Nanushuk sandstone. A possible explanation may lie in the source of the chert grains (Helmold, 2016). One of the more likely chert sources is the Mississippian-Pennsylvanian Lisburne Group carbonates that are widespread in the allochthons of the Brooks Range. These carbonates contain ubiquitous, large (cobble- to boulder-sized), bed-parallel, diagenetic chert nodules. As these nodules weather and erode from the Lisburne, they are concentrated in the coarsest detritus. Abundant silt to very-fine sand-sized chert grains should ultimately be produced with continued transport and abrasion if its solubility is comparable to that of quartz. The higher solubility of chert relative to monocrystalline quartz, combined with the greater surface area of microcrystalline chert, may result in its selective dissolution thereby increasing the relative abundance of quartz in the finer fractions (Helmold, 2016). A similar relationship between chert content and grain size is also seen in Ivishak sandstones from the North Slope of Alaska where the chert content is thought to be related to distance of transport (Atkinson and others, 1990). The coarsest detritus, having undergone little transport, contains a significant volume of chert. In the finer detritus that was transported greater distance, chert was selectively removed through abrasion relative to the more resistant monocrystalline quartz. The correlations of grain size with Qm (+ r value) and VRFs (- r value) observed in Nanushuk siltstone and sandstone from the Wainwright 1 test well (Helmold, 2016) were not evident in the current study.

A relationship between grain size and reservoir quality (porosity, permeability) is illustrated by Umiat 18 where thin sections were cut from the routine core plugs. Twenty-three (23) of the point-counted samples have corresponding porosity and permeability measurements, while one additional sample has only a porosity measurement. Two fine-grained sandstones were considered outliers and excluded from analysis; one (942.0 ft measured depth) was excluded due to excessive carbonate cement (12 percent), the other (811.6 ft measured depth) was excluded due excess detrital matrix (9 percent). There is a well-defined positive correlation between grain size and porosity for the Umiat 18 samples, with a Pearson product–moment correlation coefficient (r) of -0.85 (fig. 9B). The fine- and very-fine-grained sandstone have average porosities of 15 and 11 percent, respectively, while siltstone porosity averages 8 percent. It is difficult to quantify a similar relationship for Fish Creek 1, Square Lake 1, Grandstand 1, and Wolf Creek 3 because few samples from these wells have both grain size and

porosity data due to the lack of correlation between the petrographic and routine core analysis datasets (see above). Sparse data for Grandstand 1 and Wolf Creek 3 appear to approximate a linear relationship (fig. 9B). The entire dataset, including the regional Nanushuk data, clusters into two distinct groups. The first group displays similar ranges in porosity (less than 20 percent) and grain size as the Umiat 18 samples and has Dmax values generally greater than 7,000 ft (red dashed oval in fig. 9B). Samples from Grandstand 1 and Wolf Creek 3 are included in this group. The second group has greater porosities than the Umiat 18 samples for a given grain size, with Dmax values generally less than 7,000

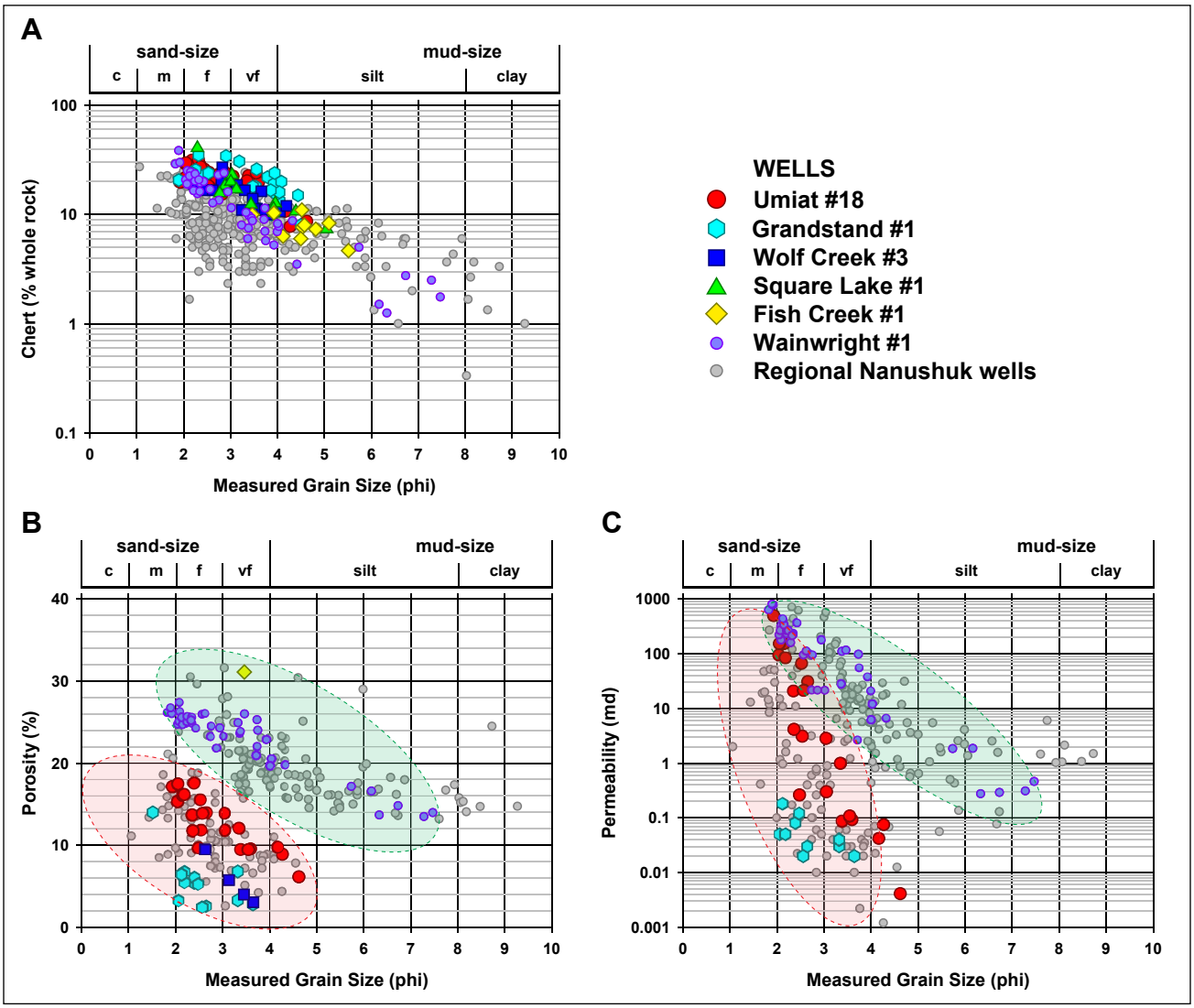

Figure 9. Cross plots of grain size, in phi units (ϕ), versus compositional and petrophysical parameters. Because grain size is given in phi (ϕ) [defined as -log2(grain size mm)], a positive correlation between variables (i.e., permeability increases with increasing grain size) is reported as a negative value of the Pearson product-moment correlation coefficient (r). To best display a linear relationship between variables, the ordinate (y-axis) representing chert is displayed with a logarithmic scale. **A**. Chert – grain size plot showing good correlation for six NPRA wells and regional samples. Chert preferentially resides in the coarser fraction of the detritus. **B**. Porosity – grain size plot showing two linear trends; one for rocks with better reservoir quality (green dashed oval) subjected to shallow to moderate burial, and the other for rocks with poorer reservoir quality (red dashed oval) subjected to moderate to deep burial. **C**. Permeability – grain size plot showing trends similar to the porosity – grain size plot. Rocks with better reservoir quality (green dashed oval) merge with rocks with poorer reservoir quality (red dashed oval) in the coarser detrital faction.

ft (green dashed oval in fig. 9B). Samples from the Wainwright 1 test well and a single sample from Fish Creek 1 are included in the latter group (fig. 9B). These two parallel trends are interpreted to result from differences in burial histories—specifically differences in Dmax, as discussed below.

Umiat 18 samples also display a pronounced positive correlation between grain size and permeability (r = -0.91), with an average permeability of 94 md in the fine-grained sandstone, 0.7 md in the very-fine-grained sandstone, and 0.04 md in the siltstone (fig. 9C). The regional Nanushuk data also cluster into two groups: one typified by the Umiat 18 and Grandstand 1 samples (Dmax > 7,000 ft), the other by the Wainwright 1 samples (Dmax < 7,000 ft). The two groups merge at higher permeability values. The existence of the two groups in the regional data is also interpreted to reflect differences in burial.

PROVENANCE SIGNALS

As detailed above, the detrital framework of Nanushuk sandstone consists largely of monocrystalline and polycrystalline quartz, chert, phyllite/schist, shale/mudstone, and detrital carbonate grains, with lesser quantities of feldspar, volcanic rock fragments, mica, and heavy minerals. Among this detritus, chert and detrital carbonate probably have the most potential to decipher the provenance of specific samples; phyllite/schist detritus could potentially be a useful indicator of provenance if combined with other techniques such as thermochronology of detrital micas, although that is beyond the scope of this report. Nanushuk sandstone in the subsurface of the eastern NPRA was derived from uplifts in the ancestral western Brooks Range, Lisburne Hills/Herald arch, and eastern Siberia (Molenaar, 1985; Houseknecht and others, 2008). The Brooks Range orogen consists of a stack of allochthons that include thick successions of carbonate, bedded chert, and silicified mudstone—many of which extend across the east-west length of the mountain belt and were likely exposed and shedding detritus during Nanushuk deposition. Allochthons that potentially supplied chert and silicified mudstone include the western parts of the Endicott Mountains (Lisburne Group, Kuna Formation, Otuk Formation), Picnic Creek (Lisburne Group-Akmalik Chert, Imnaitchiak Chert), Kelly River (Lisburne Group-Tupik Formation), Ipnavik River (Lisburne and Etivluk Groups), and Nuka Ridge (Etivluk Group; see fig. 21 in Moore and others, 1994).

The lack of carbonate staining of thin sections from the four legacy NPRA test wells hampers definitive identification of carbonate fragments. However, analyses of the state's regional collection of Nanushuk thin sections (which have been stained for carbonate) and Umiat 18 samples suggest that most carbonate fragments are dolomite, with only a small proportion consisting of calcite. Detrital carbonate occurs in variable amounts (0–35 percent of the framework, 0–28 percent of the bulk rock) in the five wells examined in this study, with variability observed both within and between wells (figs. 10A, 11A). Samples from Grandstand 1 and Umiat 18 contain the least detrital carbonate, most having little to none. Those from Square Lake 1, Wolf Creek 3, and Fish Creek 1 contain a much wider range of detrital carbonate (fig. 11A), which is a principal lithic variant in many samples. Previous work demonstrated that Nanushuk sandstone from the Wainwright 1 well also contains significant detrital carbonate (fig 11A; Helmold, 2016). This study appears to show a pattern in aerial distribution of detrital carbonate in the Nanushuk sandstone, although the number of wells was limited. Sandstone to the southeast (Grandstand 1 and Umiat 18) contains relatively little detrital carbonate, while sandstone to the northwest (Wolf Creek 3, Square Lake 1, Fish Creek 1, and Wainwright 1) contains significantly more (figs. 1, 11A). To test the validity of this observation, the abundance of detrital carbonate in Nanushuk sandstone from five measured stratigraphic sections in the central North Slope was compared. Nanushuk sandstone from the southeastern portion of the study area

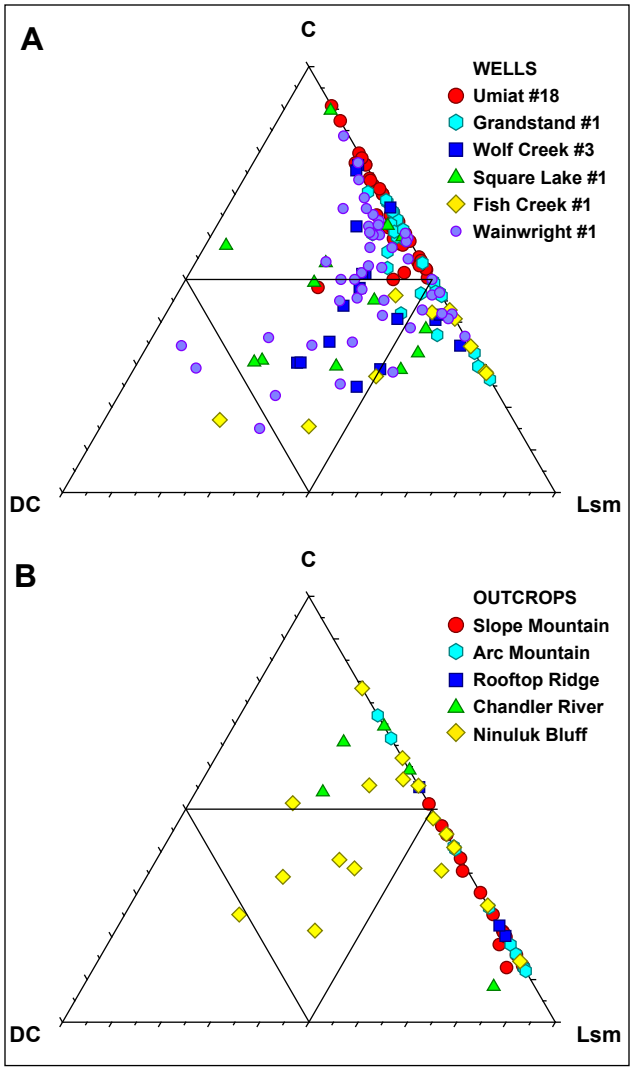

Figure 10. Chert (C) – Detrital Carbonate (DC) – Argillaceous Sedimentary/Metasedimentary Lithics (Lsm) ternary diagram detailing provenance implications for Nanushuk sandstone. The data were obtained via the traditional point-counting method in which phaneritic rock fragments are classified by their lithology (for example, granite, diorite, gabbro, gneiss). (**A**) Diagram for six NPRA wells. Nanushuk sandstone in the southeastern wells (Grandstand 1 and Umiat 18) contains little detrital carbonate while to the northwest (Wolf Creek 3, Square Lake 1, Fish Creek 1, and Wainwright 1) it contains a significant, and somewhat variable, quantity. (**B**) Diagram for five outcrop sections from the central North Slope. Nanushuk sandstone from the southeastern outcrops (Slope Mountain, Arc Mountain, and Rooftop Ridge) contains little to no detrital carbonate, while that to the northwest (Chandler River and Ninuluk Bluffs) contains significantly more. The trend seen in outcrop parallels the subsurface trend.

(Slope Mountain, Arc Mountain, and Rooftop Ridge) contains little to no (range 0–1 percent bulk rock, mean 0.07 percent) detrital carbonate (figs. 10B, 11B), while sandstone from the northwest (Chandler River and Ninuluk Bluff) contains a significantly greater quantity (range 0–17 percent bulk rock, mean 4.6 percent).

Potential sources of detrital carbonate in Nanushuk sandstone include the Mississippian-Pennsylvanian Lisburne Group in the Endicott Mountains allochthon and in uplifts in the Lisburne Hills/Herald arch area that contain abundant carbonate rocks, including thick dolomite sections. In addition, limestones of the Baird Group, which is present in the Kelly River, Ipnavik, and Nuka Ridge allochthons in the western Brooks Range, also are potential sources of detrital limestone in Nanushuk sandstone. It seems probable that these grains were derived from allochthons in the western Brooks Range and uplifts in the Herald arch. It is uncertain if detrital carbonate could survive long-distance fluvial transport from sources in eastern Siberia, a present-day distance of approximately 1,000 km.

RESERVOIR QUALITY

General Considerations

Reservoir quality (porosity, permeability) of the Nanushuk siltstone and sandstone from the 5 wells in this study (fig. 12A) varies widely from very poor (5 percent porosity, 0.002 md permeability; Umiat 18, 741 ft measured depth) to excellent (31 percent porosity, 4110 md permeability; Fish Creek 1, 2970 ft measured depth). For the Umiat 18 samples, as noted above, variation in reservoir quality, with exception of cemented samples, is largely controlled by depositional energy as signaled by grain size. It is presumed that variations in reservoir quality within Fish Creek 1, Square Lake 1, Grandstand 1, and Wolf Creek 3 are also controlled largely by depositional energy, although grain-size data are insufficient to affirm

that relationship. Porosity-permeability data for the regional Nanushuk samples plot in two distinct groups: one that mimics the trend exhibited by the Umiat 18, Grandstand 1, and Wolf Creek 3 samples (red dashed oval in fig. 12A), and a second parallel trend, represented by the Fish Creek 1 (single data point) and Wainwright 1 samples, that has higher porosity values for a given permeability (green dashed oval in fig. 12A). The disparity in reservoir quality between the two groups is interpreted to result from differences in burial, specifically the maximum burial the rocks experienced (fig. 12B). The high-porosity group consists almost exclusively of samples with a Dmax of less than 7,000 ft, while samples from the low-porosity group consistently have Dmax greater than 7,000 ft (fig. 12B). The Dmax value of 7,000 ft was determined empirically by analyzing the entire set of available data and testing which Dmax value provided the best discrimination between the two trends.

Differences in reservoir quality based on modal data are graphically illustrated in a PFC (Porosity-Framework-Cement) diagram (fig. 13); a technique originally proposed by Franks and Lee

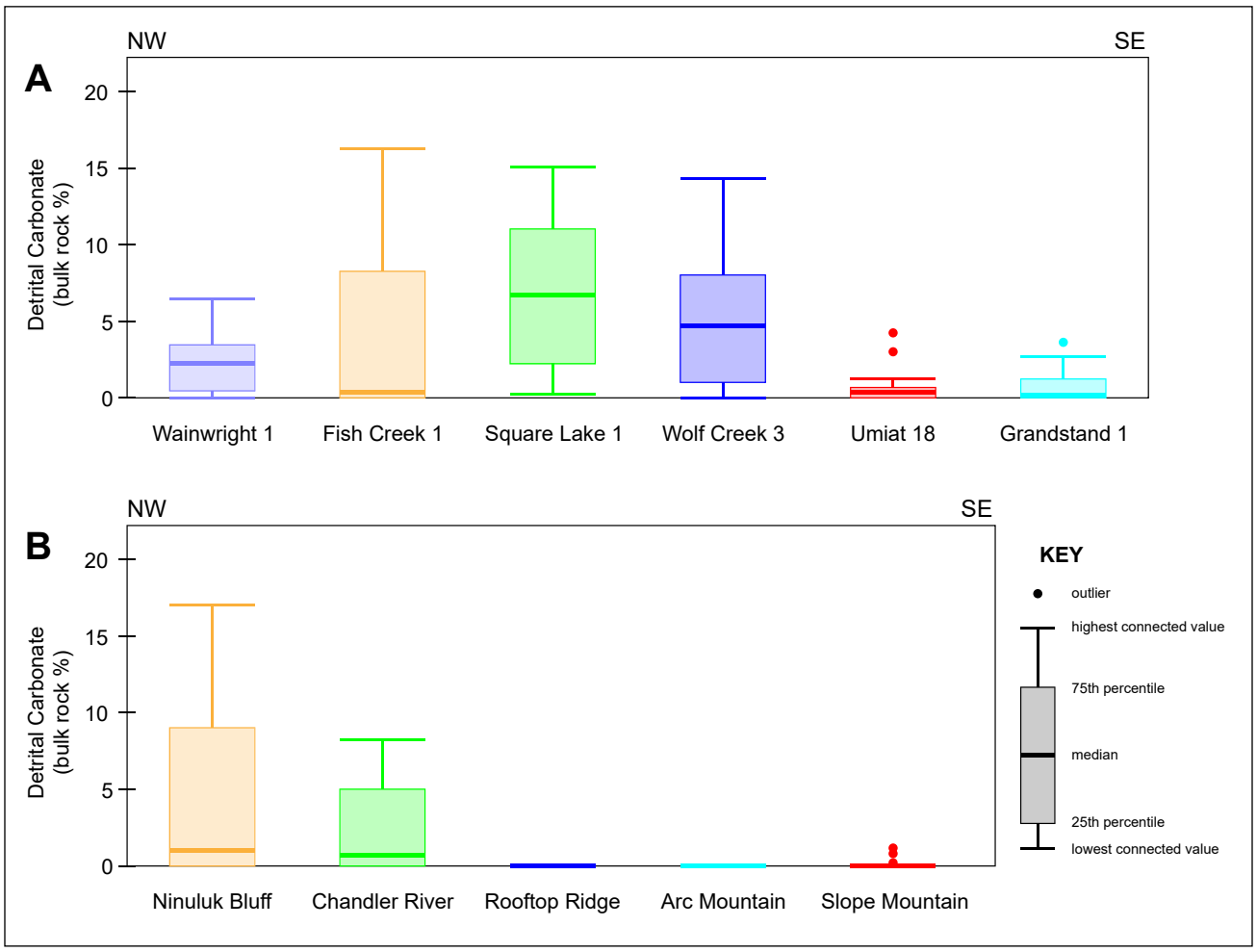

Figure 11. Boxplots for detrital carbonate (in bulk rock percent). The rectangular box represents the range between the 25th and 75th percentiles of the values; the heavy line within the box is the median value. The upper and lower whiskers represent the ranges of the highest connected and lowest connect values, respectively. Dots above the upper whiskers are outlier values. The statistics are calculated by Data Desk (Velleman, 1998). **A**. Boxplots for six NPRA wells; one extreme outlier for the Fish Creek 1 well (value of 28 percent bulk rock) was excluded from the figure for the sake of compactness but was included in statistical calculations. **B**. Boxplots for five outcrop sections from the central North Slope. Both the subsurface and outcrop data exhibit detrital carbonate amounts, and to a lesser extent variability, that increase from southeast to northwest.

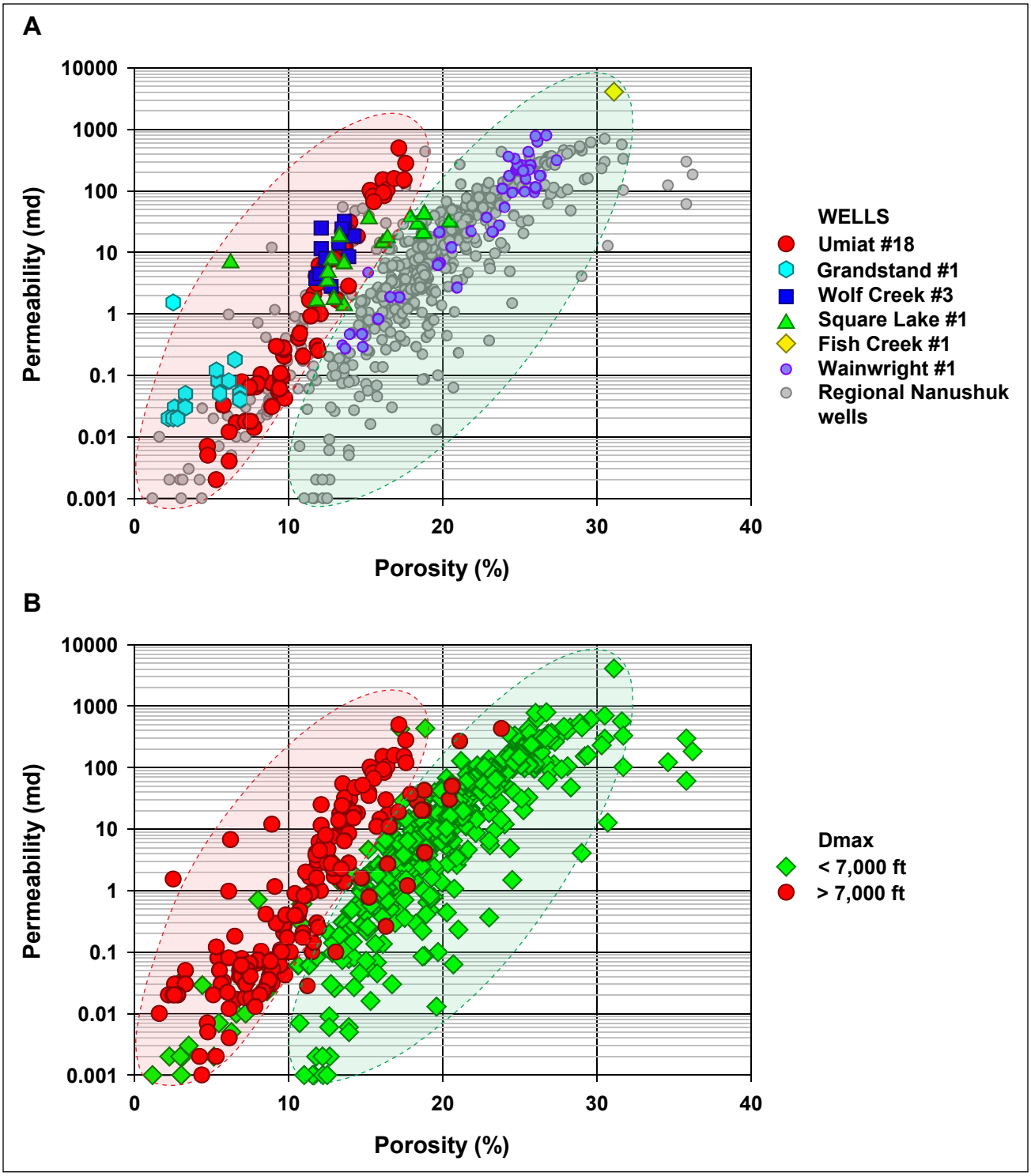

Figure 12. Porosity–permeability cross plot showing reservoir quality of Nanushuk sandstone from six NPRA wells and associated regional samples. Two parallel trends are evident: One for rocks with higher porosity (green dashed oval) and the other for rocks with lower porosity (red dashed oval). **A**. Samples are coded by well. Sandstone from Fish Creek 1 and Wainwright 1 is characteristic of the better reservoir-quality rock that has not been deeply buried, while sandstone from Square Lake 1, Grandstand 1, Wolf Creek 3, and Umiat 18 is characteristic of the poorer reservoir-quality rock subjected to moderate to deep burial. **B**. Same plot shown in A, with samples coded by Dmax. Most of the samples within the green oval have a Dmax of less than 7,000 ft, while those within the red oval have a Dmax greater than 7,000 ft. This supports the interpretation that the two parallel trends result from differences in Dmax.

(1994). The Fish Creek 1 samples fall largely into the "compacted reservoir" area of the diagram while the Square Lake 1, Grandstand 1, and Wolf Creek 3 samples largely plot in the "compacted non-reservoir" field. The Umiat 18 samples lie in both the "compacted reservoir" and "compacted non-reservoir" fields. The regional Nanushuk samples are largely confined to the "compacted reservoir" and "compacted non-reservoir" fields, although several plot in the "preserved reservoir" portion of the diagram. A limited number of the Square Lake 1 and regional samples lie in the "cemented non-reservoir" field attesting that porosity is largely destroyed by compaction. This is confirmed by a cross plot of compactional porosity loss (COPL; Lundegard, 1992) versus cementational porosity loss (CEPL) which shows a similar relationship (fig. 14). The vast majority of Fish Creek 1, Square Lake 1, Grandstand 1, Wolf Creek 3, Umiat 18, and regional Nanushuk samples have COPL values of 25–45 percent with corresponding CEPL values of less than 10 percent confirming that, for most samples, mechanical compaction plays a much larger role in porosity destruction than cementation.

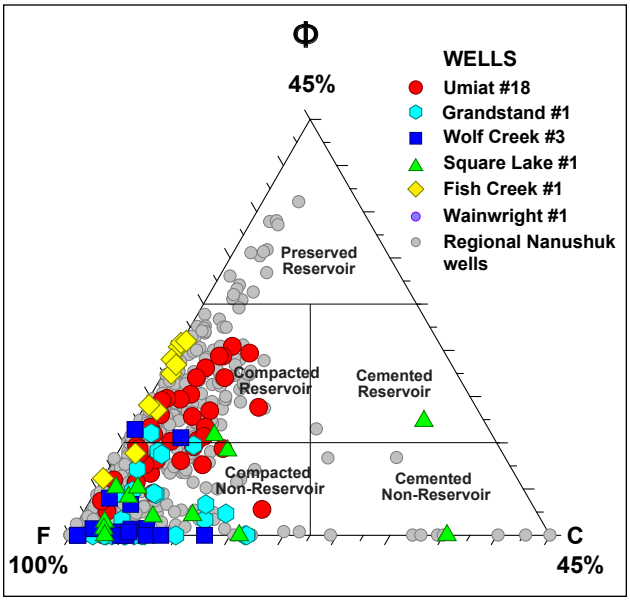

Figure 13. Porosity (Φ) – Framework Grains (F) – Cement (C) ternary diagram showing reservoir quality of six NPRA wells and regional Nanushuk siltstone and sandstone. Wolf Creek 3, Square Lake 1, and many of the Uniat 18 samples plot in the "compacted non-reservoir" area of the diagram while most of the Fish Creek 1 and the remaining Umiat 18 samples plot in the "compacted reservoir" field. The regional Nanushuk samples plot mainly in the "compacted non-reservoir" and "compacted reservoir" fields, although a few plot in the "preserved reservoir" and "cemented non-reservoir" fields. This confirms that porosity loss in Nanushuk sandstone is dominantly through compaction. Diagram modified from Franks and Lee (1994); used with permission.

Forward-Looking Predictions

In sedimentary basins where calibration datasets are available, regression analysis has proved an effective method for predicting reservoir quality (Scherer, 1987; Bloch, 1991; Byrnes and Wilson, 1991; Bloch and Helmold, 1995). This is especially true for sandstone that contains less than 10 percent cement or in which only small volumes of sandstone are highly cemented. In the latter case, inclusion of highly cemented samples in the regression analyses can yield overly pessimistic forecasts. One approach is to exclude highly cemented samples from the input data, thereby yielding predictions for only uncemented or moderately cemented sandstone. This is a viable approach when the highly cemented samples occur in thin zones (e.g., carbonate streaks) or as isolated concretions. The rationale from an exploration perspective, is that these thin, highly cemented zones are not representative of the overall reservoir and their presence will have little impact on whether the host sandstone can produce hydrocarbons. Previous studies have shown that Brookian sandstones of the North Slope, in which compaction is the dominant mechanism of porosity destruction, are good candidates for regression analysis (Smosna, 1989). This is particularly true for the Cretaceous Torok and Nanushuk Formations, and slightly less so for the Seabee Formation.

Previous work on Torok and Seabee reservoirs has established that reservoir quality expected in a prospect can be forecast reasonably well by utilizing Dmax as the predictor (independent) variable and porosity and permeability as the response (dependent) variables in regression analyses (Helmold and others, 2006). In partially exhumed sedimentary basins, Dmax is calculated by adding the amount of

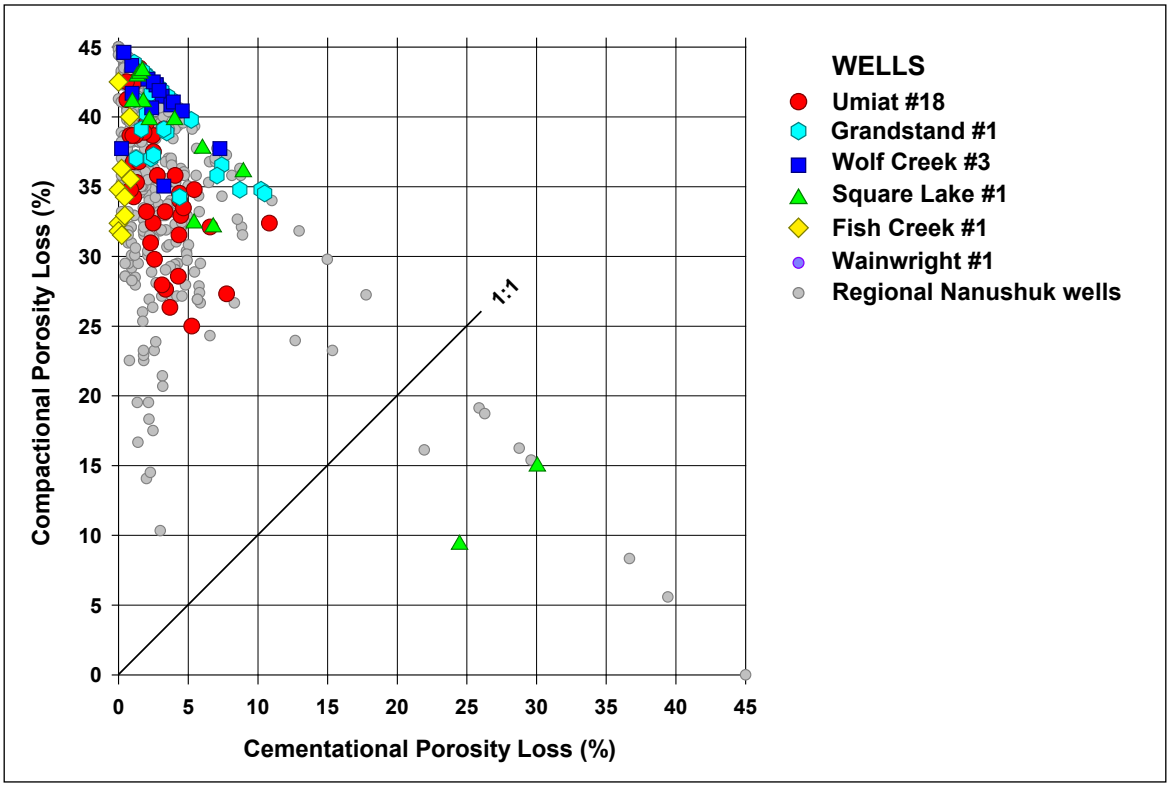

Figure 14. Cross plot of compactional porosity loss versus cementational porosity loss for six NPRA wells and regional Nanushuk siltstone and sandstone. Samples with cementational porosity loss greater than 45 percent are arbitrarily set to the assumed maximum depositional intergranular volume of 45 percent. The diagonal line (1:1) represents equal porosity loss by compaction and cementation. Porosity loss in most samples was largely through compaction. Diagram modified from Lundegard (1992).

denuded section to the current burial depth. Burns and others (2005) utilized sonic-porosity well logs to estimate the amount of sedimentary section eroded on the North Slope, thereby enabling the value of Dmax to be estimated for any exploration well. A contour map of eroded section for the central North Slope displays a generally uniform increase in the thickness of eroded section, and hence Dmax, from the Barrow Arch in the north to the Brooks Range deformation front in the south (fig. 15). Fish Creek 1 is located along the northern Alaska coastline where the thickness of eroded section is estimated at 1,103 ft (fig. 15, modified from Burns and others, 2005). That amount added to the current burial depths of Fish Creek samples, yields maximum depths of burial (Dmax) ranging from 4,074 to 4,136 ft (figs. 15, 16). Similarly, Wainwright 1 experienced 2,762 ft of denudation, with corresponding Dmax values of 2,944 to 4,263 ft (figs. 15, 16; Helmold, 2016). Most geologists consider burial less of than 5,000 ft as shallow to moderate. In contrast, Grandstand 1, Wolf Creek 3, and Umiat 18 are located 80 to 100 miles south of the Beaufort Sea where estimates of removed overburden are much greater (fig. 15, table 1). Specifically, at Umiat 18 the amount of denudation is estimated at 6,485 ft (fig. 15, modified from Burns and others, 2005), resulting in Dmax values ranging from 7,199 to 7,496 ft (figs. 15, 16). Grandstand 1 and Wolf Creek 3 are more extreme examples; the thickness of eroded section at Grandstand 1 is estimated at 8,084 ft (fig. 15, modified from Burns and others, 2005), resulting in Dmax values ranging from 8,326 to 10,596 ft (figs. 15, 16). For Wolf Creek 3 the amount of denudation is estimated at 7,191 ft, yielding Dmax values ranging from 8,724 to 10,711 ft (figs. 15, 16). Many of the southern wells in the regional dataset have similar burial histories with maximum depths of burial

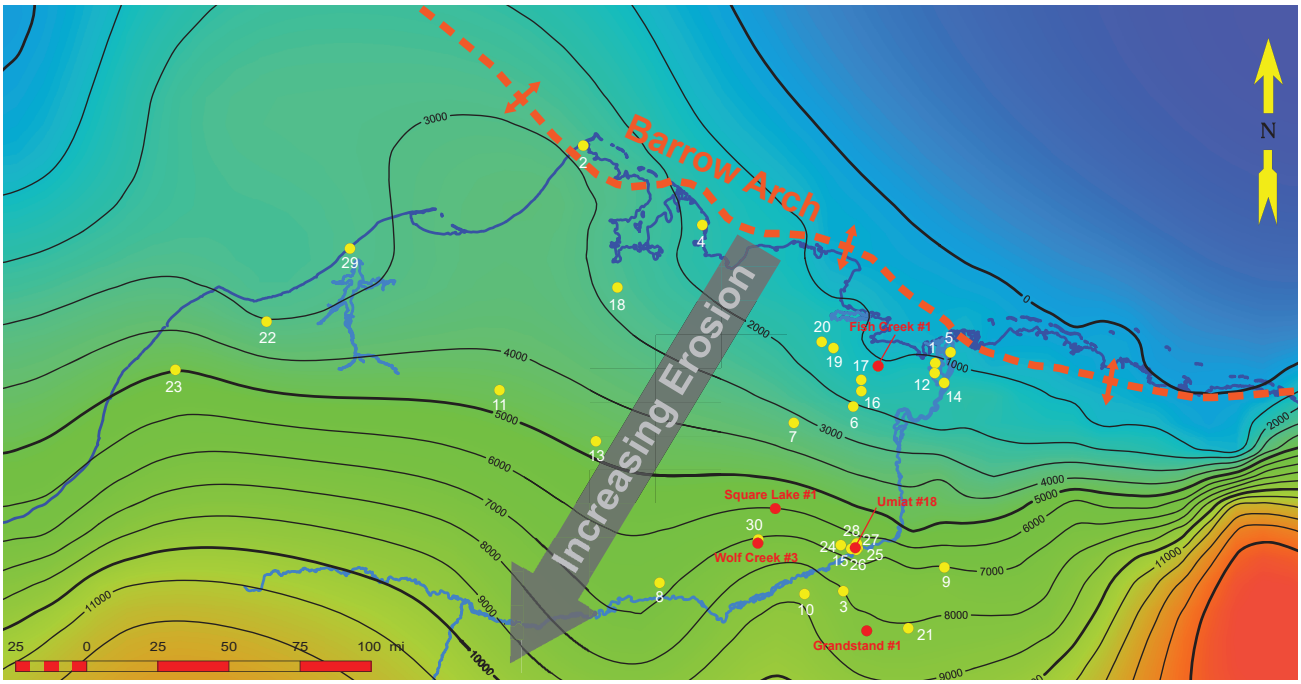

Figure 15. Contoured map of the central north slope of Alaska showing estimates of the thickness of Brookian strata removed by erosion (in feet). Red circles show the location of the five NPRA wells in this study; yellow circles show locations of thirty (30) wells for which petrographic data are available for Nanushuk sandstone (see table 1 for list). The large arrow shows the regional trend of increasing amounts of erosion to the south. Contours were generated from the data of Burns and others (2005) using GeoAtlas—the mapping module of GeoGraphix.

approaching 10,000 ft (figs. 15, 16); such values are traditionally considered deep burial.

Using available data, two sets of linear regression models for porosity-Dmax and permeability-Dmax relationships were developed for Nanushuk sandstone. Samples known or suspected to have greater than 10 percent carbonate cement were excluded from the analyses. One model (full-dataset model) uses all available porosity, permeability, and Dmax data (fig. 16, table 3), while the other (mean-value model) uses mean values of porosity, permeability, and Dmax calculated for each well (fig. 17). The two models give similar results, although with differing degrees of complexity. The mean-value analysis produces a plot (fig. 17) in which data points representing individual wells better conform to the regression line thereby yielding a higher correlation coefficient (r = -0.82 for porosity). Although this plot is more visually appealing, it hides the true intricacy of the data. Analysis of the full dataset (fig. 16) yields a lower correlation coefficient (r = -0.79 for porosity) but allows for a better understanding of the factors controlling reservoir quality. For any conventional core in each well, individual samples have similar values of Dmax (within 30 to 60 ft—the standard length of conventional core barrels) and form nearly vertical lines in the plot (fig. 16). Two factors are thought to govern the reservoir quality of Brookian sandstone: depositional environment, which is considered a local control; and depth of burial, which is deemed a regional factor. The large spread in porosity and permeability for any given value of Dmax (i.e., any given core) illustrates the primary (local) control depositional environment has on reservoir quality. This realization is lost in the mean-value model. Both analyses illustrate the secondary (regional) control that burial history has on reservoir quality. The porosity-Dmax plot yields a more tightly constrained relationship (higher correlation coefficient) than the permeability-Dmax plot in both the mean-value and full-dataset models. This is to be expected

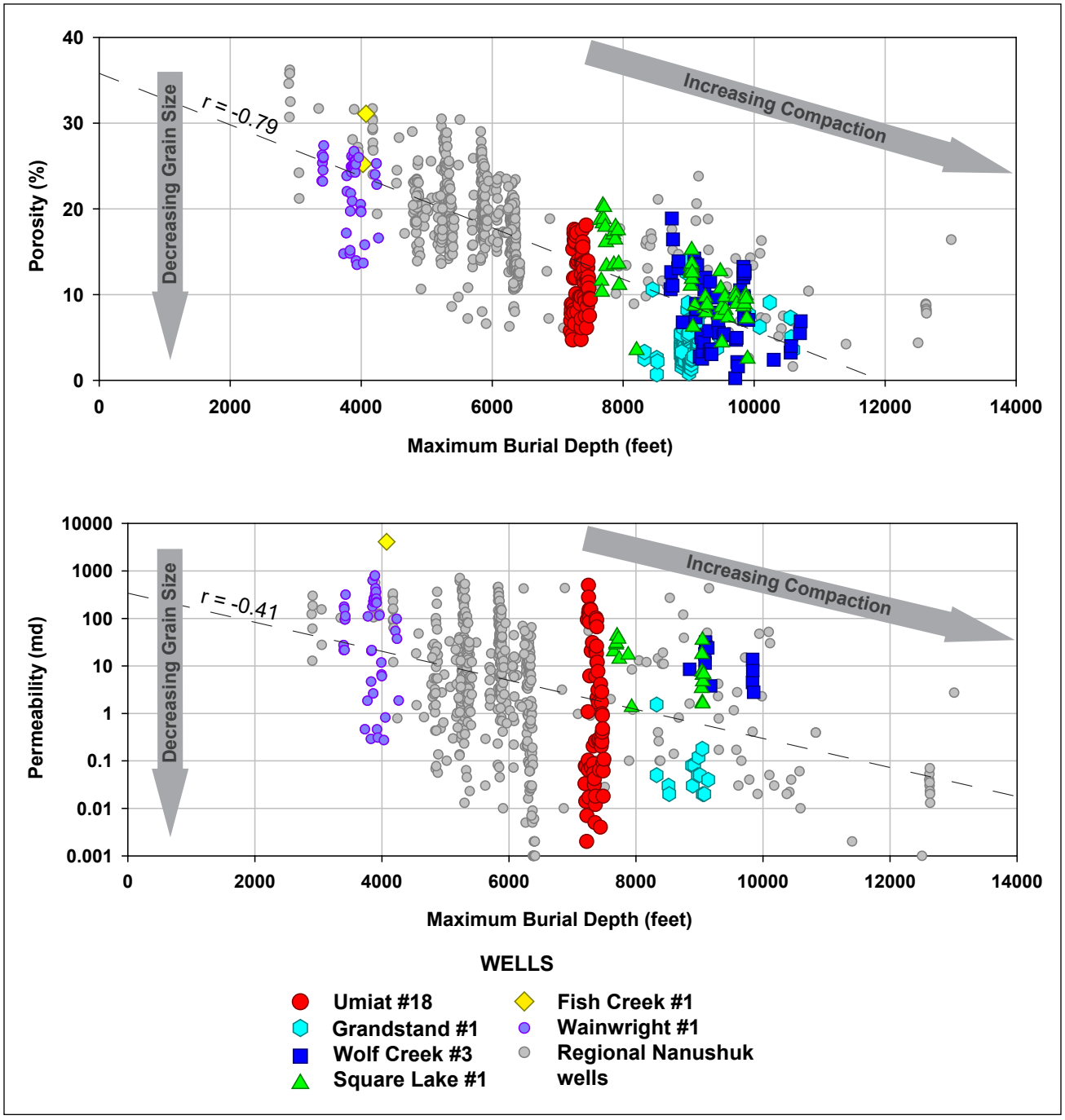

Figure 16. Cross plots of reservoir quality versus maximum burial depth (Dmax) for six NPRA wells and regional Nanushuk samples. All available data were plotted (compare with fig. 17) except for samples with > 10 percent carbonate cement. The arrows depict the two major controls on Nanushuk reservoir quality: depositional environment (grain size as proxy) and compaction. At any given value of Dmax, reservoir quality is largely controlled by depositional energy as signaled by grain size. At the regional scale, compaction has a significant effect on reservoir quality. **A**. Porosity versus Dmax plot; Wainwright 1 samples are indicative of shallow samples (~ 4,000 ft Dmax) while those from Wolf Creek 3 are representative of deeply buried rocks (> 9,000 ft Dmax). **B**. Permeability versus Dmax plot. Permeability data have a larger standard deviation than porosity data.

Table 3. Linear regression models to predict porosity and permeability of Nanushuk sandstone from maximum burial depth (Dmax). The models use all available porosity, permeability, and Dmax data; samples with greater than 10% carbonate cement are excluded (fig. 16). When applied to pre-drill predictions, an estimate of the maximum burial depth of the reservoir yields predictions for the mean values of core porosity and permeability. Estimates of the range of individual values are given by the mean ± 1 σ. Coefficient of porosity intercept = 35.7982, coefficient of porosity slope = -0.00301337, coefficient of log(permeability) intercept = 2.53536, coefficient of log(permeability) slope = -0.000308174.

All Data						
	Porosity Regression			Permeability Regression		
Dmax	Porosity	Porosity - 1σ	Porosity + 1σ	Permeability	Permeability - 1σ	Permeability + 1σ
1,000	32.8	25.5	40.1	168.728	8.186	3477.891
2,000	29.8	22.5	37.1	82.987	4.026	1710.575
3,000	26.8	19.5	34.1	40.817	1.980	841.333
4,000	23.7	16.4	31.0	20.075	0.974	413.803
5,000	20.7	13.4	28.0	9.874	0.479	203.526
6,000	17.7	10.4	25.0	4.856	0.236	100.103
7,000	14.7	7.4	22.0	2.389	0.116	49.235
8,000	11.7	4.4	19.0	1.175	0.057	24.216
9,000	8.7	1.4	16.0	0.578	0.028	11.910
10,000	5.7	0.0	13.0	0.284	0.014	5.858
11,000	2.7	0.0	9.9	0.140	0.007	2.881
12,000	0.0	0.0	7.3	0.069	0.003	1.417
13,000	0.0	0.0	7.3	0.034	0.002	0.697
14,000	0.0	0.0	7.3	0.017	0.001	0.343

given the large range of permeability in sandstone. The predicted values of porosity and permeability derived from the regression models are essentially mean values for a given value of Dmax. Estimates of the range in individual values of porosity and permeability are obtained by adding (high end of range) and subtracting (low end of range) the value of one sigma of the entire population from the mean (table 3). When using these regression models to forecast reservoir quality prior to drilling, it is important to keep in mind the implied assumptions: 1) petrology of the target sandstone is comparable to that in the modeled wells, and 2) the depositional environments in the target well are akin to those represented in the modeled wells. The greatest expected source of error in the forecasts lies in the possible occurrence of depositional facies that were not present in the modeled wells. Similar regression analyses for Torok and Seabee sandstones have proven useful in predicting reservoir quality prior to drilling (Helmold and others, 2006) and have led to a better understanding of the regional distribution of reservoir sandstone on the North Slope (table 4).

Musings on the Big Picture

Reservoir quality of Nanushuk sandstone is largely controlled by two separate and independent processes: depositional environment, which establishes a local control, and compaction, which constitutes a regional control (fig. 16). Many facets of sediment deposition influence reservoir quality, such as grain size, sorting, bioturbation, laminations, sedimentary structures, and clay content to name a few. Given the disparate and incomplete datasets used in this and other regional studies, grain size emerges as a useful parameter that is often measured during sedimentologic and petrographic studies. While not a direct analog, grain size can be used as a proxy for depositional environment, more specifically as a measure of depositional energy. At the local-con-

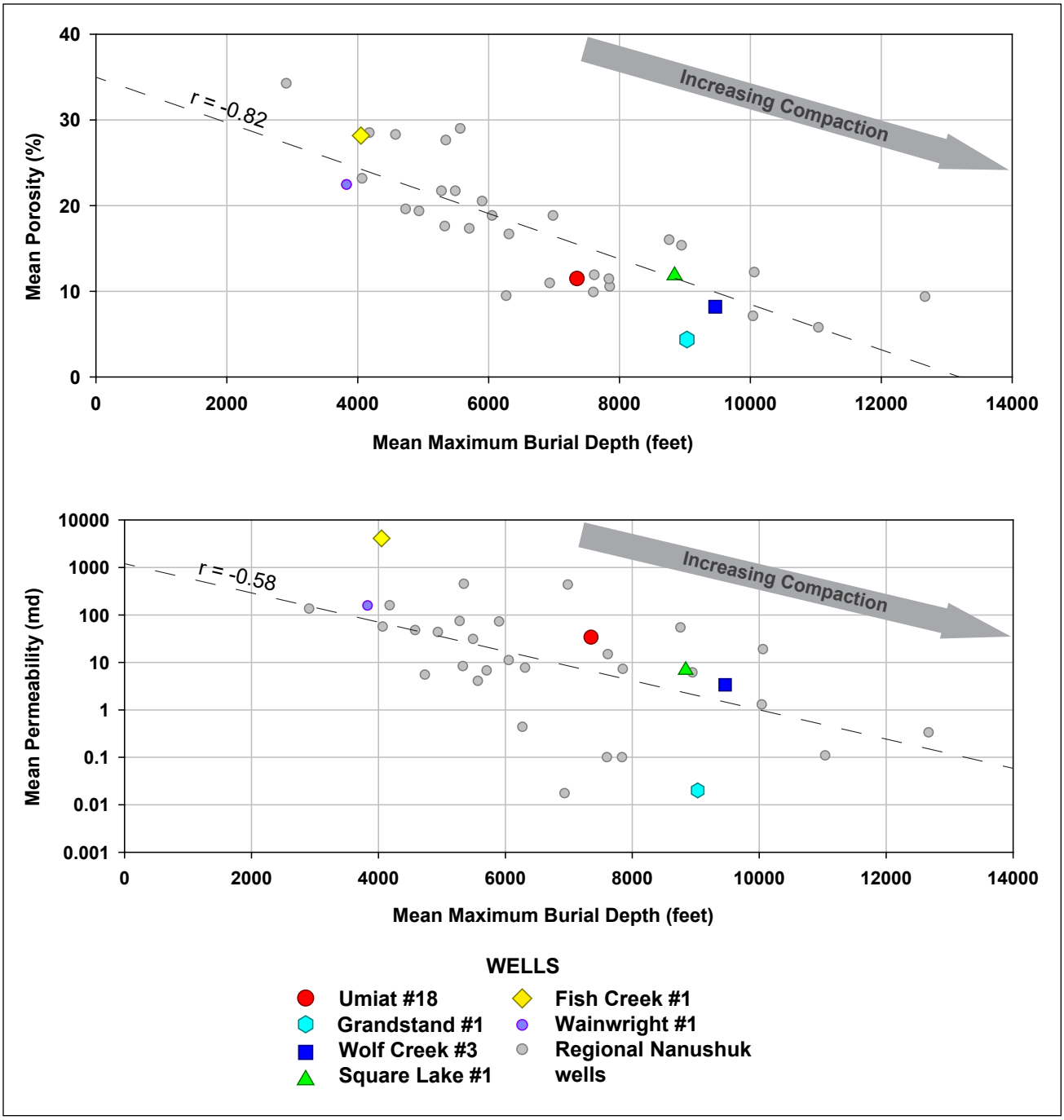

Figure 17. Cross plots of reservoir quality (as mean porosity and mean permeability) versus mean maximum burial depth (Dmax) for six NPRA wells and regional Nanushuk samples. Mean values are plotted by well (compare with fig. 16); samples with > 10 percent carbonate cement were excluded from the means. The arrow depicts the regional control compaction has on reservoir quality; the local control of depositional environment, as indicated by grain size, is not evident from plots of mean values. Correlation coefficients are greater than for plots incorporating all the data (fig. 16), but complexity of the data is hidden. **A**. Porosity versus Dmax plot; Wainwright 1 is indicative of shallow samples (~ 4,000 ft Dmax) while Wolf Creek 3 is representative of deeply buried rocks (> 9,000 ft Dmax). **B**. Permeability versus Dmax plot.

Table 4. Predictions of reservoir quality of Torok and Seabee sandstone from maximum burial depth (Dmax). Regression model uses all available data; samples with >10 percent carbonate cement are excluded. Predicted values are mean porosity and permeability. Dmax values < 8,000 ft (green zone) yield productive reservoirs, Dmax values of 8,000–9,000 ft (yellow zone) yield marginal reservoirs, sandstone with >9,000 ft Dmax (red zone) are non-productive. Estimates of the range of individual values are given by the mean ± 1 σ. Coefficient of porosity intercept = 37.6734, coefficient of porosity slope = -0.00274949, coefficient of log(permeability) intercept = 3.29548, coefficient of log(permeability) slope = -0.000431553.

			Mean Porosity				Mean Permeability			
Well	Formation	Dmax	$Ø_{predicted}$	$Ø_{actual}$	$Ø_{predicted \pm 1\sigma}$	$Ø_{actual \pm 1\sigma}$	$K_{predicted}$	K_{actual}	$K_{predicted \pm 1\sigma}$	$K_{actual \pm 1\sigma}$
Kalubik 2	Torok	5,814	21.7	18.4	15.8–27.5	15.0–21.9	6.12	8.08	0.39–95.3	0.0–25.6
Kalubik 1	Torok	5,969	21.3	20.0	15.4–27.1	17.5–22.5	5.24	13.97	0.34–81.7	0.0–28.2
Bergschrund 1	Torok	7,002	18.4	13.9	12.6–24.3	4.0–9.9	1.88	3.00	0.12–29.3	0.0–6.9
Tarn 2N-313	Seabee	7,198	17.9	20.5	12.0–23.7	16.9–24.2	1.55	37.11	0.10–24.1	0.0–105.2
Tarn 3	Seabee	7,259	17.7	15.2	11.9–23.6	12.2–18.3	1.45	1.49	0.09–22.7	0.0–5.3
Tarn 2	Seabee	7,417	17.3	16.3	11.4–23.1	12.7–19.9	1.24	3.43	0.08–19.4	0.0–10.3
Tarn 4	Seabee	7,502	17.0	15.6	11.2–22.9	11.0–20.2	1.14	1.65	0.07–17.8	0.0–4.7
Aklaq 2	Torok	7,542	16.9	13.3	11.1–22.8	9.4–17.3	1.10	1.90	0.07–17.1	0.4–3.5
Cirque 3	Seabee	7,638	16.7	14.8	10.8–22.5	11.9–17.7	1.00	1.79	0.06–15.6	0.0–2.6
Meltwater North 2A	Seabee	7,683	16.5	16.9	10.7–22.4	12.2–21.7	0.95	6.94	0.06–14.9	0.0–17.7
Nanuk 1	Torok	7,691	16.5	15.5	10.7–22.4	13.8–17.2	0.95	2.08	0.06–14.8	0.0–4.3
Nanuk 2	Torok	7,754	16.4	15.8	10.5–22.2	13.7–17.9	0.89	3.70	0.06–13.9	0.0–7.9
Meltwater North 2	Seabee	7,839	16.1	13.1	10.3–22.0	9.6–16.6	0.82	1.99	0.05–12.7	0.0–8.7
Bermuda 1	Torok	7,860	16.1	20.3	10.2–21.9	18.3–22.3	0.80	11.83	0.05–12.5	0.7–22.9
Meltwater North 1	Seabee	7,864	16.1	16.7	10.2–21.9	12.5–20.9	0.80	6.72	0.05–12.4	0.0–19.5
Trailblazer A1	Torok	8,119	15.4	8.2	9.5–21.2	7.0–9.3	0.62	0.02	0.04–9.6	0.0–0.0
Aklaq 2	Torok	8,261	15.0	11.7	9.1–20.8	8.3–15.1	0.54	0.30	0.03–8.4	0.0–0.8
Trailblazer H1	Torok	8,293	14.9	8.4	9.0–20.7	7.0–9.9	0.52	0.04	0.03–8.1	0.0–0.1
Atlas 1	Torok	8,320	14.8	13.9	8.9–20.6	12.2–15.7	0.51	0.45	0.03–7.9	0.0–1.0
Aklaq 2	Torok	8,637	13.9	11.6	8.1–19.8	9.1–14.0	0.37	0.20	0.02–5.8	0.0–0.3
Kokoda 1	Torok	8,666	13.8	10.0	8.0–19.7	8.8–11.2	0.36	0.08	0.02–5.6	0.0–0.1
Aklaq 2	Torok	8,913	13.2	11.4	7.3–19.0	8.5–14.3	0.28	0.20	0.02–4.4	0.0–0.3
Aklaq 2	Torok	9,069	12.7	11.7	6.9–18.6	10.7–12.7	0.24	0.10	0.02–3.8	0.1–0.2
Meltwater South 1	Seabee	9,086	12.7	11.5	6.8–18.5	9.5–13.5	0.24	0.35	0.02–3.7	0.0–1.6
Cronus 1	Torok	9,200	12.4	10.0	6.5–18.2	–	0.21	–	0.01–3.3	–
Aklaq 2	Torok	9,302	12.1	5.7	6.2–17.9	5.3–6.1	0.19	0.10	0.01–3.0	0.0–0.1
Caribou 1	Torok	9,768	10.8	5.7	5.0–16.7	2.7–8.8	0.12	0.01	0.01–1.9	0.0–0.03
Hunter A	Torok	9,781	10.8	9.3	4.9–16.6	7.8–10.7	0.12	0.08	0.01–1.8	0.0–0.19
Caribou 1	Torok	10,074	10.0	8.9	4.1–15.8	6.5–11.3	0.09	0.07	0.01–1.4	0.02–0.12
Caribou 1	Torok	10,288	9.4	9.1	3.5–15.2	7.5–10.8	0.07	0.04	0.00–1.1	0.02–0.05
Grizzly 1	Torok	10,820	7.9	5.9	2.1–13.8	4.1–7.7	0.04	–	0.00–0.7	–
Heavenly 1	Torok	11,995	4.7	9.9	0.0–10.5	8.0–11.8	0.01	–	0.00–0.2	–

trol level, porosity and permeability are largely a function of depositional energy of the depositing currents which can be estimated by grain size of the detritus. Higher-energy depositional environments are characterized by coarser-grained detritus which typically have better reservoir quality. Conversely, lower-energy depositional environments consist of finer-grained detritus that exhibit poor reservoir quality. From a regional-control perspective porosity and permeability of Brookian sandstone is reduced as the rock, regardless of grain size or depositional environment, is buried to greater depths. Hence, on the North Slope there is a decrease in overall reservoir quality from north to south corresponding to progressively greater uplift, denudation, and maximum burial. Sandstone that has not seen significant burial (vicinity of the Beaufort Sea) is characterized by large spreads in porosity and permeability. This variability is controlled almost exclusively by depositional energy as signaled by grain size. In contrast, sandstone that has undergone deep burial (vicinity of Brooks Range deformation front) displays narrower ranges in porosity and permeability; reservoir quality being controlled by both depositional energy and compaction (figs. 16, 17).

Another important conclusion is that provenance does not exert a significant control on reservoir quality for the majority of Nanushuk samples examined in this study. Despite the variability in chert (related to grain size) and detrital carbonate (related to aerial distribution) content noted above, most samples have a somewhat uniform composition characterized by an abundance of argillaceous sedimentary and metasedimentary rock fragments. These lithic fragments are highly susceptible to ductile grain deformation; hence burial history, particularly maximum burial depth, of the sandstone is a critical factor in determining its reservoir potential. Recent work (Helmold and others, 2021) suggests there is more variability in Nanushuk composition than noted in the samples of this report. Nanushuk sandstone having a more quartzose composition and containing silica cement in the form of quartz overgrowths has been reported from outcrop samples collected from measured stratigraphic sections in the central North Slope (Helmold and others, 2021). The presence of significant overgrowths relegates this sandstone to a distinctly different diagenetic pathway than the more argillaceous lithic-rich variants. Additional work is needed to pinpoint similar quartzose sandstone in the subsurface.

Based on analysis of datasets in this report, it is possible to make general conclusions concerning the relationships between porosity, permeability, and maximum burial depth for Brookian sandstone of the North Slope. Uncemented and lightly cemented sandstone that was subjected to limited burial should show a wide range in porosity and permeability with reservoir quality largely controlled by depositional energy as indicated by grain size, sorting, mica and detrital matrix content, and lateral continuity of clay and mudstone laminations. Porosity values approaching 45 percent (presumed depositional porosity) can be expected for coarser-grained detritus with little mica, clay, or laminations of finer-grained sediment. Finer-grained, more mica- and clay-rich, or laminated sandstone should have lower porosity, potentially approaching 10–15 percent (fig. 18). As sandstone is subjected to increased burial, the overall variability of porosity and permeability is expected to decrease. Deep burial (>10,000 ft) results in significant mechanical compaction that reduces both the mean value and range of porosity and permeability, with porosities typically less than 10 percent. The theoretical data cloud in a porosity-Dmax cross plot for sandstone will tend to form a right trapezoid, with a longer base at lower burial depth and a shorter base at greater burial (fig. 18). (Note on terminology: a right trapezoid is a convex quadrilateral with one pair of parallel sides and two adjacent right angles. The parallel sides are termed the bases of the trapezoid, while the non-parallel sides are called the legs of the trapezoid.) The theoretical data cloud in a permeability-Dmax cross plot should show a similar shape. The actual porosity-Dmax data for Nanushuk sandstone presented in this report (fig. 16A) fall short of the idealized trend due to the dearth of samples with minimal burial (low Dmax). It is anticipated

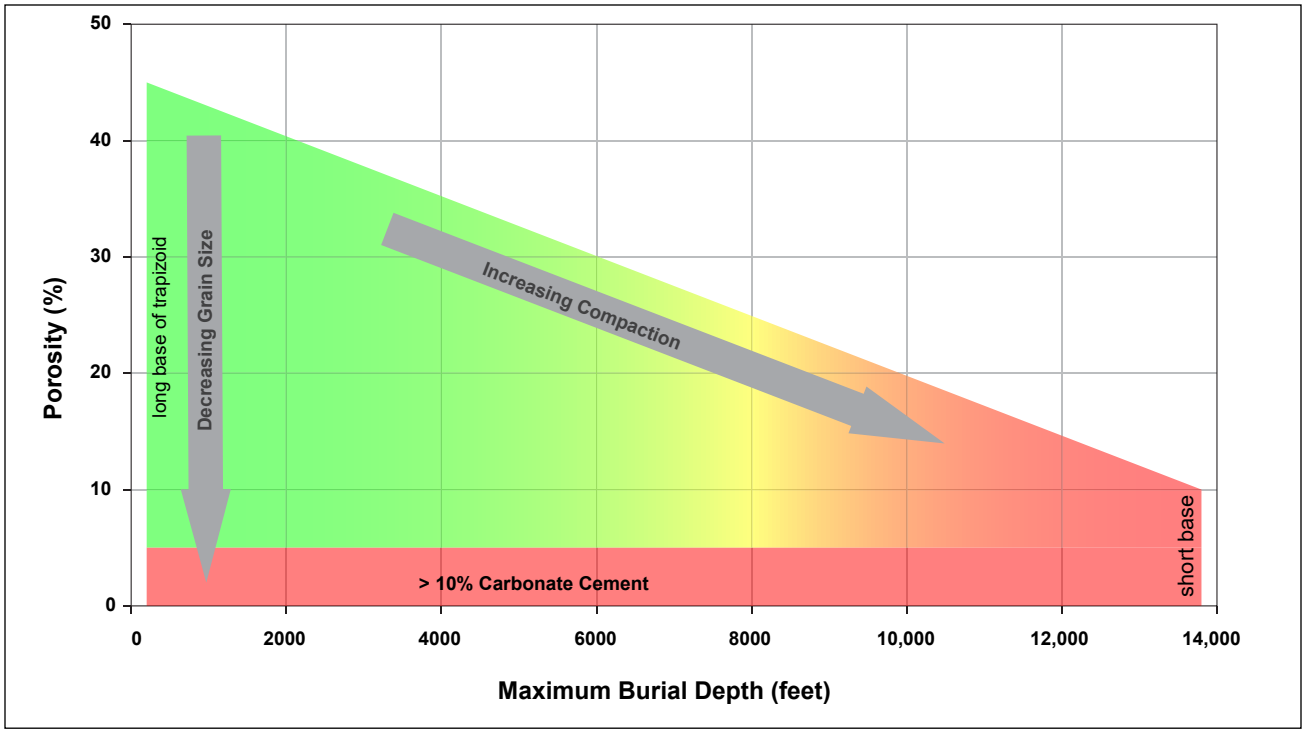

Figure 18. Theoretical plot of porosity versus maximum burial depth (Dmax) showing the idealized right trapezoid shape of the data cloud, with a longer base at lower burial depth and a shorter base at greater burial. Sandstone with >10 percent carbonate cement occurs as a narrow band with low porosity along the right-angle leg of the trapezoid. The green–yellow–red color shading shows the relative extent of reservoir quality; a value of ~8,000 ft Dmax marks the approximate boundary between productive and non-productive Brookian reservoirs. The arrows signify local (depositional energy as indicated by grain size) versus regional (compaction) controls on reservoir quality. A theoretical plot of permeability versus Dmax should have a similar shape.

the cloud from a larger dataset would more nearly resemble the theoretical quadrilateral.

The presence of significant cement, particularly diagenetically early cement, alters the appearance of the cross plot. Sandstone with appreciable cement (typically > 10 percent) will have poor reservoir quality regardless of its burial history and will plot as a narrow band with low porosity and permeability along the right-angle leg of the trapezoid (fig. 18).

Similar generalizations can be made for theoretical porosity-permeability cross plots of sandstone in the basin. Regardless of burial, the porosity-permeability trend for sandstone in any given well should plot as a diagonal line (fig. 19). Sandstone subjected to shallow burial will plot on the right-hand portion of the diagram (higher porosity values), while more deeply buried sandstone will plot farther to the left (lower porosity values). Both the local control of depositional environment as signaled by grain size and the regional control of compaction can be delineated on the plots.

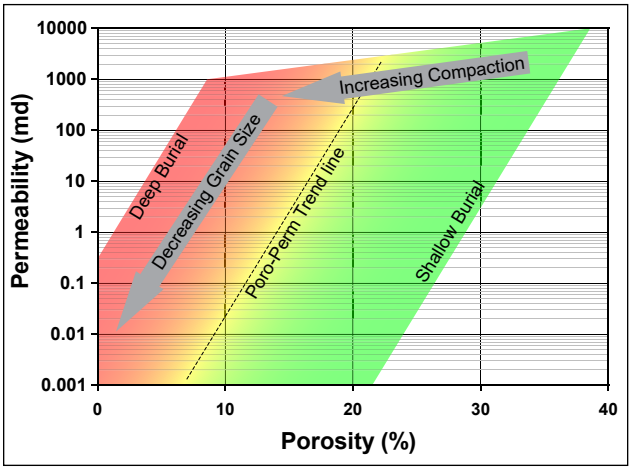

Figure 19. Theoretical plot of porosity versus permeability showing idealized parallel trends exhibited by Brookian sandstone subjected to shallow (green zone), moderate (yellow zone), and deep burial (red zone). The arrows signify local (depositional energy as indicated by grain size) versus regional (compaction) controls on reservoir quality.

ACKNOWLEDGMENTS

Funding for this work was provided by the State of Alaska. The Alaska Geologic Materials Center provided thin sections from the Fish Creek 1, Square Lake 1, Grandstand 1, and Wolf Creek 3 wells; the assistance of Kurt Johnson and Jean Riordan is greatly appreciated. Corri Feige, DNR Commissioner, was instrumental in gaining access to material and data from the Umiat 18 core. Linc Energy granted access to thin sections and routine core analyses from the core. Leonard Sojka, Malamute Energy, Inc., facilitated the loan of this material to DGGS/DOG. Insightful formal reviews by Andrew Dewhurst, Colby VanDenburg, Nina T. Harun, Ellen Daley, and Astrid Makowtiz were helpful in improving the final report.

REFERENCES

Ahlbrandt, T.S., Huffman, A.C., Fox, J.E., and Pasternack, I., 1979, Depositional framework and reservoir-quality studies of selected Nanushuk Group outcrops, North Slope, Alaska, *in* Ahlbrandt, T.S., ed., Preliminary geologic, petrologic, and paleontologic results of the study of Nanushuk Group rocks, North Slope, Alaska: U.S. Geological Survey Circular 794, p.14–31.

Atkinson, C.D., McGowen, J.H., Bloch, S., Lundell, L.L., and Trumbly, P.N., 1990, Braidplain and deltaic reservoir, Prudhoe Bay Field, Alaska: *in* Barwis, J.H., McPherson, J.G., and Studlick, J.R.J., eds., Sandstone Petroleum Reservoirs, Springer-Verlag, p. 205–224.

Bartsch-Winkler, S., 1979, Textural and mineralogical study of some surface and subsurface sandstones from the Nanushuk Group, western North Slope, Alaska, *in* Ahlbrandt, T.S., ed., Preliminary geologic, petrologic, and paleontologic results of the study of Nanushuk Group rocks, North Slope, Alaska: U.S. Geological Survey Circular 794, p. 61–76.

———1985, Petrography of sandstones of the Nanushuk Group from four measured sections, central North Slope, Alaska, *in* Huffman, A.C., Jr., ed., Geology of the Nanushuk Group and related rocks, North Slope, Alaska: U.S. Geological Survey Bulletin 1614, p. 75–95.

Bartsch-Winkler, S., and Huffman, A.C., Jr., 1988, Sandstone petrography of the Nanushuk Group and Torok Formation, *in* Gryc, George, ed., Geology and exploration of the National Petroleum Reserve in Alaska, 1974 to 1982: U.S. Geological Survey Professional Paper 1399, p. 801–831.

Basu, A., Young, S.W., Suttner, L.J., James, W.C., and Mack, G.H., 1975, Re-evaluation of the use of undulatory extinction and polycrystallinity in detrital quartz for provenance interpretations: Journal of Sedimentary Petrology, v. 45, no. 4, p. 873–882.

Blatt, H., 1982, Sedimentary Petrology: New York, NY, W. H. Freeman and Company, 564 p.

Blatt, H., Middleton, G.V., and Murray, R., 1980, Origin of Sedimentary Rock (2nd edition): Englewood Cliffs, NJ, Prentice-Hall, 782 p.

Bloch, S., 1991, Empirical prediction of porosity and permeability in sandstone: American Association of Petroleum Geologist Bulletin, v. 75, no. 7, p. 1,145–1,160.

Bloch, S., and Helmold, K.P., 1995, Approaches to predicting reservoir quality in sandstones: Association of Petroleum Geologist Bulletin, v. 79, no. 1, p. 97–115.

Boggs, S., Jr., 2009, Petrology of Sedimentary Rocks (2nd edition): New York, NY, Cambridge University Press, 600 p.

Burns, W.M., Hayba, D.O., Rowan, E.L., and Houseknecht, D.W., 2005, Estimating the amount of eroded section in a partially exhumed basin from geophysical well logs: An example from the North Slope *in* Haeussler, P.J., and Galloway, J.P., eds., Studies by the U.S. Geological Survey in Alaska: U.S. Geological Survey Professional Paper 1732-D, p. 1–18.

Byrnes, A.P., and Wilson, M.D., 1991, Aspects of porosity prediction using multivariate linear regression [abs.]: American Association of Petroleum Geologist Bulletin, v. 75, p. 548.

Collins, F.R., 1959, Test Wells, Square Lake and Wolf Creek Areas Alaska: U.S. Geological Survey Professional Paper 305-H, p. 423–484.

Crowder, R.K., 1989, Deposition of the Fortress Mountain Formation, *in* Mull, C.G., and Adams, K.E., eds., Bedrock geology of the east-

ern Koyukuk basin, central Brooks Range, and east-central Arctic Slope along the Dalton Highway, Yukon River to Prudhoe Bay, Alaska, Volume 2: Alaska Division of Geological & Geophysical Surveys Guidebook 7-20, p. 293–301. http://doi.org/10.14509/24134

Decker, J.E., 1985, Sandstones modal analysis procedure: Alaska Division of Geological & Geophysical Surveys Public Data File 85-3, 38 p.

Decker, J.E., and Helmold, K.P., 1985, The effect of grain size on detrital modes: A test of the Gazzi-Dickinson point-counting method– Discussion: Journal of Sedimentary Petrology, v. 55, p. 618–620.

Decker, P.L., 2010, Brookian sequence stratigraphic framework of the northern Colville foreland basin, central North Slope, Alaska (poster and presentation): DNR Spring Technical Review Meeting, Anchorage, April 21–22, 2010: Alaska Division of Geological & Geophysical Surveys, 30 p., 1 sheet. http://doi.org/10.14509/21861

Folk, R.L., 1974, Petrology of sedimentary rocks: Hemphill Publishing Co., Austin, TX, 182 p.

Fox, J.E., 1979, A summary of reservoir characteristics of the Nanushuk Group, Umiat Test Well 11, National Petroleum Reserve in Alaska, *in* Ahlbrandt, T.S., ed., Preliminary geologic, petrologic, and paleontologic results of the study of Nanushuk Group rocks, North Slope, Alaska: U.S. Geological Survey Circular 794, p. 42–53.

Fox, J.E., Lambert, P.W., Pitman, J.K., and Wu, C.H., 1979, A study of reservoir characteristics of the Nanushuk and Colville Groups, Umiat Test Well 11, National Petroleum Reserve in Alaska: U.S. Geological Survey Circular 820, 47 p.

Franks, S.G., and Lee, M.K., 1994, Preliminary report on diagenesis of upper Cook Inlet sandstones: Atlantic Richfield Company report, 46 p.

Garrity, C.P., Houseknecht, D.W., Bird, K.J., Potter, C.J., Moore, T.E., Nelson, P.H., and Schenk, C.J., 2005, U.S. Geological Survey 2005 oil and gas resource assessment of the central North Slope, Alaska: play maps and results: U.S. Geological Survey Open-File Report 2005-1182, 25 p.

Gillis, R.J., Decker, P.L., Wartes, M.A., Loveland, A.M., and Hubbard, T.D., 2014, Geologic map of the south-central Sagavanirktok Quadrangle, North Slope, Alaska: Alaska Division of Geological & Geophysical Surveys Report of Investigation 2014-4, 24 p., 2 sheets, scale 1:63,360. http://doi.org/10.14509/29138

Gryc, George, 1988, Introduction and role of the U.S. Geological Survey, *in* Gryc, George, ed., Geology and exploration of the National Petroleum Reserve in Alaska, 1974 to 1982: U.S. Geological Survey Professional Paper 1399, p. 1–12.

Helmold, K.P., 2016, Sedimentary petrology and reservoir quality of Albian-Cenomanian Nanushuk Formation sandstones, USGS Wainwright #1 test well, western North Slope, Alaska, *in* LePain, D.L., ed., Stratigraphic and reservoir quality studies of continuous core from the Wainwright #1 coalbed methane test well, Wainwright, Alaska: Fairbanks, Alaska, Alaska Division of Geological and Geophysical Surveys Report of Investigations 2016-3-3, p. 37–58. https://doi.org/10.14509/29657

Helmold, K.P., Campaign, W.J., Morris, W.R., Hastings, D.S., and Moothart, S.R., 2006, Reservoir quality and petrophysical model of the Tarn deep-water slope-apron system, North Slope, Alaska: Pacific Section, American Association of Petroleum Geologists annual meeting, Anchorage, Alaska.

Helmold, K.P., LePain, D.L., and Harun, N.T., 2021, Qualitative assessment of composition and reservoir quality of Albian–Cenomanian Nanushuk Formation sandstones, measured outcrop sections, central North Slope, Alaska: Alaska Division of Geological & Geophysical Surveys Raw Data File 2021-13, 7 p. https://doi.org/10.14509/30746

Herriott, T.M., Wartes, M.A., Decker, P.L., Gillis, R.J., Shellenbaum, D.P., Willingham, A.L., and Mauel, D.J., 2018, Geologic map of the Umiat-Gubik area, central North Slope, Alaska: Alaska Division of Geological & Geophysical Surveys Report of Investigation 2018-6, 55 p.

Houseknecht, D.W., 2019, Petroleum systems framework of significant new oil discoveries in a giant Cretaceous (Aptian-Cenomanian) clinotherm in Arctic Alaska: American Association of

Petroleum Geologists Bulletin, v. 103, no. 3, p. 619–652.

Houseknecht, D.W., Bird, K.J., and Schenk, C.J., 2008, Seismic analysis of clinoform depositional sequences and shelf-margin trajectories in Lower Cretaceous (Albian) strata, Alaska North Slope: Basin Research, v. 21, no. 5, p. 644–654. https://doi.org/10.1111/j.1365-2117.2008.00392.x

Houseknecht, D.W., and Schenk, C.J., 2001, Depositional sequences and facies in the Torok Formation, National Petroleum Reserve–Alaska (NPRA), *in* Houseknecht, D.W., ed., NPRA Core Workshop: Petroleum Plays and Systems in the National Petroleum Reserve–Alaska, p. 179–199.

Huffman, A.C., Ahlbrandt, T.S., Pasternack, I., Stricker, G.D., and Fox, J.E., 1985, Depositional and sedimentologic factors affecting the reservoir potential of the Cretaceous Nanushuk Group, central North Slope, Alaska, *in* Huffman, A.C., ed., Geology of the Nanushuk Group and related rocks, North Slope, Alaska: U.S. Geological Survey Bulletin 1614, p. 61–74.

Ingersoll, R.V., Bullard, T.F., Ford, R.L., Grimm, J.P., Pickle, J.D., and Sares, S.W., 1984, The effect of grain size on detrital modes: A test of the Gazzi-Dickinson point-counting method: Journal of Sedimentary Petrology, v. 54, p. 103–116.

Johnsson, M.J., and Sokol, N.K., 2000, Stratigraphic variation in petrographic composition of Nanushuk Group sandstones at Slope Mountain, North Slope, Alaska, *in* Kelley, K.D., and Gough, L.P., eds., Geologic studies in Alaska by the U. S. Geological Survey, 1998: U.S. Geological Survey Professional Paper 1615, p. 83–100.

LePain, D.L., and Kirkham, R.A., 2001, Potential reservoir facies in the Nanushuk Formation (Albian-Cenomanian), central North Slope, Alaska: Examples from outcrop and core, *in* Houseknecht, D.W., ed., NPRA core workshop: Petroleum plays and systems in the National Petroleum Reserve in Alaska: SEPM Core Workshop 21, p. 19–36.

LePain, D.L., McCarthy, P.J., and Kirkham, R.A., 2009, Sedimentology and sequence stratigraphy of the middle Albian-Cenomanian Nanushuk Formation in outcrop, central North Slope, Alaska: Alaska Division of Geological & Geophysical Surveys Report of Investigation 2009-1 v. 2, 76 p., 1 sheet. http://doi.org/10.14509/19761

Lundegard, P.D., 1992, Sandstone porosity loss; a "big picture" view of the importance of compaction: Journal of Sedimentary Petrology, v. 62, no. 2, p. 250–260.

Molenaar, C.M., 1985, Subsurface correlations and depositional history of the Nanushuk Group and related strata, North Slope, Alaska, *in* Huffman, A.C., ed., Geology of the Nanushuk Group and related rocks, North Slope, Alaska: U.S. Geological Survey Bulletin 1614, p. 61–74.

Molenaar, C.M., Egbert, R.M., and Krystinik, L.F., 1988, Depositional facies, petrography, and reservoir potential of the Fortress Mountain Formation (Lower Cretaceous), central North Slope, Alaska *in* Gryc, George, ed., Geology and exploration of the National Petroleum Reserve in Alaska, 1974 to 1982: U.S. Geological Survey Professional Paper 1399, p. 257–280.

Moore, T.E., Wallace, W.K., Bird, K.J., Karl, S.M., Mull, C.G., and Dillon, J.T., 1994, Geology of northern Alaska, *in* Plafker, George, and Berg, H.C., eds., The Geology of Alaska: Geological Society of America, p. 49–138.

Mull, C.G., Houseknecht, D.W., and Bird, K.J., 2003, Revised Cretaceous and Tertiary stratigraphic nomenclature in the Coleville Basin, northern Alaska: U.S. Geological Survey Professional Paper 1673, 51 p.

Paxton, S.T., Szabo, J.O., Ajdukiewicz, J.M., and Klimentidis, R.E., 2002, Construction of an intergranular volume compaction curve for evaluating and predicting compaction and porosity loss in rigid-grain sandstone reservoirs: American Association of Petroleum Geologist Bulletin, v. 86, no. 12, p. 2,047–2,067.

Reifenstuhl, R.R., and Loveland, Andrea, 2004, Reservoir characterization study: porosity and permeability of 148 Tertiary to Mississippian age outcrop samples, east-central Brooks Range Foothills and North Slope, Alaska: Alaska Division of Geological & Geophysical Surveys Preliminary Interpretive Report 2004-5, 21 p. https://doi.org/10.14509/3312

Robinson, F.M., 1958, Test Well Grandstand Area Alaska: U.S. Geological Survey Professional Paper 305-E, p. 317–338.

Robinson, F.M., and Collins, F.R., 1959, Core Test, Sentinel Hill Area and Test Well Fish Creek Area, Alaska: U.S. Geological Survey Professional Paper 305-I, p. 485–520.

Scherer, M., 1987, Parameters influencing porosity in sandstones: A model for sandstone porosity prediction: American Association of Petroleum Geologist Bulletin, v. 71, no. 5, p. 485–491.

Shimer, G.T., McCarthy, P.J., and Hanks, C.L., 2014, Sedimentology, stratigraphy, and reservoir properties of an unconventional, shallow, frozen petroleum reservoir in the Cretaceous Nanushuk Formation at Umiat field, North Slope, Alaska: Association of Petroleum Geologist Bulletin, v. 98, no. 4, p. 631–661.

Smosna, Richard, 1989, Compaction law for Cretaceous sandstones of Alaska's North Slope: Journal of Sedimentary Petrology, v. 59, no. 4, p. 572–584.

Szabo, J.O., and Paxton, S.T., 1991, Intergranular volume (IGV) decline curves for evaluating and predicting compaction and porosity loss in sandstones [abs.]: Association of Petroleum Geologist Bulletin, v. 75, no. 3, p. 678.

Velleman, P.F., 1998, Learning data analysis with the student version of Data Desk 6.0: Ithaca, New York, Addison-Wesley, 362 p.

Wartes, M.A., 2008, Evaluation of stratigraphic continuity between the Fortress Mountain and Nanushuk Formations in the central Brooks Range foothills—Are they partly correlative?, *in* Wartes, M.A., and Decker, P.L., eds., Preliminary results of recent geologic field investigations in the Brooks Range Foothills and North Slope, Alaska: Alaska Division of Geological & Geophysical Surveys Preliminary Interpretive Report 2008-1C, p. 25–39. http://doi.org/10.14509/16087

Wilson, F.H., Hults, C.P., Mull, C.G., and Karl, S.M., 2015, Geologic Map of Alaska: U.S. Geological Survey Scientific Investigations Map 3340, pamphlet 197p., 2 sheets, scale 1:1,584,000. http://pubs.er.usgs.gov/publication/sim3340 (on DVD)